



## Deliverable D4.34 - Innovative Design of a 10MW Steel-Type Jacket

Agreement n.:	308974
Duration	November 2012 – October 2017
Co-ordinator:	DTU Wind

The research leading to these results has received funding from the European Community's Seventh Framework Programme FP7-ENERGY-2012-1-2STAGE under grant agreement No. 308974 (INNWIND.EU).



---

#### PROPRIETARY RIGHTS STATEMENT

This document contains information, which is proprietary to the "INNWIND.EU" Consortium. Neither this document nor the information contained herein shall be used, duplicated or communicated by any means to any third party, in whole or in parts, except with prior written consent of the "INNWIND.EU" consortium.

---

# Document information

Document Name:	<b>Innovative design of a 10MW steel-type jacket</b>
Document Number:	<b>Deliverable D4.34</b>
Author:	<b>Mathias Stolpe, W. Njomo Wandji, Anand Natarajan (DTU) Rasoul Shirzadeh, Martin Kühn (UOL) Daniel Kaufer (Rambøll)</b>
Document Type	Report
Dissemination level	PU
Review:	<b>WP Leader</b>
Date:	<b>2016-06-17</b>
WP:	<b>4 Offshore Foundations and Support Structures</b>
Task:	<b>4.3 Design of Offshore Support Structures</b>
Approval:	Approved by Author

## TABLE OF CONTENTS

TABLE OF CONTENTS .....	3
1 INTRODUCTION.....	5
2 REVIEW OF THE INNOVATIVE 10MW WIND TURBINE.....	6
2.1 Background.....	6
2.2 Implementation of Wind Turbine Innovations.....	7
2.2.1 Description of the performed studies .....	7
2.2.2 Description of the load mitigation concepts.....	8
2.3 Design Load Verification .....	9
2.4 Conclusions .....	13
3 IMPROVED STEEL JACKET DESIGN .....	14
3.1 Design Methodology.....	14
3.1.1 General .....	14
3.1.2 Natural Frequency Analysis .....	14
3.1.3 Ultimate Limit State .....	14
3.1.4 Fatigue Limit State .....	15
3.1.5 Design Assumptions .....	15
3.1.6 Integrated Load Simulation Approach .....	16
3.1.7 Damping Model .....	17
3.1.8 Soil Properties .....	17
3.1.9 Load Cases and Load Combinations .....	17
3.1.10 Superelement of the Jacket Model .....	18
3.2 Review of Component Innovations.....	19
3.3 Computer Model.....	22
3.3.1 Design Tools .....	22
3.3.2 Support Structure and Foundation .....	22
3.3.3 Rotor-Nacelle-Assembly and Tower.....	23
3.4 Design Results.....	24
3.4.1 Natural Frequency Analysis .....	24
3.4.2 Ultimate Limit State .....	25
3.4.3 Fatigue Limit State.....	26
3.4.4 Summary of the Jacket Geometry and Masses.....	27
3.5 Cost Estimation .....	28
3.5.1 Unit Price Approach .....	28
3.5.2 Advanced Cost Model for Fabrication.....	28
4 MODULARIZED JACKET DESIGN.....	31
4.1 Background.....	31
4.2 Optimization Methodology .....	32
4.3 Fatigue Load Results and Lifetime.....	34
4.3.1 Met-Ocean Conditions .....	34
4.3.2 Hydro-Servo-Aero-Elastic Load Simulation .....	34
4.3.3 Critical Stress Loads and Lifetime .....	35
4.3.4 Stress Concentration Factors.....	36

4.3.5	SN-Curves .....	37
4.3.6	Damage Accumulation.....	37
4.3.7	Fatigue Lifetime .....	38
4.4	Monopile Design at 50 m Water Depth.....	38
4.4.1	Met-Ocean Conditions and Hydro-Servo-Aero-Elastic Load Simulation .....	38
4.4.2	Predesign: Resonance Avoidance.....	39
4.4.3	Load Assessment, Ultimate Limit State and Stability Limit State .....	39
4.4.4	Fatigue Limit State.....	40
4.5	Summary of the three Developed Concepts .....	41
5	CONCLUSIONS.....	43
6	REFERENCES.....	45
	APPENDIX A – JACKET SUPERELEMENT .....	46
	Mass matrix:.....	46
	Damping matrix.....	49
	Stiffness matrix.....	52
	APPENDIX B – TOWER MODEL .....	55
	APPENDIX C – SOIL PROFILE .....	56
	APPENDIX D – FATIGUE LIVES OF TUBULAR JOINTS .....	57
	APPENDIX E – GEOMETRY OF THE JACKET.....	58
	APPENDIX F – GEOMETRY OF THE MONOPILE .....	67

## 1 INTRODUCTION

The report shows the results of the bottom-fixed support structure designs for the 10MW wind turbine class. It makes use of the findings from the concept studies of previous deliverables of the Task 4.3, the component innovations (with respect to steel type jackets) developed in Task 4.1 and also from innovations coming from other WPs. The support structure designs use the most rational and promising innovations. A selection of the innovation is made and the reasoning is given in the appropriate sections. Consequently the deliverable is a collaborative work between different work packages.

The innovative designs are compared against the reference jacket given in D4.31 (ref. /1/) or if more appropriate to the predecessor obtained during the concept study in D4.32. Besides the structural parameters the cost model from WP1 will be used to evaluate the cost saving potential (CAPEX) of the designs.

The design procedure is in accordance to the standards and guidelines for offshore support structures. As a minimum requirement ultimate limit state analyses (ULS), fatigue limit state (FLS) analyses and natural frequencies analysis (NFA) are carried out in order to allow fair comparisons to the reference jacket design.

The following analyses and designs are carried out by the project partners:

- Load reduction and performance of the innovative 10MW wind turbine model by University Oldenburg, see Chapter 2,
- Update of the reference jacket including innovations and improvements from WTB, controller, damping and structural optimization by Ramboll, see Chapter 3,
- Optimization using modularized steel frame jackets and lattice towers by DTU, see Chapter 4),
- Cost comparison of support structure designs against the reference jacket from D4.31

## 2 REVIEW OF THE INNOVATIVE 10MW WIND TURBINE

### 2.1 Background

In recent years, the size of wind turbines is dramatically increased beyond the 5 MW class to reduce the cost of energy. The design of support structures for such large machines is still a challenging task as the rotor diameter and tower height are exceeding 100 m. The support structure eigenfrequencies are analysed in the early stage of the design procedure to prevent significant resonances between the structural frequencies and excitations from the waves, rotor frequency, and higher harmonics. This can be acquired via the Campbell diagram which plots the eigenfrequency of the entire wind turbine system against the rotor speed including the harmonic excitations 1P, 3P, etc. Figure 2-1 plots qualitatively the rotor rotational frequency (1P) and blade passing frequency (3P) ranges along with the first eigenfrequency of the support structure as a function of the wind turbine size. In the design procedure of large offshore wind turbines, 7.5+ MW, with jacket foundations, a strong and severe blade passing (3P) resonance is expected at low rotor speeds ref /15/.

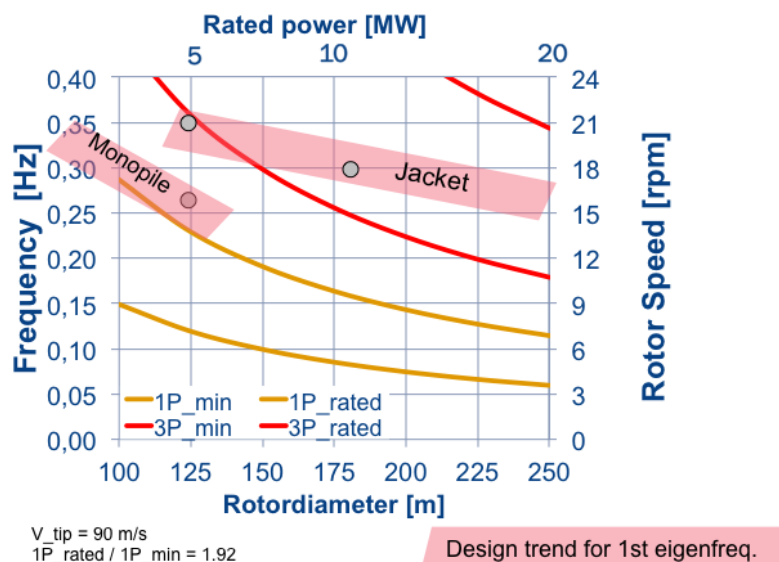
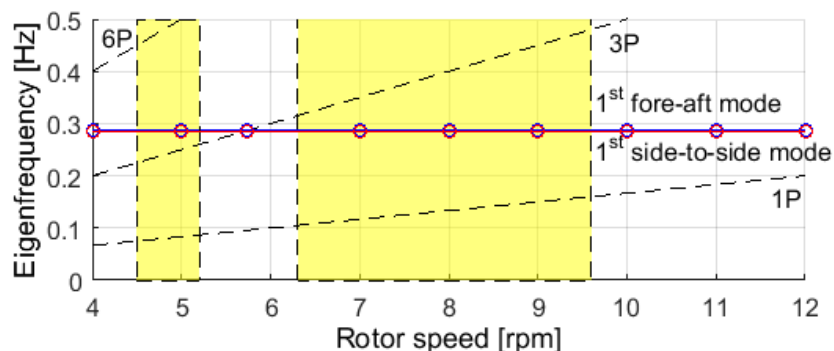


Figure 2-1: Design trends on first design eigenfrequency and the rotor and blade resonance ranges for three-bladed offshore turbines in the 5 to 20 MW class ref /15/.

Figure 2-2 shows the Campbell diagram for the 10MW INN WIND.EU reference turbine. It can be seen that at the rotor speed of 5.7 rpm, the blade passing frequency coincides with the first natural frequency of the system. The rotor frequency (1P) is however not problematic as it is found far outside of the operational region. In order to reduce the dynamic excitation, a rotor speed exclusion zone between 5.2 rpm and 6.3 rpm is considered. Compared to the initial exclusion zone chosen in the preliminary stage ref /16/, the exclusion zone is shifted downward due to the modified eigenfrequencies. This causes an extra modification of the cut-in speed from 5 rpm to 4.5 rpm.



**Figure 2-2: Campbell diagram of the INN WIND.EU 10 MW reference turbine. The yellow marked areas represent the operational range of the turbine. The cut-in speed is modified to avoid overlapping with the exclusion zone.**

The larger the blades and the supporting structure of the wind turbine, the higher the bending loads and strongly increased fatigue loads are experienced by critical components e.g. tower base. Innovations are targeted in lowering the loads experienced by the support structure. This goal can be met through a variety of load mitigation strategies e.g. implementation of passive or (semi) - active damping devices and different control and regulation concepts. Nowadays, the application of a tower mass damper (TMD) is becoming increasingly practical for the load mitigation of large wind turbine structures. Previous works have shown the potential for integration of the TMDs in the tower top location ref /17/. In addition, different solutions have been proposed for the application of semi-active or active dampers, e.g. toggle-brace viscous damper, tuned liquid column damper (TLCD), magnetorheological (MR) damper and hybrid mass dampers, see ref. /18/, /19/ and /20/.

To control the dynamic excitation of the supporting structure, two innovative concepts are designed and integrated in the INN WIND 10 MW reference turbine. In the first study, the results of the integration of a passive structural damper to reduce the support structure loads are presented. A passive tuned mass damper (TMD) is designed to realize the best configuration according to the calculated tower base lifetime and damage equivalent loads (DELs). During the second innovative concept, the numerical model of a diagonal-brace viscous damper is developed. Aeroelastic simulations are performed in DNV GH Bladed software ref /21/ for the offshore 10MW INN WIND reference wind turbine mounted on a jacket structure. The loads calculated for the innovative concepts are then compared with the reference turbine. The improved loads data obtained from the integrated design are most likely to extend the lifetime of the support structure with a positive impact on the economic aspects.

## 2.2 Implementation of Wind Turbine Innovations

### 2.2.1 Description of the performed studies

The performed studies on the innovative concepts are based on the offshore 10 MW INN WIND.EU reference wind turbine ref /1/. The 3D turbulent wind field with the Kaimal spectrum is generated for six random seeds while the wave kinematics is modelled based on the irregular wave model with the JONSWAP spectrum. No yaw misalignment angle is assumed in this analysis. The design load case (DLC) 1.2 ref /1/ is considered and fatigue loads are calculated during the full operating wind speed range. The wind and wave characteristics are listed in Table 2-1.

**Table 2-1: Environmental conditions for the wind and wave parameters**

V [m/s]	Long. Turb. I [%]	Lat. Turb. I [%]	Vert. Turb. I [%]	Hs [m]	Tp [s]	Occurance [hours/year]
4	20.4	16.3	10.2	1.1	5.88	874.7
6	17.5	14	8.75	1.18	5.67	992.8
8	16	12.8	8	1.31	5.67	1181.8
10	15.2	12.16	7.6	1.48	5.74	1076.3
12	14.6	11.68	7.3	1.7	5.88	1137.2
14	14.2	11.36	7.1	1.91	6.07	875.6
16	13.9	11.12	6.95	2.19	6.37	764.7
18	13.6	10.88	6.8	2.47	6.71	501.3
20	13.4	10.72	6.7	2.76	6.99	336.0
22	13.3	10.64	6.65	3.09	7.4	289.4
24	13.1	10.48	6.55	3.42	7.8	130.4

### 2.2.2 Description of the load mitigation concepts

The two load mitigation innovative concepts introduced in the Deliverable 4.13 ref /7/ can be integrated in the final design of the jacket to ensure an optimised and affordable design. Figure 2-3 represents the schematic models of two integrated innovative concepts considered in this load mitigation investigation. The time series of the wind loads combined with the hydrodynamic loads are calculated for each innovative concept and used in the calculation of the Ultimate Limit State (ULS) and Fatigue Limit State (FLS). Here in this study only one wind-wave misalignment is considered. Although the tuned mass dampers are a common design for current commercial wind turbines, but the initial INN WIND.EU 10MW reference jacket is designed without considering the any damper in the tower. As a consequence, the initial jacket design is not optimised and needs further improvements. Therefore, the integration of a TMD has the potential to improve the jacket design by reducing the interface loads.

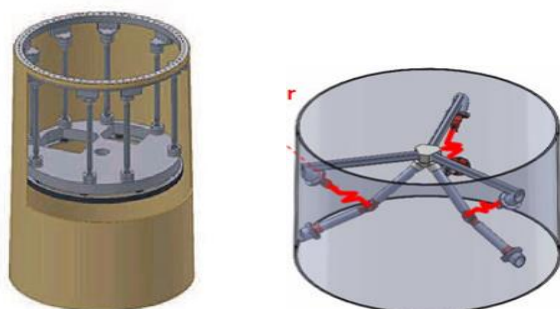


**Figure 2-3: Innovative concepts considered to be integrated into the Reference INN WIND.EU wind turbine, passive TMD (left) and the toggle brace damper (right)**

For both innovative concepts, the fatigue loads are calculated at the tower base and the interface loads are delivered to Ramboll to establish a new jacket design analysis with improved loads. The new designed jacket structure will be imported in the Bladed software and the optimization loop can be repeated to achieve an improved design.

In the first study, the tower top is equipped with a tuned mass damper and the damage equivalent loads (DELs) are calculated at the tower base at different wind speeds. According to /17/, the TMD mass is approximately either 8% of the nacelle mass or 6% of the tower top mass. Other studies propose to use a value between 2-4% of the modal mass associated with the fundamental lowest eigenfrequency which is commonly used for civil engineering structures /17/. In this analysis, a parameter study for a TMD with mass ratios of 1% and 2% is performed.

The second part describes the mathematical representation of a viscous damper. Up to now, only passive dampers are coming into practice for the wind turbines and both semi-active and active dampers are still under development. A Simulink model is developed for a viscous damper and is connected to Bladed via an external Dynamic-Link Library (DLL). The optimal location of the damper is a challenging task. In this study, we assume that the viscous damper system is installed at the tower top, which has the largest lateral motion and thus results in higher damping efficiency. The design formulas for a viscous damper system are based on the study described in /22/. For a system represented in Figure 2-3, the following relation exists:

$$u_D = fu \quad (2-1)$$

where  $u_D$  is the relative displacement along the axis of the damper,  $u$  is the structural drift and  $f$  is the magnification factor. Also, the horizontal component of the force exerted by the damper on the structure,  $F$ , is obtained from:

$$F = fF_D \quad (2-2)$$

with  $F_D$ , the damper force. For a viscous damper, the damper force along its axis is written as below:

$$F_D = C\dot{u}_D^\alpha \quad (2-3)$$

where  $C$  is the damping coefficient of the damper,  $\dot{u}_D$  represents the relative velocity between the ends of the damper and  $\alpha$  is the damper nonlinearity. If we combine Equations (2-3) and (2.1) the magnitude of the damping force can be expressed as:

$$F_D = f^2 C \dot{u}^\alpha = C_0 |\dot{u}|^\alpha \text{sgn}(\dot{u}) \quad (2-4)$$

The new damping coefficient  $C_0 = f^2 C$  has an important impact on the damper force. The magnification factor depends on the configuration of the bracing system. This damper force is applied to the structure to mitigate the external forces exerted on the structure. Several strategies can be used in the semi-active control and regulation. One of the most practically available parameter is the acceleration which can be measured easily by the accelerometers.

The accelerations at the ending points of the damper where it is attached to the tower are measured. The corresponding velocities can be attained by integration of the measured accelerations at the ends of the damper. The damper force is then obtained using the velocities and damping coefficient and then applied to the attached points of the damper and tower. The damper behaves as a passive device if a fixed and constant damping coefficient is assumed. The damping coefficient, however, can be provided to the controller as a lookup table which is calculated and scheduled based on the external or operating conditions. For such a damper, it acts semi-actively as an optimal damper force is applied for each situation. In this study, however, a constant damping coefficient is chosen at all wind speeds. In the next section, the results of two innovative concepts in the load reduction of the foundation will be shown.

### 2.3 Design Load Verification

In this section, the results of the load verification with the integration of two discussed innovative concepts are discussed. Figure 2-4 and Figure 2-5 demonstrate the DELs of the tower base moment in the fore-aft (My) and side-to-side (Mx) directions, respectively. Mx and My are represented in the global coordinate system with X and Y axes pointing towards the north and west, respectively, when nacelle is faced to the inflow wind. It should be mentioned that these results are only for one set of load setup where the wind-wave misalignment angle is zero. The influence of the TMD is not significant in the fore-aft direction, especially near the rated wind speed, while the TMD can effectively mitigate the fatigue loads in the sideways direction.

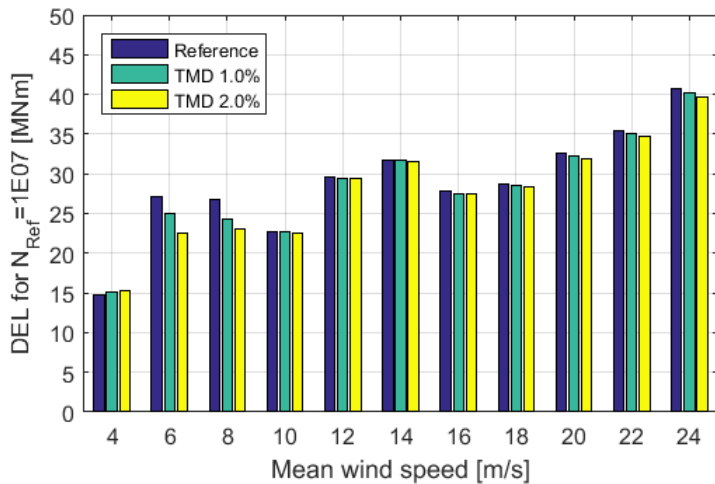


Figure 2-4: DELs of the tower base moment in fore-aft, My, direction for different mass ratios of the TMD

This is in agreement with findings of Kuhnle (ref. /7/) where it has been shown that the DELs can be improved by the application of a tuned mass damper at the tower top location. In addition, the application of the tuned mass damper is more effective for the sideways direction which is due to the low aerodynamic damping in this direction. The aerodynamic damping is the dominant phenomenon in the fore-aft direction and therefore the performance of the TMD is marginal in this direction. Except for DELs in the fore-aft direction in a region around the rated wind speed, the TMD effectively dissipates side-to-side loads in the whole operational range.

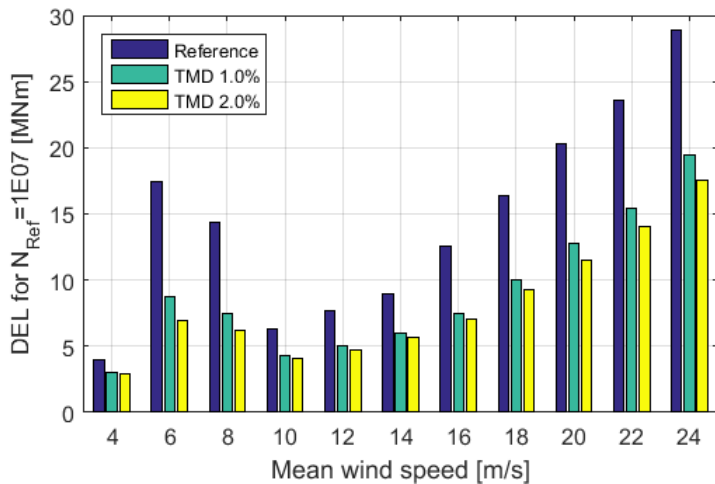


Figure 2-5: DELs of the tower base moment in sideways, Mx, direction for different mass ratios of the TMD

The maximum reduction of DELs occurs in the sideways direction with a TMD with the mass ratio of 2% at the wind speed of 6 m/s which corresponds to a 60% reduction with respect to the reference turbine configuration. The lifetime weighted equivalent loads of the tower base moments for the reference turbine and integrated TMD are demonstrated in Figure 2-6. The values are normalised with respect to the fore-aft DELs for the reference turbine. This can be concluded that the DELs are improved for the integrated design.

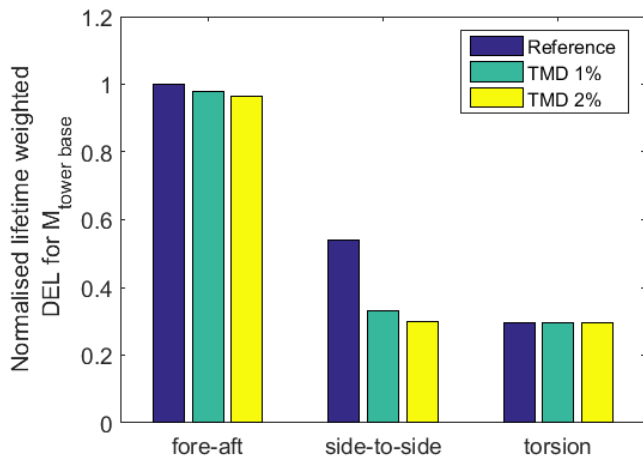
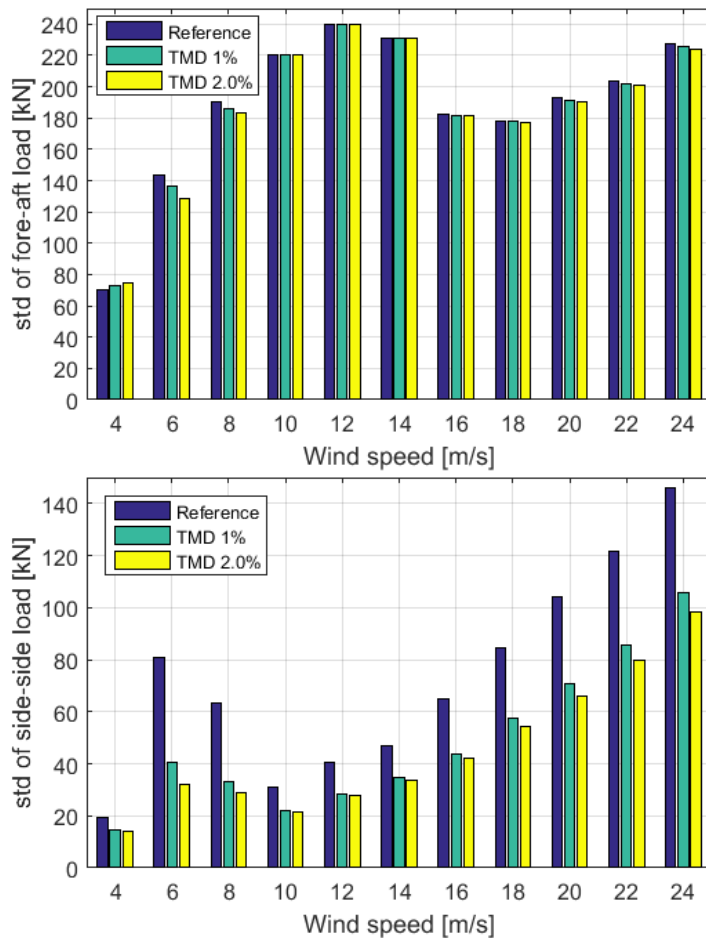
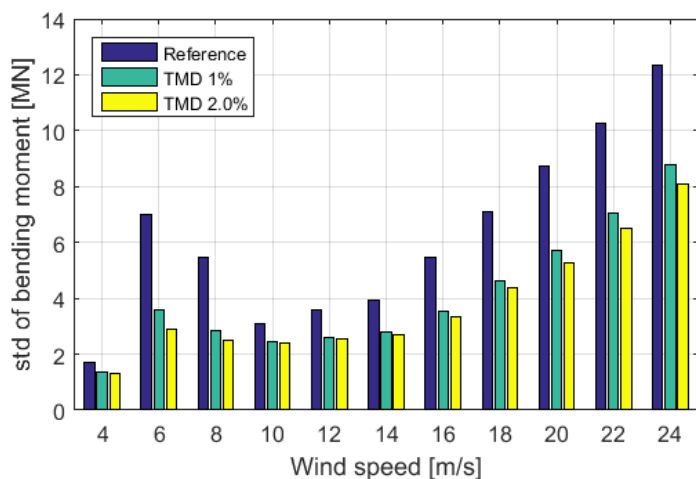


Figure 2-6: Lifetime weighted DELs of the tower base moments for different mass ratios of the TMD

For design purposes, the load comparison of the old and new interface loads is helpful. The reduced interface loads and moments improve the new jacket dimensions designed by the foundation designer. The tower base standard deviation of the interface loads in the fore-aft and sideways directions and the fore-aft moments for the DLC 1.2 are shown in Figure 2-7. Similar to DELs, the forces and moments are significantly reduced in the side-side direction. The new improved loads and moments are considered in the optimisation and refining the improved jacket which is designed by Ramboll.



(Figure continuous on next page)



**Figure 2-7: Comparison of the tower base loads and moments for the reference and innovative design**

As explained in the last section, the second innovative concept is a viscous damper installed at the tower top location. Three diagonal viscous dampers with 120° phase shifting i.e. 0° towards north, 120° and 240°, are considered. The model of the viscous damper is created in Simulink and is called through an external controller at every time steps. During a preliminary analysis, the damping coefficient of the viscous damper is increased step by step and the displacement of the nacelle is monitored to realize the situation with the maximum vibration dissipation. The Bladed simulations are carried out according to DLC 1.2 with the viscous damper integrated in the reference turbine.

A typical time interval of the nacelle displacements in the fore-aft and side-to-side directions are demonstrated in Figure 2-8. It is obvious that the tower top vibration, especially in the sideways direction, is greatly dissipated compared to the reference wind turbine.

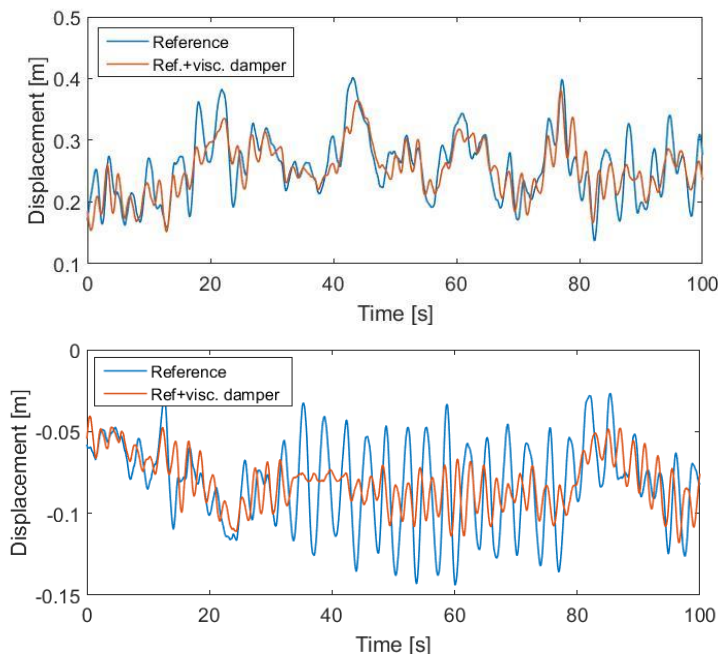


**Figure 2-8: Nacelle displacement in the fore-aft (up) and side-to-side directions at wind speed of 12 m/s**

The tower base DELs of the bending moments in the fore-aft and sideways directions are plotted in Figure 2-9 and Figure 2-10, respectively. It should be noted that these plots are for a load setup where the wind-wave misalignment is zero. It can be seen that the DELs are remarkably decreased in both directions. The maximum load reduction, i.e. around 69%, occurs in the sideways direction at the wind speed of 6 m/s. In addition, the lowest loads reduction occurs near the rated wind speed where the highest variations of aerodynamic forces happen.

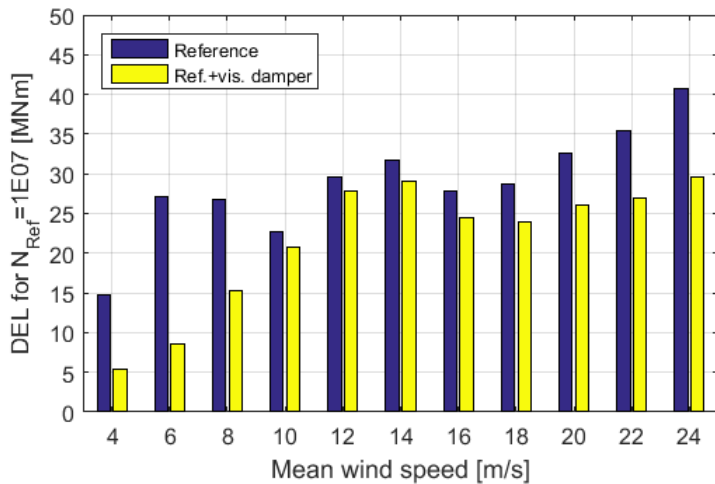


Figure 2-9: Tower base moment DELs in the fore-aft direction with integration of a viscous damper

Although these results are calculated only for one wind-wave misalignment angle, the interface loads and moments calculated for the full load setup are most likely result in optimized jacket geometry.

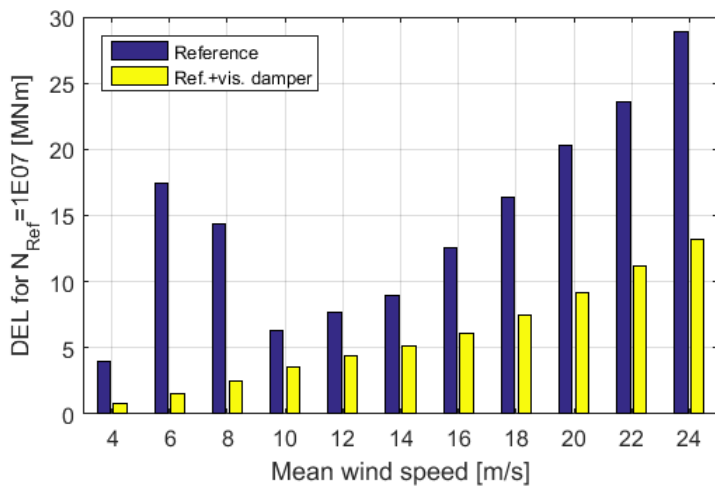


Figure 2-10: Tower base moment DELs in the side-to-side direction with integration of a viscous damper

## 2.4 Conclusions

This chapter presents the results of the integration of two innovative concepts in the 10MW INN WIND.EU reference wind turbine. These two innovative concepts are: a passive TMD and a diagonal viscous damper. The improved interface loads are obtained and compared with the reference turbine and considered in the design of the new jacket.

The major contributions and conclusions of this work are:

- It can be concluded that for the load setup where inflow wind is aligned with the wave direction, the DELs in the sideways direction, where no aerodynamic damping is active, can be lowered up to 29% and 59% compared to the reference case for respectively a TMD and viscous damper. In this condition, the impact of the TMD in the fore-aft direction is however not significant while the viscous damper gives remarkably lowered loads in both directions.
- The integration of the innovative concepts could have a positive impact on the lifetime of the system. The integration of the developed innovative concepts could be considered for an optimized jacket design with reduced entire mass and applied loads for the INN WIND 10 MW reference wind turbine.

### 3 IMPROVED STEEL JACKET DESIGN

#### 3.1 Design Methodology

##### 3.1.1 General

The final design of the innovative jacket for the 10MW wind turbine is given in subsequent chapters. The applied methodologies for the design load calculations and design assessment are the identical to the reference jacket, ref. /1/. The governing standards are the IEC 61400-3, DNV-OS-J101, DNVGL-RP-005 and NORSOK N-004 see ref. /2/, /3/, /4/ and /5/ accordingly. All in all this ensures comparability between the baseline jacket design and the new jacket design including innovations from the work packages.

The design optimization of the reference jacket is elaborated based on the following analyses:

- Natural Frequency Analysis (NFA)
- Ultimate Limit State (ULS)
- Fatigue Limit State (FLS)

Transport, Vortex induced vibrations boat impact and grouted connections are neglected.

##### 3.1.2 Natural Frequency Analysis

The natural frequency analysis (NFA) is carried out to determine the natural frequencies of the integrated foundation and wind turbine structure. The objective is to ensure that the natural frequencies of the overall structure comply with the allowable frequency band specified by the turbine vendor. The first natural frequency of the integrated system is determined based on a soft and stiff configuration. The parameters for marine growth thickness, corrosion allowance, water levels, soil profiles and scour are adapted to account for these conditions. Characteristically, for jacket support structure the bandwidth between these two configurations is rather low. Hence, the natural frequency can be adapted easier and more efficient by changing the tower stiffness than the jacket stiffness.

##### 3.1.3 Ultimate Limit State

The purpose of the extreme event analysis is to ensure that the jacket structure is capable of supporting the WTG for the least favourable combination of environmental load conditions. The ultimate limit state (ULS) analysis is conducted for both characteristic and design soil conditions. Full corrosion allowance, maximum marine growth, varying water levels, extreme waves, extreme currents, extreme wind loads and appropriate load safety factors according to /2/ are considered. A calculation of SLS criteria such as permanent rotation is neglected, which is seen not design driving for jackets; it can be a requirement from the wind turbine and influences pile penetration.

The ULS design criterion for steel members is to keep the maximum member utilization ratio equal to or below 1.00, with this value being the ratio of the actual design stress in the member divided by the design material yield strength.

The extreme event analysis uses partial safety factors to determine the design loads. Normal loads (N) and abnormal loads (A) are considered in the ULS. In case of the pile-soil utilization check, gravity and buoyancy loads are considered unfavourable for the piles under maximum compression and favourable for the piles under maximum tension.

**Table 3-1: Partial safety factors for loads, according to /2/**

ULS partial load safety factor, $\gamma_f$				SLS, $\gamma_f$
Type of design situation			Favourable permanent loads <sup>1)</sup>	
N Normal	A Abnormal	T Transport and erection	All design situations	
1.35	1.10	1.50	0.90	1.00

<sup>1)</sup> Favourable gravity or buoyancy loads if significantly relieve the total response

### 3.1.4 Fatigue Limit State

The foundations have been designed to fulfil the DNV recommended practice, ref. /4/. The design has been performed with a target operational lifetime of 25 years and two additional years for installation and decommission. The fatigue analyses have been performed characteristically, but a Design Fatigue Factor (DFF) of three (3) has been applied for design purposes. This allows the design to survive without any service inspection. Thereby, if the target lifetime is 27 years, a design life time of 81 years is required.

The fatigue damage is determined using an S-N curve approach combined with appropriate stress concentration factors, SCFs, which consider the change in thickness and transitions between cylindrical- and conical sections and tubular joints by joint classification according to Efthymiou, /9/. An overview of the applied SN-curves is given in Table 3-2.

**Table 3-2: Applied SN-curves for FLS**

	Description	S-N Curve		Valid for
		In and below splash zone	Above splash zone	
1	Element Fatigue	DNV-D-W	DNV-D-A	Circumferential welds welded from both sides
		DNV-F-W	DNV-F-A	Circumferential welds welded from one side on a temporary or permanent backing strip without fillet welds
2	Tubular Joints	DNV-T-W	DNV-T-A	Circumferential welds welded from both sides
3	Attachment fatigue with SCF	DNV-D-W <sup>1)</sup>	DNV-D-A <sup>1)</sup>	Internally and externally
4	J-tube hole fatigue with SCF	DNV-B2-W <sup>2)</sup>	DNV-B2-A <sup>2)</sup>	Internally and externally

<sup>1)</sup> With appropriate SCF=1.61 as determined by FE analysis

<sup>2)</sup> With appropriate SCF=2.50 as determined by FE analysis

### 3.1.5 Design Assumptions

The general layout of the jacket has been maintained, which means that the jacket has four legs and four levels of X-bracings. The water depth is 50mMSL. Reducing the number of braces and legs has been studied in additionally. The aim was to reduce the surface area which is prone to wave action and thus reduce the loading on the structure. The jacket for this site is mainly driven by wind turbine fatigue loads and less by the wave action, which limits the intended effect.

The bottom elevation of the transition piece is determined by the maximum wave crest, sea level rise and an additional safety air gap. According to the reference design the lower elevation is approximately 17.8m and finally defined to 18m. The transition piece design height is 8m, which is considered to be the minimum height and results in a width to height ratio of approximately 2:1. The interface elevation between WTG tower and transition piece is therefore 26m.

The boundary conditions regarding soil, marine growth, corrosion protection systems, secondary steel elements and water levels is in accordance with the site conditions used in the reference jacket design, ref /1/. Secondary steel on the foundation structures is included in the analyses by applying appropriate wave areas, volumes, masses and stress concentration factors. Marine growth, shielding and blocking of nearby members are also considered for the appurtenances. They attract wave loads and increase the inertia of structure, but do not contribute to the stiffness of the model. Marine growth of 100mm is taken into account between -40mMSL and +2mMSL. The corrosion protection system is a combined system of anodes, coating and corrosion

allowance. The coating lifetime is assumed to be 15 years in the splash zone, after this time an external corrosion allowance of 0.3mm/year is taken into account. Internal corrosion is not considered. The water level range is between 3.29mMSL (highest still water level) and -2.37mMSL (lowest still water level). The secondary steel components are not part of the design. The dimensions are based on experience from other commercial projects in order to consider the additional loads on these structures. The following items of secondary steel are taken into account:

- One boat landing (inclusive two bumper and sea access ladder)
- Rest platform
- Upper access ladder
- TP flange
- Anodes
- Two external J-tubes for caballing

The tubular members of the jacket are based on standardized diameter and wall thickness, where possible, to ensure a cost-efficient design. Usually steps of full inches are used for diameters of the piles, jacket leg and braces. Wall thickness increments of 1/4th inch are mainly considered. For reasons of optimisation individual sections have smaller increments of 1/8th inch. The design is considered to yield an estimate of the overall layout, dimensions and masses of the jacket, pile and transition piece. These are:

- Cross sections of legs
- Cross sections of braces
- Layout and node coordinates
- Pile geometries
- Wall thicknesses
- Mass of jacket, piles and transition piece

### 3.1.6 Integrated Load Simulation Approach

The design loads are based on sequential integrated wind turbine and foundation analyses with exchange of superelements and interface loads. The jacket design calculations are based on force time series instead of simplified damage equivalent loads. In a first step a superelement of the initial reference jacket has been derived and implemented in the wind turbine load simulation. The design load cases are performed and the interface forces at tower bottom are saved for the subsequent jacket design. These interface forces (in the present case as wind-only loads) are combined with the wave loads from wind-correlated sea states. The stresses in the jacket members are calculated and further processed in the post-processing for ULS and FLS design checks. Figure 3-1 illustrates the load simulation method between the foundation designer and wind turbine designer to calculate the design loads.

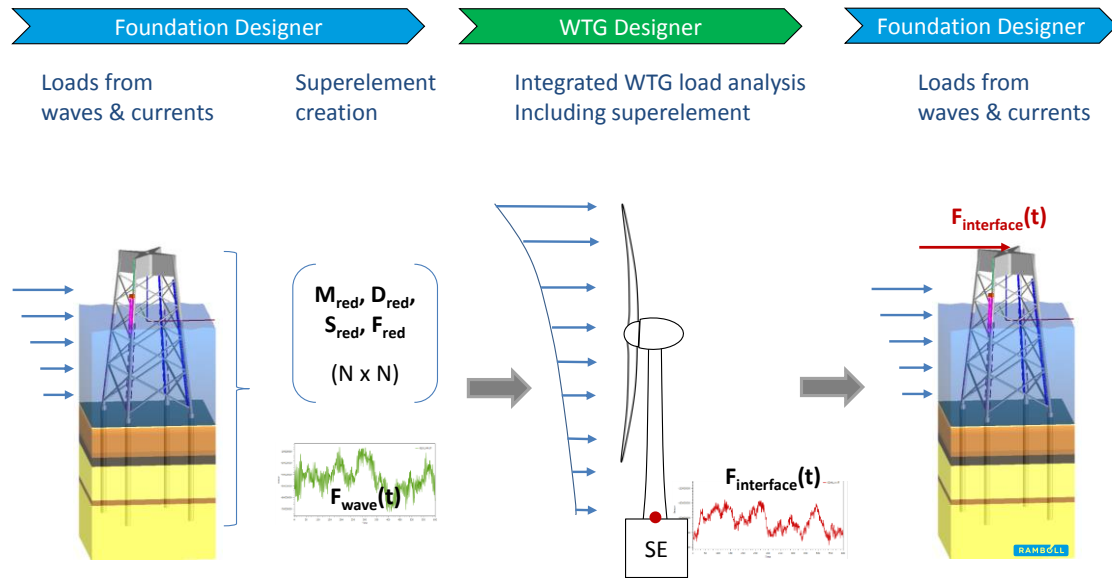


Figure 3-1: Load iteration for support structure design

The integrated models used by the foundation designer and WTG designer have to be compared by means of modal properties of the models. This means that the NFA results of the full system should agree. However smaller differences will be present as the foundation design tools use a simplified model of the rotor-nacelle-assembly in the NFA calculations. The flexibility of the rotor is not captured in this model.

### 3.1.7 Damping Model

The support structure damping is based on Rayleigh damping parameters. This means that stiffness and mass proportional damping is considered, with the following relation:

$$C = \alpha M + \beta K$$

The Rayleigh coefficients  $\alpha$  and  $\beta$  are calculated from the critical damping values  $\zeta_{1/2}$  defined for the first and second natural frequencies  $\omega_{1/2}$ . The following calculations are performed:

$$\alpha = \frac{2\omega_1\omega_2}{\omega_2^2 - \omega_1^2} * (\zeta_1\omega_2 - \zeta_2\omega_1) \quad \text{with } \omega = \frac{2\pi}{T}$$

$$\beta = \frac{2(\zeta_2\omega_2 - \zeta_1\omega_1)}{\omega_2^2 - \omega_1^2} \quad \text{with } \omega = \frac{2\pi}{T}$$

The critical damping  $\zeta_{1/2}$  for the jacket foundation is assumed to be 0.7% (i.e. 4.4% logarithmic decrement). The corresponding eigenperiods of the offshore model are given in the NFA results, refer to Chapter 3.4.1.

The superelement of the jacket contains the appropriate damping parameters.

### 3.1.8 Soil Properties

The soil is modelled using P-y, T-z and Q-w curves. The curves are derived from a defined soil profile, which is the same as for the reference jacket design. The profile is given in Appendix C – Soil Profile.

### 3.1.9 Load Cases and Load Combinations

The design load cases used in the reference design are taken over, which are based on the IEC 61400-3 guideline. This ensures comparability of the reference design with the innovative design results. A short summary of the design load cases is given below. More detailed information can

be found in Appendix 5 in /1/. The selected load cases are a subset of design load cases. In a detailed design thousands of load cases are to be considered.

The jacket will be considered for a number of different load combinations to produce the most severe loading on the structure. The following basic loads are considered:

- Gravitational and inertial loads
- Aerodynamic loads: Wind loads
- Hydrodynamic loads: Wave and current loads
- Hydrostatic buoyancy loads

For **ULS** the DLC 2.1, 2.3, 6.1 and 6.2 are taken into account with 6 directions (half-cycle with 6 sectors and 30° steps) to determine the governing wind loads at interface elevation. The extreme load cases for maximum bending moments and for maximum torsion are found and subsequently combined with the appropriate wave loads for the jacket design calculations. The following parameters have been considered when simulating the loads:

- 6 load directions
- 1 wind speed
- Yaw errors of -8°, 0° and +8°
- 6 seeds per scenario
- Randomly varying seeds
- Extreme waves with recurrence period of 50 years
- Wind, wave and currents are aligned

For **FLS** the DLC 1.2 & 6.4 are taken into account directional with a full cycle having 12 sectors and 30° steps. The following parameters have been considered when simulating the wind loads:

#### DLC 1.2

- 12 load directions
- 11 wind speeds (4, 6, 8, 10, 12, 14, 16, 18, 20, 22 and 24 m/s)
- Yaw error of -8°
- 2 seeds per scenario
- Randomly varying seeds
- Wind correlated random sea states based on JONSWAP spectra
- A total of  $12 \cdot 11 \cdot 1 \cdot 2 = 264$  cases

#### DLC 6.4

- 12 load directions
- 2 wind speeds (2 and 30 m/s)
- Yaw error of -8°
- 2 seeds per scenario
- Randomly varying seeds
- Wind correlated random sea states based on JONSWAP spectra
- A total of  $12 \cdot 2 \cdot 1 \cdot 2 = 48$  cases

### 3.1.10 Superelement of the Jacket Model

Several methods exist for reducing the size of structural models by condensation of a number of degrees of freedom (DOF) from the system or subsystem under consideration. Hereby, the dimensions of system matrices as well as load vectors are reduced, allowing for faster analyses and facilitates efficient load and data exchange processes. This reduced system is often denoted as superelement.

The initial superelement of the jacket is derived from the static reduction method according to Guyan's approach. The overall jacket and foundation model is represented by 6x6 reduced mass, damping and stiffness matrix as described in the reference jacket model, ref. /1/. The conserved master node is the interface node at TP-tower intersection. This superelement is applied in the first load iteration with the 10MW INN WIND.EU reference wind turbine to determine the interface loads being applied for the innovative jacket design.

A more advanced superelement including local modes of the innovative jacket will be calculated and appended to this report, see Appendix A – Jacket Superelement. It is a significant improvement for the accuracy of dynamic problems and can be applied in subsequent WTG load iterations. A Craig-Bampton superelement, ref /6/, reduced to 36 degrees of freedom (DOF) is derived. It has six physical DOF, representing the interface node at the TP–tower-interface and further 30 internal DOF, which are modal degrees of freedom. The number of internal modes to be considered depends on the exciting frequencies of the loads. Each mode correlates with a certain natural frequency. The number of modes should be large enough to capture the relevant exciting dynamic loads. It is possible to consider all modes in the superelement, however this would be only a transformation without reduction of DOF.

The transformation matrix  $T$  of the original jacket model according to Craig-Bampton is based on the model matrix  $\Phi_{ss}$  and the stiffness matrix relation of master and slave DOF, index  $m$  and  $s$  respectively. The modal matrix is found from the eigenvalue solution of the undamped equations of motion. The model matrix contains only the selected number of internal eigenvectors (i.e. 30) of the jacket subsystem and is sorted ascending after the natural frequency.

$$T = \begin{bmatrix} I & 0 \\ -K_{ss}^{-1}K_{sm} & \Phi_{ss} \end{bmatrix} \quad \text{with } I = \begin{bmatrix} 1 & \dots & 0 \\ \vdots & \ddots & \vdots \\ 0 & \dots & 1 \end{bmatrix}$$

The reduced mass, stiffness and damping matrix are then obtained by matrix multiplication of the transformation matrix with the original system.

$$M_{red} = T^T M T, \quad C_{red} = T^T C T, \quad K_{red} = T^T K T, \quad F_{red} = T^T F$$

### 3.2 Review of Component Innovations

Different innovations for jacket type support structures have been developed and assessed in Task 4.1, ref. /7/ and /8/. The component innovations can be classified into four categories, which are shown in Figure 3-2: manufacturing, materials, soil and foundation and load reduction.

All innovations from the material category are not considered in the steel jacket design. Those innovations consider sandwich material for braces and joints, which will be part of the hybrid jacket of Deliverable 4.35.

The soil and foundation innovation consider vibro-driven piles, semi-floater and suction bucket foundations, whereas only the vibro-driven piles and buckets can be applied to the jacket. However, the foundation of a jacket is mainly loaded by axial tension and compression loads, which finally lead to optimizing the penetration length of the piles or the length of the bucket skirt to ensure sufficient soil bearing capacity. On the other hand the foundation of the jacket has only minor effects on the design of the jacket itself. The major improvement of the innovations from soil and foundation can be found in reducing installation costs. The positive cost effects are from lower noise emission during installation, thus cheaper equipment costs, and faster installation.

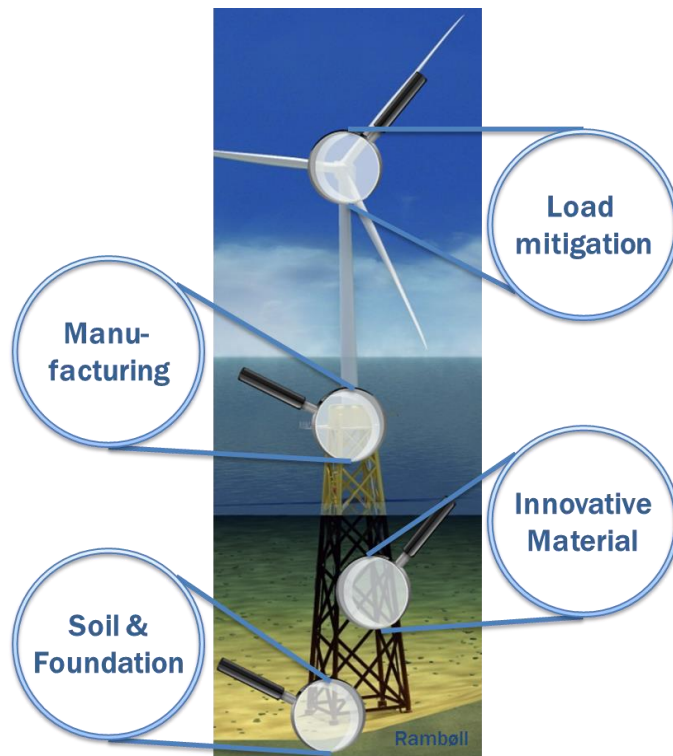


**Figure 3-2: Component innovations from Task 4.1 for jacket support structures**

The innovations from manufacturing consider the optimized transition piece (TP), which is shown in Figure 3-3, and an improved layout of the jacket. Both have been iterated for the final innovative jacket design. The width of the new TP is adapted to the new jacket top width. The overall TP mass is increased and results in approximately 258 tons. The initial TP design study of Task 4.1, based on the dimensions of the reference jacket, had a mass of 211 tons (ref /7/).

The assembly strategies of the jacket can improve the fabrication costs significantly and the studies showed up to 20% lower costs, ref /7/. The tubular elements are continuous from joint to joint and thus become heavier than required, while the number of welds is reduced dramatically for efficient assembly. Unfortunately the assembly-optimized jacket has a negative effect on the fatigue damage and it was not possible to fulfil the FLS criteria under the given design conditions. Stronger local deflection in the braces occur which increases the damage in the joints. It has been found that the jacket elements need individual adapted geometry to fulfil the design criteria, which is contrary to the aims of assembly strategies for mass production and prevents the application for the innovative design update.

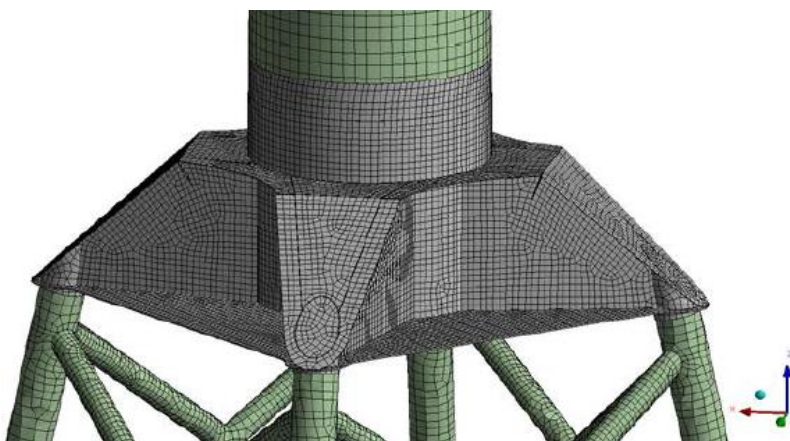


**Figure 3-3: Innovative TP design**

Significant improvement can be achieved by load mitigation. The improvements from the rotor blade innovations, damping system and control strategies for load mitigation have strong effect on the overall support structure design.

An innovative blade design from WP2 has been implemented in the innovative wind turbine model and a load calculation study has been performed for different configurations of the offshore wind turbine. The fatigue loads have been reduced up to 8%. The results are shown in Figure 3-4.

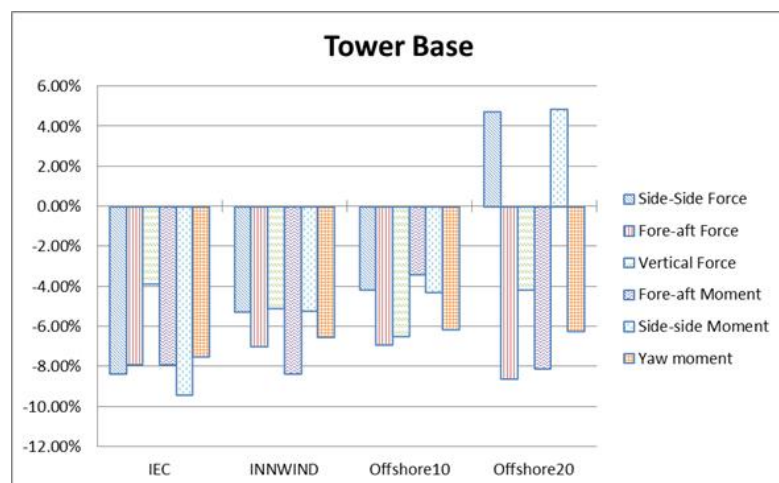


Figure 3-4: Fatigue load reduction (DEL) at tower base by innovative rotor blades.

The vibration absorber mounted in the near of the tower bottom showed its potential to reduce the governing loads, but at the same time increases the complexity, installation effort and production costs. The concept is currently not applicable due to design space requirements and the fixation of the heavy vibration absorber is seen problematic. The current offshore concept has only a small air gap of 3.8m between blade tip and TP top.

The tower mass damper can be included which adds an additional weight of 0.5% of the modal mass of the fundamental support structure frequency, i.e. approximate 4.3 tons have to be taken into account for the reference design. The load mitigation effect varies between the different load components. Load reduction of the sidewise bending moment at the tower base up to 25% has been achieved. The negative effect on the CAPEX and maintenance should be compensated by the savings in other components. Such systems are considered to be robust and to be easily and cheap to maintain.

Active load reduction technology has been implemented for the reduction of the thrust around rated wind speed by the so called Peak Shaver. The effect of the Peak Shaver is a trade-off between load mitigation and capacity factor.

Tower damping in fore-aft directions by active collective pitch control or individual pitch control has been suggested. Tower damping in sideways direction is suggested by usage of individual pitch control and generator control. However the controller innovations (functionalities) have not been applied in the design load calculations directly as the implementation could not be incorporated into the integrated wind turbine model together with the other innovations due to compatibility reasons. Further work on the transition of innovations developed with high fidelity models to integrated and more robust models, which can be used in design purposes, is required.

The following innovations have been considered to improve the reference jacket design:

- Load mitigation from RNA innovations aiming on reduction of fatigue loads
- Optimized transition piece with improved load transition into the jacket
- Jacket layout and geometry optimization
- Vibro-driven piles

### 3.3 Computer Model

#### 3.3.1 Design Tools

The support structure design is made with the computer software ROSAP. It is developed by Ramboll as a tool to solve the problems commonly arising in analyses of fixed offshore steel platforms. During recent years the program package has been extended to solve problems regarding offshore wind turbine support structures. In this project ROSAP is used to design the jacket structure.

ROSAP is a software package consisting of various tools, which consider the governing standards for the design of offshore structures:

- WAVGEN = wave kinematics program
- ROSA = Static and dynamic analysis of space frame structures
- STRETCH = Member stress check
- TUBJOI = Punching shear check of joints
- PILMAX = Soil-pile bearing capacity checks
- FATIMA = Fatigue analysis program
- FATCOM = Fatigue damage combination program
- PREBOM = Pre-bill of material and intersection analysis

#### 3.3.2 Support Structure and Foundation

A general view with the conceptual main dimensions is shown in Figure 3-5. The leg and brace elements are modelled with non-linear beam-elements. Most parts are made of tubular cross sections using standardized sizes for diameter and wall thickness. Conical transition sections placed at the legs and some design critical brace ends. Can and stubs are used to strengthen the tubular joints. An additional mudline brace is avoided in the model. K-, Y- and X-joints are used to connect the braces and legs. Local joint flexibilities are considered to improve the flexibility of the connections.

The jacket is supported by pre-installed piles. The grouted connection between the piles and the jacket is approximated as rigid link. A more sophisticated FE analysis should be used in detailed design to optimize the overlapping length. However, it has limited effect on the jacket itself. Pile elements are used for the part of the structure below mudline, which allows for modelling of non-linear pile-soil interaction based on the P-y, T-z and Q-w soil load-deformation curves. The design considers scour effects around the piles. Additional scour protection is not required.

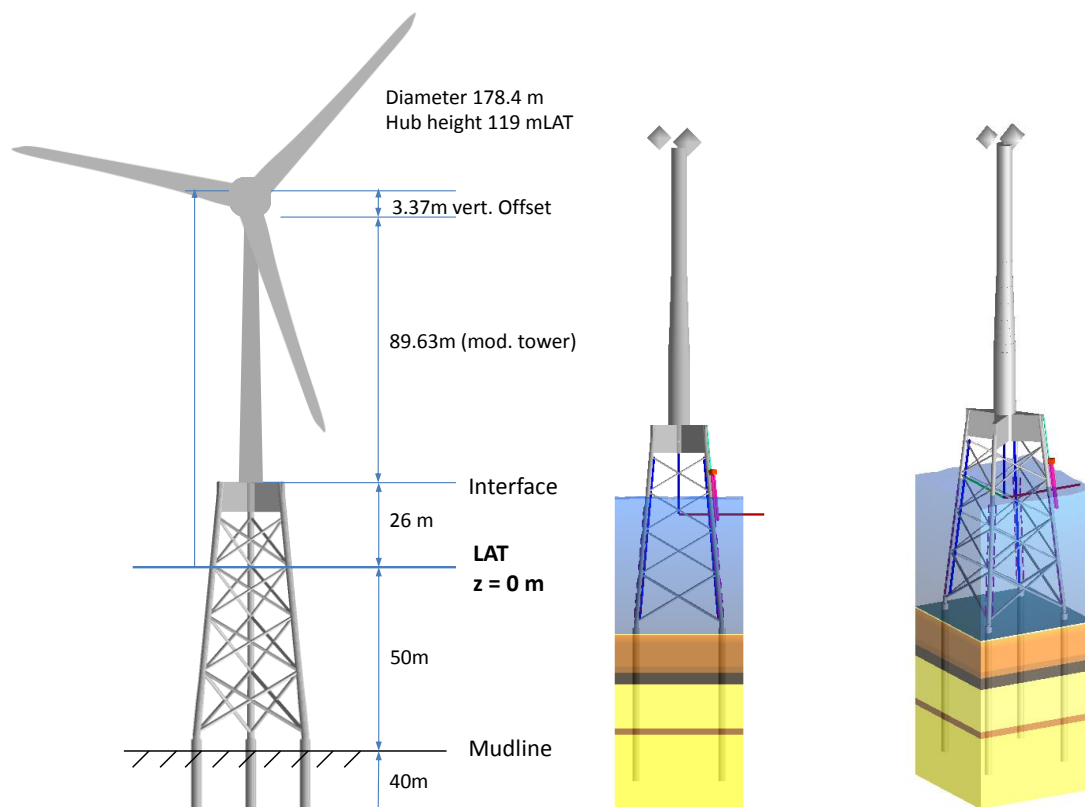


Figure 3-5: Concept drawing (left) and jacket model in ROSA (right)

Attached appurtenances (e.g. boat landing, etc.) are modelled as point masses or distributed mass, surfaces and volumes. In such way they attract wave loads, but do not contribute to the stiffness of the primary steel structure. Most attachments are welded on the jacket legs. For fatigue analysis an appropriate SN-curve is applied.

### 3.3.3 Rotor-Nacelle-Assembly and Tower

The RNA and tower model is included to accurately determine the dynamic response of the entire structure and to evaluate the natural frequencies. The wave forces induce additional inertia loads on the superstructure which need to be considered in conceptual design approaches of isolated wind and wave fatigue damage. The latter one is not required in case of the sequential integrated load calculation approach, which is also applied in the innovative design (Figure 3-1).

A modified tower of the reference 10MW wind turbine is used. Initially this tower was a land-based tower, which was adapted to the interface heights. Furthermore an optimization due to buckling analysis has been carried out during the reference jacket design, ref. /1/. A drawing of the tower model is given in Appendix B – Tower model.

The wind turbine is approximated by a lumped point with condensed mass and inertias to represent the rotor blades, hub, and nacelle. The estimated properties are given in Table 3-3. These appurtenances are applied eccentrically on the tower top.

Table 3-3: Lumped Rotor-Nacelle-Assembly data

RNA properties at tower top		
Lumped mass	[kg]	676723
Moment of inertia $I_x$	[kgm <sup>2</sup> ]	1.66 e8
Moment of inertia $I_y$	[kgm <sup>2</sup> ]	1.27 e8
Moment of inertia $I_z$	[kgm <sup>2</sup> ]	1.27 e8

### 3.4 Design Results

#### 3.4.1 Natural Frequency Analysis

The natural frequencies of the integrated overall structure are calculated for three different scenarios. The “soft” scenario considers full marine growth, corrosion and highest water level and scour. The “fatigue” scenario estimate realistic environmental boundary condition, such as mean water level, half corrosion allowance and maximum marine growth. The “stiff” scenario represents conditions right after installation to cover the upper bound. Table 3-4 shows the results for the first nine frequencies and Figure 3-6 illustrates the mode shapes of the first five modes and mode nine. The latter one is the first strong local mode where mainly braces are amplified. The frequencies are slightly smaller compared to the reference jacket.

**Table 3-4: Natural frequency results of the full model**

Mode #	Soft	Fatigue	Stiff	Mode
1	0.2625	0.2627	0.2636	1 <sup>st</sup> global bending
2	0.2641	0.2642	0.2651	1 <sup>st</sup> global bending
3	0.9417	0.9428	0.9538	1 <sup>st</sup> torsion
4	1.1864	1.1991	1.3658	2 <sup>nd</sup> global bending
5	1.2084	1.2228	1.4459	2 <sup>nd</sup> global bending
6	1.5996	1.6048	1.8789	3 <sup>rd</sup> global bending
7	1.7137	1.7172	1.9420	3 <sup>rd</sup> global bending
8	1.8442	1.8571	2.4340	2 <sup>nd</sup> torsion
9	1.9283	1.9362	2.4438	Local x-braces

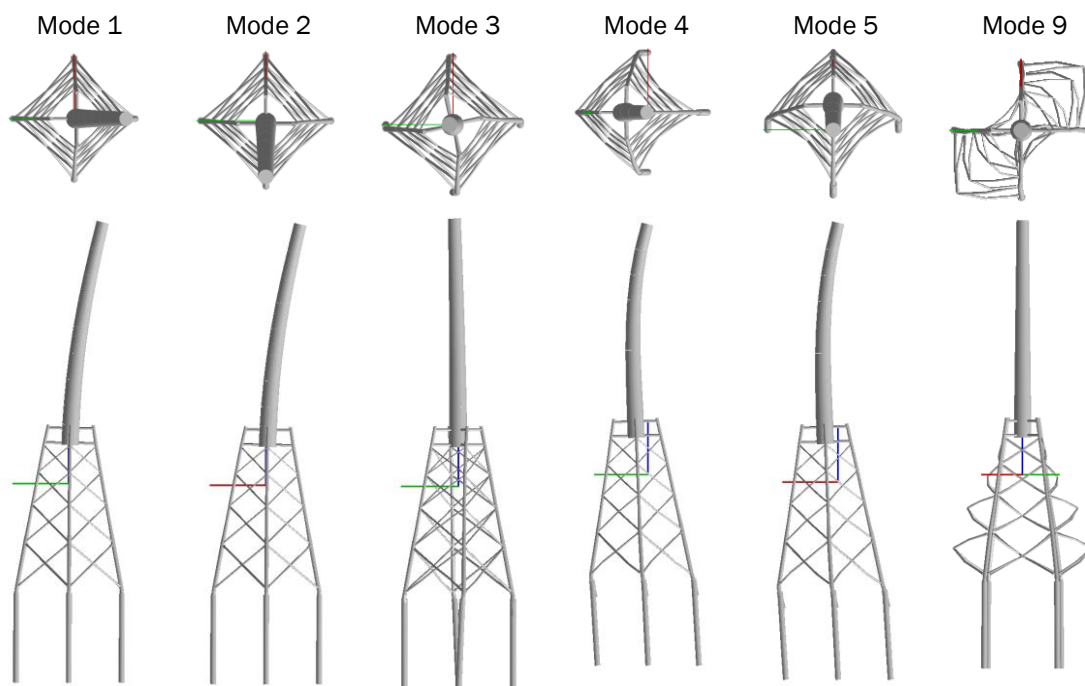


**Figure 3-6: Mode shapes (soil profiles and TP superelement not shown)**

### 3.4.2 Ultimate Limit State

#### 3.4.2.1 Steel Utilization

The design loads are extracted from the design load cases given in section 3.1.9. The governing load sets results from the scenarios with lowest still water level. Table 3-5 shows the maximum wind loads at the tower bottom. This results in more steep extreme waves at this site and in the higher utilization. These wind loads are combined with appropriate wave and current loads. Wind and wave impacting the support structure have been applied from directions parallel to the diagonal of the jacket footprint and perpendicular to the sides of the jacket structure.

The jacket structure has been checked against allowable stresses, loss of stability and punching shear stresses. As can be seen from Table 3-6 and Table 3-7, all utilisation-ratios are below 1.0. It is seen from the utilisation-ratios of the jacket braces, legs and the X-and K-joints that ULS is not governing the jacket design.

**Table 3-5: Maximum design loads for ULS at interface.**

Governing Load Component	DLC	Included Load Factor	V <sub>Res</sub> [MN]	M <sub>Res</sub> [MNm]	M <sub>T</sub> [MNm]
Shear Force V <sub>Res</sub> / Bending Moment M <sub>Res</sub>	2.3	1.10	2.797	255.370	02.395
Torsional Moment M <sub>T</sub>	1.2	1.35	1.141	128.427	49.189

**Table 3-6: Maximum utilization ratios of tubular members**

Component	Utilisation-ratio [-]
Legs	0.84
Braces	0.78
Piles	0.92

**Table 3-7: Maximum utilization ratios of joints**

Component	Utilisation-ratio [-]
X-joints	0.77
K-joints	0.37

#### 3.4.2.2 Pile-Soil Capacity

The pile bearing capacity check is based on design loads from overall ULS calculations and distinguishes for tension and compression scenarios. The design loads are combined with plastic soil conditions, which include further soil strength safety factors for friction, shear strength and axial capacity. The safety factors are 1.15, 1.25 and 1.25 accordingly. The maximum design loads are given in Table 3-8.

**Table 3-8: Pile design loads at pile head**

Scenario	Axial	V Shear	W Shear	Torsion	V bending	W bending
					[kNm]	
Compression	-25633	-5911	-5	-13	5	17994
Tension	16009	4951	-8	-34	-37	-17305

Additionally, a vertical load deflection analysis is carried out to determine the optimal pile penetration length. As shown in Figure 3-7 the bearing capacity is driven by tension scenarios and result in a minimum penetration of 36m, whereas the smallest deflection of the pile head is given for approximately 37m penetration length. The final design considers 38m penetration length to be on the safe side.

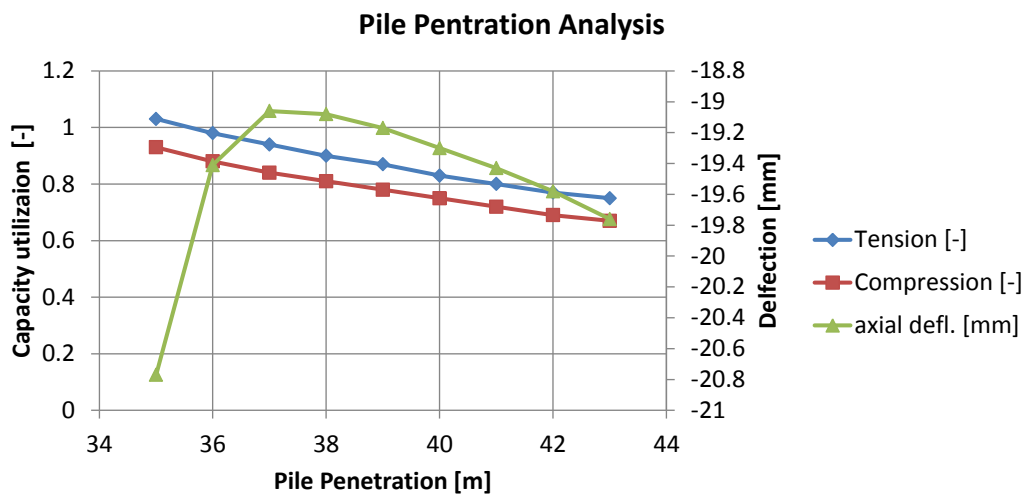


Figure 3-7: Results of pile penetration analysis

### 3.4.3 Fatigue Limit State

The results from the reference jacket design showed possible resonance problems at the lower bound of the 3p rotor frequency. This region occurs at lower wind speeds of 4-6m/s. In order to reduce the resonance excitation the stiffness of the jacket should be lowered. The first natural frequency has been reduced by approximately 7% compared to the reference jacket design of deliverable D4.31, /1/. This can be achieved mainly by changing the width of the jacket top and bottom rather than adaption of individual cross sections. However, a compromise has to be found between reduction of overall stiffness and consequently increasing the stresses in the structure due to the smaller framework dimensions. Finally the layout has been optimized to improve the damage of the critical joints.

The fatigue lives have been calculated for all leg and brace elements, tubular joints, attachment welds and cut-outs. The design lifetime is 81 years (DFF of three times 27years operation, see section 3.1.4). This means that the characteristic hot-spot stresses are used in the damage calculation using the appropriate SN-curves, which ensures correct application of the bi-linear SN-curves. Table 3-9 shows the minimum lifetimes per structural detail. Typically for jacket structures are the low tubular joint fatigue lives, which require wall thickness increase at the stub and can sections. The possible thickness jump to the free tubular member is limited and a thickness transition with gradient 1:4 is considered. The wall thickness optimization is done in steps of ¼ inches, hence the normal butt welds can result in conservative lifetimes. The minimum tubular joint fatigue lives across the jacket are given in Appendix D –Fatigue Lives of Tubular Joints.

Table 3-9: Minimum fatigue life in [years] per detail (design lifetime = 81 years)

Detail	Location	S-N curve	Min. fatigue life	With post weld treatment
2-sided circumferential welds	Legs	DNV-D	130	-
	Piles	DNV-D	>100	-
1-sided circumferential welds	Braces	DNV-F	>100	-
Attachment welds	Legs	DNV-D + SCF	>270	-
J-tube hole	Legs	DNV-B2 + SCF	>350	-
X-joints	Brace to Brace	DNV-T	102	-
K-joints	Brace to Leg	DNV-T	35	>81*

For some welding details of the jacket post-weld treatment by fabrication has to be applied to guarantee the design lifetime. It concerns only some K-joints. The application is possible if the failure mode of cracking is not from the weld root, which is usually the case as the membrane stresses on the inside of the joint or circumferential weld are lower. However this has not been

checked. Typical weld improvements are weld profiling by machining or grinding, weld toe grinding, TIG dressing and Hammer peening. According to DNV recommendations, ref. /4/, the fatigue life can be increased up to a factor of 3.5 for steel material with yield strength higher the 350MPa, which is used also in the current jacket design.

### 3.4.4 Summary of the Jacket Geometry and Masses

An overview of the final main jacket properties and its components is given in Table 3-10. More detailed drawings are given in Appendix E – Geometry of the Jacket. It should be noted that the design changes compared to the reference jacket are significant. This requires further load iterations with the wind turbine before continuing the design optimization in order to ensure accurate interface loads for the present jacket structure. However this has not been achieved in the scope of the project and therefore it can be assumed that further improvements are possible.

**Table 3-10: Design summary of the jacket concept**

Jacket general	Dimensions	Value
Base Width	[m]	33
Top Width	[m]	16
Interface elevation	[mMSL]	26
Transition Piece height	[m]	8
Number of horizontal braces		none
<b>Number of legs</b>		4
Jacket legs outer diameter (upper / lower leg)	[mm]	1422/1828
Jacket legs maximum wall thickness	[mm]	108
Jacket legs minimum wall thickness	[mm]	38.1
<b>Number of x-braces levels</b>		4
Max. Upper x-braces diameters (outer)	[mm]	610
Max. Upper x-braces wall thicknesses	[mm]	31.8
Max. Middle upper x-braces diameters (outer)	[mm]	711
Max. Middle upper x-braces wall thicknesses	[mm]	34.9
Max. Middle lower x-braces diameters (outer)	[mm]	812
Max. Middle lower x-braces wall thicknesses	[mm]	31.8
Max. Lower x-braces diameters (outer)	[mm]	914 / 1168
Max. Lower x-braces wall thicknesses	[mm]	41.3
<b>Number of Piles</b>	[-]	4
Pile penetration	[m]	38
Pile diameter	[mm]	2540
Pile wall thicknesses	[mm]	25.4 - 44.5
Pile top elevation above mudline (Stick-out length)	[m]	1.50
Overlap length (grout length)	[m]	7.5
<b>Mass</b>		
Jacket structure (primary steel)	[t]	1093
Transition Piece	[t]	258
Steel Appurtenances (estimation)	[t]	48
Piles (all)	[t]	342
Grout (estimation)	[t]	125
Total (including grout)	[t]	1866
<b>Natural frequency overall structure</b>		
1 <sup>st</sup> eigenfrequency (1 <sup>st</sup> bending mode)	[Hz]	0.2635

### 3.5 Cost Estimation

#### 3.5.1 Unit Price Approach

The fabricators estimate the costs for fabrication by using lumped unit prices, which depend solely on the mass of the structure. The three main components are individually addressed in such way. These are the transition piece, the jacket and the piles. The lumped prices are mainly based on experience gained during realized projects and might be influenced on current market boundary conditions. The reference jacket and also the INN WIND.EU cost models, ref. /10/, are based on this approach for the cost studies. The unit prices as of 2012 are applied to maintain the comparability within the project. Current market prices are most probably different.

This approach automatically leads to mass optimized structures to reduce the overall costs, although the approach neglects any separation in terms of the type of welding, preparation work and complexity of the structure itself. The cost contributions of the innovative jacket design are compared against the reference jacket design in Table 3-11. Overall a cost saving of approximately -12.2% has been achieved, which is solely a consequence of mass reduction of the components.

**Table 3-11: Substructure fabrication cost estimation based on lumped unit prices**

	Component	Unit costs [€/ton] <sub>2012</sub>	Component Mass [ton]	Sum of costs [€]
Reference jacket design	TP	5000	330	1,650,000
	Jacket	4800	1210	5,808,000
	Driven-piles	1200	380	456,000
	<b>Total</b>			<b>7,914,000</b>
Innovative jacket design	TP	5000	258	1,290,000
	Jacket	4800	1093	5,246,400
	Driven-piles	1200	342	410,400
	<b>Total</b>			<b>6,946,800</b>
<b>Total cost reduction</b>				<b>-12.2%</b>

#### 3.5.2 Advanced Cost Model for Fabrication

##### 3.5.2.1 Description of the Model

A more detailed cost model has been applied to address more precisely the fabrication cost shares of the jacket primary steel. It considers the main cost contributors by addressing raw material of steel, welding, coating and assembly (Figure 3-8). The reference jacket design and the innovative jacket design are analysed with the same assumptions for each cost contribution. This ensures a fair comparison and results in a more accurate cost reduction potential. Secondary steel is neglected as it is very similar between both designs.

The transition piece cost comparison only considers the material costs for the steel pipes or plates as well as the welding costs with respect to welding length and welding volume. Any further costs, e.g. coating, secondary steel items or equipment are not considered. However, since the primary steel is governing the overall TP costs, this is deemed a sufficient approach in order to evaluate the cost differences between the reference TP and the innovative TP design.

The TP material costs are calculated based on internally available (however confidential) unit values [€/ton] depending on the wall thickness of each plate or tubular part. For the welding costs a constant unit value [€/cm<sup>3</sup>] has been applied based on Ramboll's internal data.

The foundation pile elements are joined together by automated welding and as such are mass-production components. Due to the large experience with these structures it can be assumed that the lumped unit price [€/ton] is suited to compare the costs, which means that the pile fabrication costs are still driven by its mass.

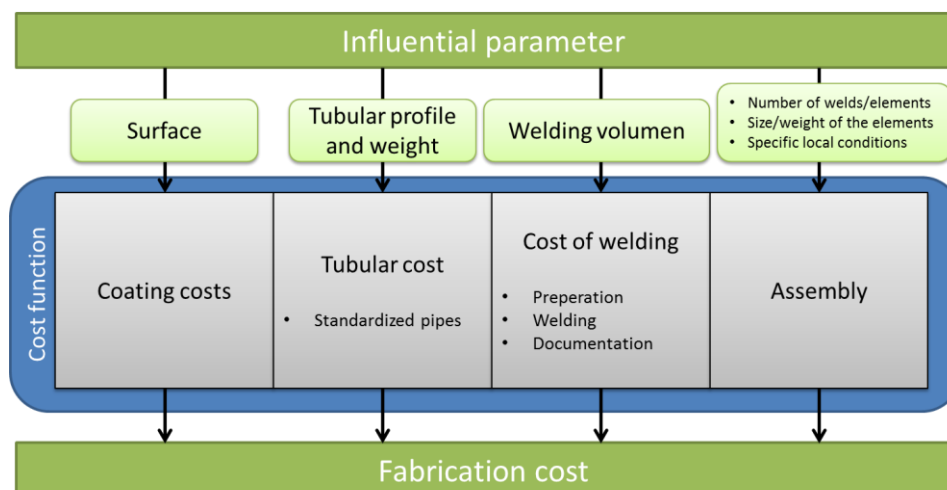


**Figure 3-8: Structure of the fabrication cost model**

#### Costs of tubular members

The costs for tubular members consist of their material and processing costs. Different tubular cross-sections cause different processing costs due to different manufacturing processes, e.g. due to standardize or individual manufacturing. Consequently, each tubular cross-section has a specific cost factor depending on its dimension and manufacturing characteristics. Hence, the tubular cost of each pipe is the product of its weight and a specific cost factor.

#### Coating costs

Coating is for protection from corrosion and depends on the surface area of the jacket. Coating cost is the smallest share of the fabrication costs and remains virtually unchanged by varying the geometrical parameters.

#### Cost of welding

Cost of welding includes the preparation of the welds, the welding, the documentation and the man hours. This cost depends on the welding volume and the welding process. A special distinction must be made between manual and automated welding. Automated welding is less expensive than manual welding, but not every weld can be performed by automated welding. The costs of welding are generally of the same order as the costs for the tubular members. In order to quantify the welding costs, cost factors are introduced which are multiplied by the volume of the respective weld.

#### Assembly costs

Special attention must be paid to the assembly costs. Assembly costs mainly depend on the number of tubular members to be welded. Furthermore there are dependences on the specific local conditions (e.g. size of the assembly hall, location of the assembly hall). The calculation of this cost – which is only indicative - is based on the fabricator's experience.

### 3.5.2.2 Results

The cost distribution of the reference jacket and the innovative jacket are given in Figure 3-9. It can be seen that the cost distribution has changed and finally a total costs reduction of -5.4% has been achieved with this cost model, although the jacket mass reduction is approximately -9.7%. Which clearly points out that a mass optimization of a structure does not necessarily reduce the overall costs of a jacket. This is a consequence of the layout optimization to reduce the fatigue damage to guarantee a sufficiently safe design. Standard tubular pipes have been substituted by non-standard pipes at the lower part of the jacket, which make the material contribution more expensive. Also the overall width of the jacket is different, which affects the length of braces. Furthermore the welding volume of some nodes is higher of the innovative jacket and the increased costs could not be compensated by the reduced number of normal circumferential butt welds.

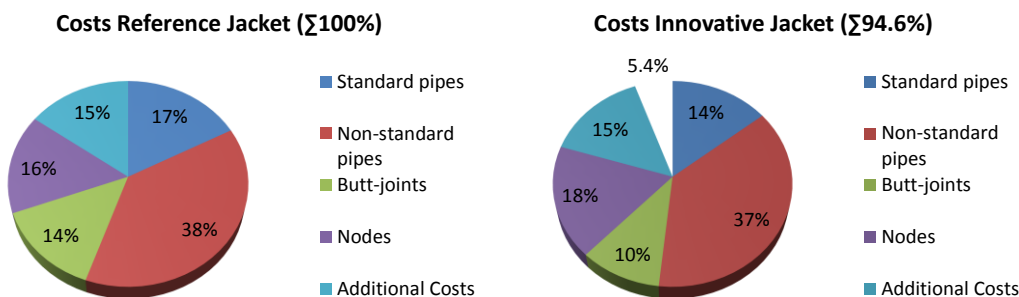


Figure 3-9: Comparison of cost distribution, only jacket primary steel (no TP/piles)

The cost reduction for the transition piece is shown in Figure 3-10. The reference TP is the 4-Strut concept and the innovative jacket design utilised the optimised Box-Extreme concept. The reduction of approximately 60% is driven mainly by the costs for welding. The 4-strut concept requires significant reinforcements at the centre column due to the punch-through effect caused by the inclined brace connection and thus has a large welding volume. A more detailed description of the welding calculation of the TP concepts can be found in /7/.

### Normalised Primary Steel Fabrication Costs

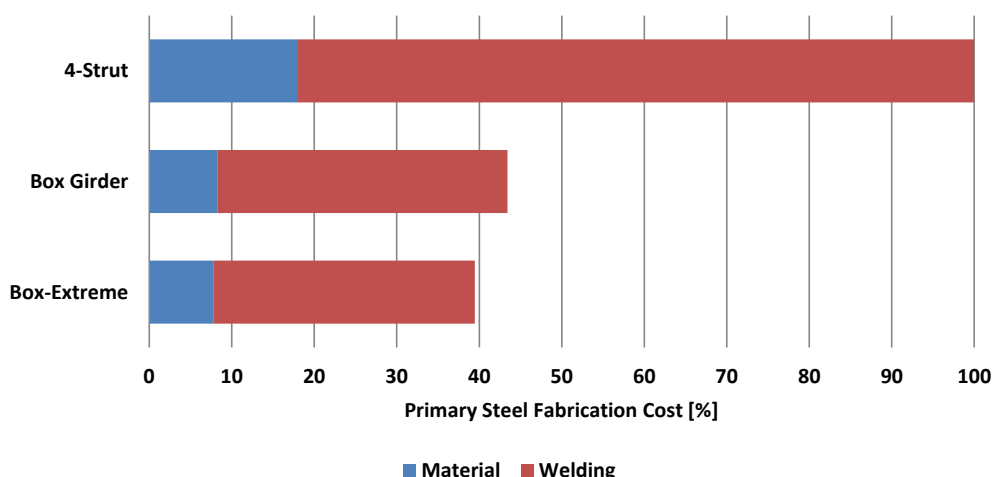


Figure 3-10: Normalized primary steel fabrication costs of transition piece concepts.

As explained above the piles are still compared by its unit prices. Therefore the cost reduction is proportional to the mass reduction of the component. The total mass of all piles have been reduced by 38 tons, which is approximately 10%.

All in all this ends up in a total cost reduction of approximately -17% for the innovative steel type jacket design. The considered component innovations are successfully implemented in the design optimization of the offshore support structure. Table 3-12 shows the cost reduction summary.

Table 3-12: Substructure fabrication cost estimation based on fabrication cost model

	Component	Reference costs [€]	Fabrication cost reduction	Final costs [€]
Innovative jacket design	TP	1,650,000	-60%	660,000
	Jacket	5,808,000	-5.4%	5,494,368
	Driven-piles	456,000	-10%	410,400
	<b>Total</b>	<b>7,914,000</b>		<b>6,564,768</b>
<b>Total cost reduction</b>				<b>-17.05%</b>

## 4 MODULARIZED JACKET DESIGN

### 4.1 Background

The reference jacket design for the 10 MW wind turbine was completed in deliverable D4.31 ref. /1/. This concept had a significant design drawback due to high amplification of the wind driven loads at the first natural frequency (0.287 Hz), which was very close to the 3P frequency (3 times rotational frequency  $\sim 0.30$  Hz) of the turbine. This greatly induces high fatigue cycles and damage at mean wind speeds in the range 5 m/s – 7 m/s. Consequently the minimum expected fatigue life of the reference jacket at some of its K-joints was close to 4 years.

Subsequent to the reference jacket design, the load computations were repeated using DLC 1.2 (design load case under normal operation) using a controller that possessed an exclusion zone that minimizes the time spent by the turbine at rotor speeds that excite the support structure. Figure 4-1 depicts the wind/wave input directions used and the key jacket braces/legs examined. The rotor speed exclusion zone is able to reduce the loading on the jacket nodes most affected by about 20%, as shown in Figure 4-2 below. However this is still insufficient to significantly increase the fatigue life of the substructure due to the high load excitations still seen at the lower mean wind speeds.

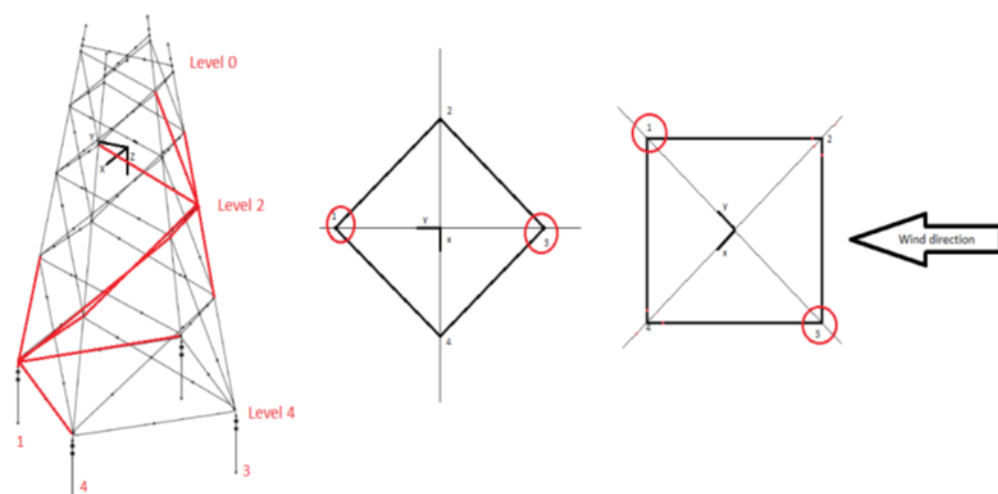


**Figure 4-1: Wind direction for DLC 1.2 and the schematic of the braces and legs as studied for load magnitudes**

Two joints as highlighted on Figure 4-1 are the node located on leg 1 at level 4 symbolized as N41 and the node located on leg 3 at level 2 symbolized as N23. Four braces are attached at each of these nodes: the braces attached to node N41 that lay on face 4-1 (LB4 and S4X4A), those laying on face 1-2 (LB1 and S1X4A) and the ones attached to N23 that lay on face 2-3 (S2X2A and S2X3A), and those laying on face 3-4 (S3X2A and S3X3A) were studied, in addition to legs 1 and 3 around the respective handled nodes.

Therefore without significantly lowering the natural frequencies of the jacket so as to be away from the 3P and 6P excitations, it is not feasible to design a jacket for the 10 MW reference turbine capable of withstanding 25 years operational lifetime. Due to the stiff structural characteristics of the jacket structure and due to the fixed hub height and water depth, lowering the natural frequency is not straight forward.

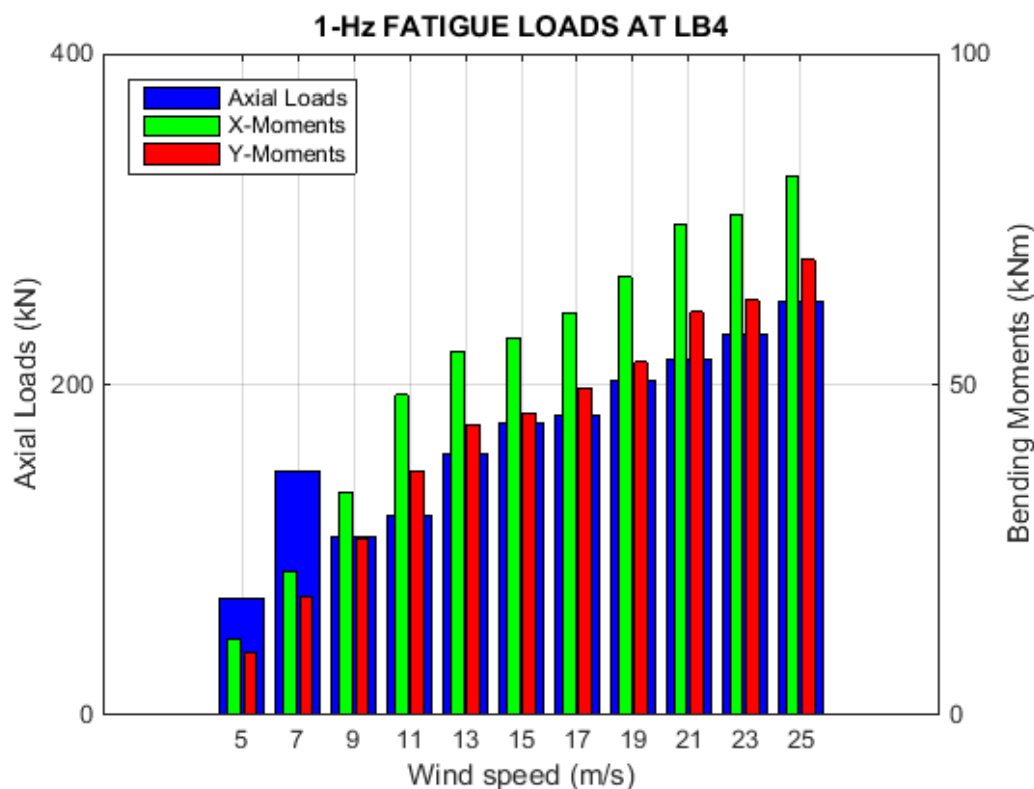


Figure 4-2: The damage equivalent loads in the lower level joints of the jacket along Leg L1 showing 3-P excitation at 7 m/s in the axial loads

Towards this target, a structural optimization solver is used, which can minimize the first natural frequency of the jacket while constraining:

- the tower top displacement for a given static load;
- The fatigue damage at critical joints
- the total mass of the jacket structure; and
- the von Mises ultimate stresses on each member for a given static load.

The fatigue limit state is considered by applying a representative load at the tower top, whose resulting stresses and selected cycles from the S-N curve are used as a measure of fatigue damage. The ULS criteria are included in the optimization problem to ensure that the resulting structure has the basic strength required. The objective function is set to reduce the first natural frequency in order to avoid the resonant excitation issues that occur for the reference jacket design.

A 3-legged and a 4-legged modular jacket substructure are now developed based on this structural optimization. The fatigue life of the two modular jackets for a 10 MW wind turbine is computed after HAWC2 load simulations using appropriate stress concentration factors as per DNV RP C203 /11/ and compared with the fatigue lifetime of a monopile substructure at 50 m water depth.

## 4.2 Optimization Methodology

The optimization methodology largely follows the approach outlined in deliverable D4.32 /12/. The main difference is that the objective function is to minimize the first natural frequency, rather than the mass. The loads, analysis models, and material parameters are exactly as described in deliverable D4.31 /1/.

The overall dimensioning and the sizing of the members in the jacket support structures for offshore wind turbines are done using a two level structural optimization approach, which is with inner design variables for one optimization loop and another set of design variables for the outer loop. The topology, i.e. the connectivity of the structure is assumed to be fixed, but can be chosen

by the user at the start of the optimization procedure. The user decides on the number of legs and the number of X-braces (for example 3 or 4) per jacket side. Two classes of design variables describe the dimensions of the jacket resulting in the two level approach. Outer variables model overall dimensions of the structure, such as foot print of the jacket and the height of the transition piece. The structural optimization also contains dimensioning of a simple space frame transition piece which connects the jacket to the tower. The jacket and the transition piece are modelled using Timoshenko beam elements. The transition piece is only designed for ultimate design states. The outer variables also model the locations of the X- and K-joints in the jacket structures. The inner design variables represent the dimensions of the members in the jacket. They represent the inner diameters and the thickness distribution of the members. Modularization is achieved by severe variable linking. The outer optimization problem is small-scale and is solved by one of the derivative free methods (i.e. pattern search) in the Matlab Optimization Toolbox. The inner problem, i.e. the dimensioning of the members in the jacket, is done using a state-of-the-art numerical optimization method that relies on gradients of objective and constraints functions. It should be noted that the final design is very dependent on the problem data (such as lower and upper bounds on diameter and thickness variables) and on the time allowed for solving the outer optimization problem. The loads are not updated during the optimization process and therefore a full HAWC2 simulation at the end of the optimization is required on the final jacket configuration to verify that the constraints are satisfied with the updated loads. The optimization tool is used to propose two different design concepts. The first is a jacket with four legs and four levels of X-braces. The second is a three legged jacket with four levels of X-braces per side. Different problem data has been used for the two designs and this can explain the results (cf. below). For the design of a jacket with four legs we have chosen to use four levels of X-braces. The lower and upper bounds on the outer design variables are listed in Table 4-1 for while the bounds on the inner design variables are listed in Table 4-2

**Table 4-1: Bounds on the outer design variables for the jacket with four legs**

Description	Lower Bound [m]	Upper bound [m]
Half base width	8	16
Half top width	4	8
Transition jacket height	8	12

**Table 4-2: Bounds on the inner design variables for the jacket with four legs**

Description	Lower Bound [m]	Upper bound [m]
Legs wall thickness	40	120
Braces etc. wall thickness	20	100
Legs inner radius	250	1500
Braces etc. inner radius	250	500

The main geometric characteristics of the final result from the optimization process for the four legged jacket are listed in Table 4-3. The diameter of the legs and braces was allowed to be larger, but the optimization process deemed the below dimensions sufficient to meet all the constraints.

**Table 4-3: Overview of the geometry and masses of the four-legged jacket**

Description	Unit	Four X-brace levels
Half base width	[m]	12.0
Half top width	[m]	7.25
Transition piece height	[m]	10.0
Jacket legs max inner radius	[mm]	297
Jacket legs max wall thickness	[mm]	74
Jacket legs min wall thickness	[mm]	45
Jacket mass (excl. transition)	[tons]	654
Transition jacket mass	[tons]	171
Total legs mass	[tons]	197
Total X-braces mass	[tons]	457

Once the DTU 10 MW reference wind turbine has been mounted on each resulting jacket, a modal analysis is performed in HAWC2 /13/, and the frequencies are presented in Table 4-4, which shows that the natural frequencies of the resulting structure have been lowered to below 3P excitation

**Table 4-4: Natural Frequencies [Hz]**

Mode	4-legged jacket	3-legged jacket
1 <sup>st</sup> bending mode Fore-Aft	0.2267	0.2475
1 <sup>st</sup> bending mode Side-Side	0.2300	0.2518
1 <sup>st</sup> Blade Asym. Flapwise Yaw	0.4417	0.4914
1 <sup>st</sup> Blade Asym. Flapwise tilt	0.5867	0.5868
1 <sup>st</sup> Blade Collective Flap	0.6288	0.6289

### 4.3 Fatigue Load Results and Lifetime

#### 4.3.1 Met-Ocean Conditions

A detailed fatigue analysis has been carried out on the two jackets resulting from the optimization process. The analysis starts with fatigue load assessment using the hydro-servo-aero-elastic software package HAWC2 /13/. The IEC 61400-3 /2/ design load case DLC 1.2 has been simulated with the met-ocean conditions shown in Table 4-5. The operational wind range is divided into 11 mean wind speed bins, which are each linked to a particular sea state characterized by an expected significant wave height and a peak spectral period. A total of 16 primary wind directions equally spaced around the jacket are used in the computation of the fatigue damage equivalent loads. The wave height is modelled based on JONSWAP spectrum at the expected value of the sea state characteristics conditional on the mean wind speed.

**Table 4-5: Met-ocean conditions used for evaluation of the fatigue load on jackets**

Wind speed [m/s]	Normal turbulence Intensity [%]	Significant wave height, Hs [m]	Peak period, Tp [s]	Expected annual frequency [hrs/yr.]
5	18.95	1.140	5.820	933.75
7	16.75	1.245	5.715	1087.30
9	15.60	1.395	5.705	1129.05
11	14.90	1.590	5.810	1106.75
13	14.40	1.805	5.975	1006.40
15	14.05	2.050	6.220	820.15
17	13.75	2.330	6.540	633.00
19	13.50	2.615	6.850	418.65
21	13.35	2.925	7.195	312.70
23	13.20	3.255	7.600	209.90
25	13.00	3.600	7.950	148.96

#### 4.3.2 Hydro-Servo-Aero-Elastic Load Simulation

HAWC2 utilizes a multibody formulation, which couples different elastic bodies together using Timoshenko beam finite elements whereby their stiffness, mass and damping are assembled into the governing equations of motion coupled to aerodynamic forces, whose aeroelastic solution is obtained using the Newmark- $\beta$  method. The blade element momentum theory supplemented with Leishman Beddoes dynamic stall model and dynamic inflow is employed to represent the rotor unsteady aerodynamics.

The Mann turbulence model is used in the load case simulation for representing the input wind turbulence over the rotor. Random Gaussian 10-minute turbulent wind realizations are used as input to simulate normal operation over the 11 mean wind speed bins in 16 equally spaced directions collinear with the rotor in each case or with  $\pm 10^\circ$  yaw misalignment. The input waves are assumed to be aligned with the wind. Random wave kinematics are computed according to

the linear Airy model with Wheeler stretching. The hydrodynamic forces are calculated based on the Morison equation evaluated from water surface to seabed. The structure is assumed to be embedded (all degrees of freedom are fully restrained) at the soil interface, implying the soil is not considered in the simulation.

This set of conditions provides  $11 \times 1 \times 3 \times 16 = 528$  10-minute load time series. Figure 4.3 provides the critical joints on the jacket with the highest fatigue damage and therefore the “hot spots”.

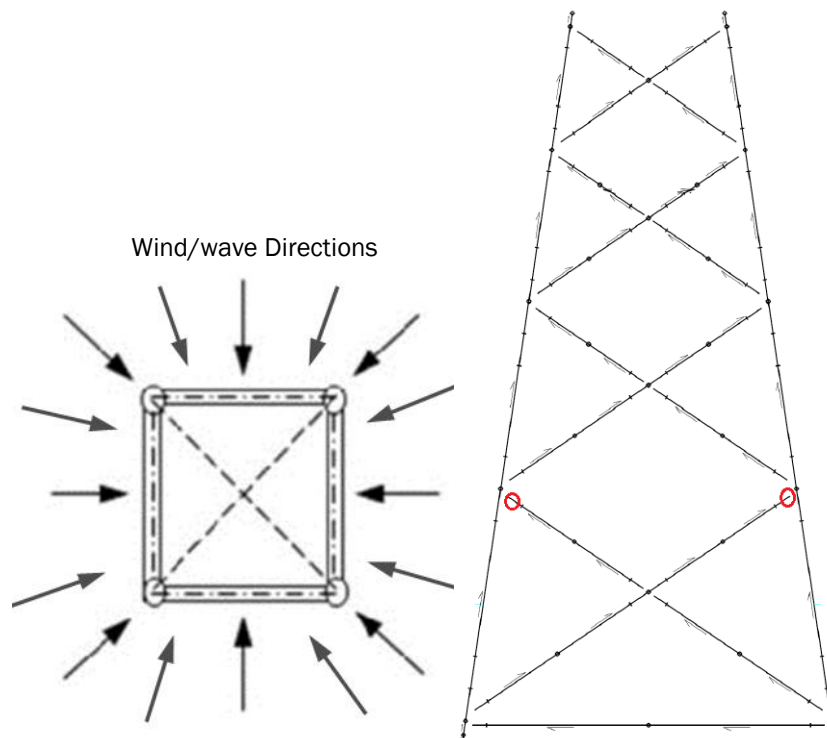


**Figure 4-3: Wind direction and critical locations. The wind is directed along positive y-axis**

Though the simulation model has been set to be as close as possible as in the Reference report D4.31, some conditions are not used:

- Corrosion allowance.
- Soil conditions and Scour.
- Appurtenances.
- Marine growth.

### 4.3.3 Critical Stress Loads and Lifetime

Deliverable D4.31 has pointed out that critical locations are the weld connections situated at the hot spots. Similarly, on the 4-legged and on the 3-legged jackets, the corresponding weld connections have been determined to be critical locations for fatigue analysis, as encircled in Figure 4-3. These connections are the joints between the braces and the corresponding legs.

The axial force and the bending moments acting at those points have been collected for stresses calculations. For instance, the axial force time series and their corresponding spectra acting at the most critical welded joint are presented in Figure 4-4, for the 4-legged jacket. For stress evaluation at K-joint’s crowns and saddles, attention has been taken to express the internal loads in terms of axial forces, in-plane and out-of-plane bending moments.

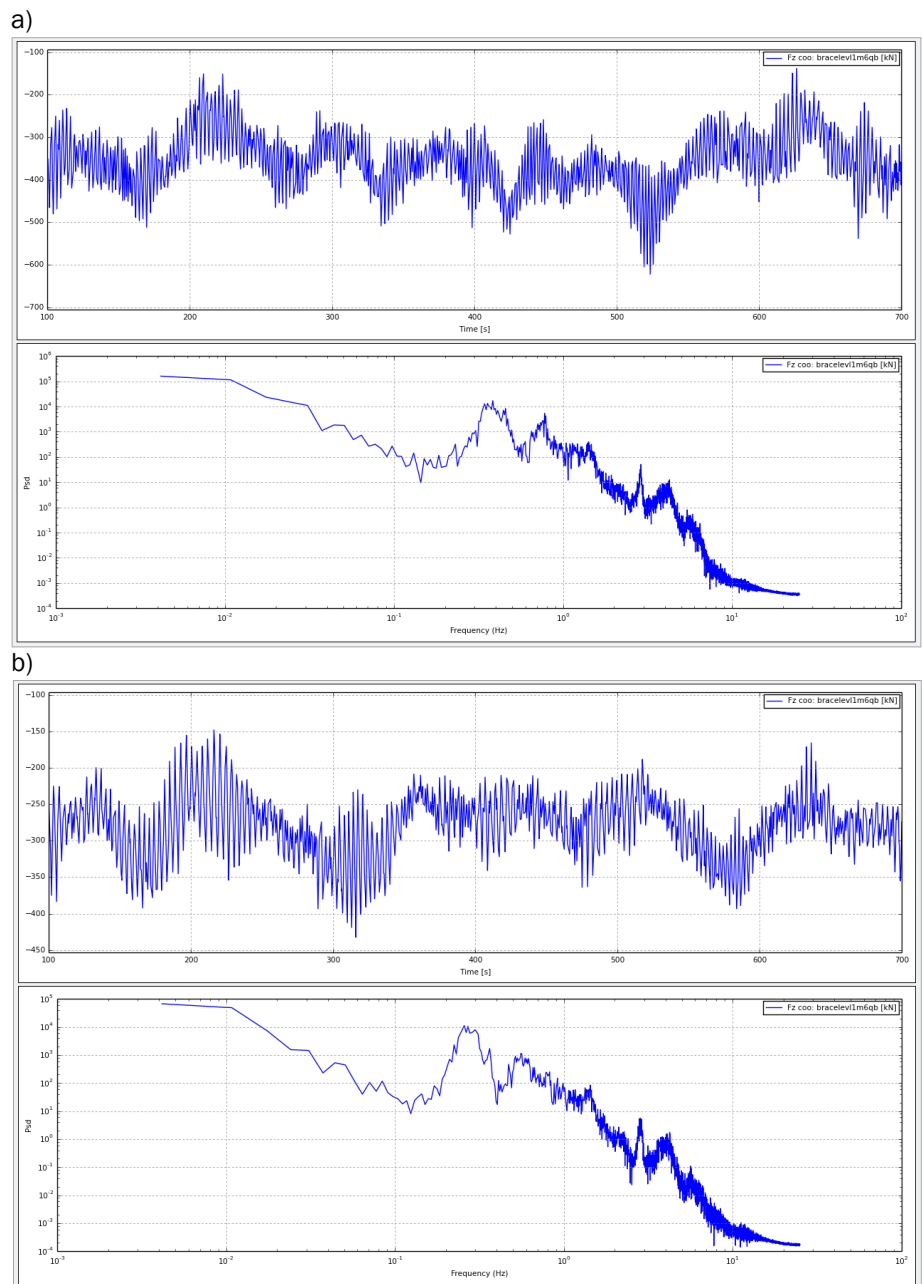
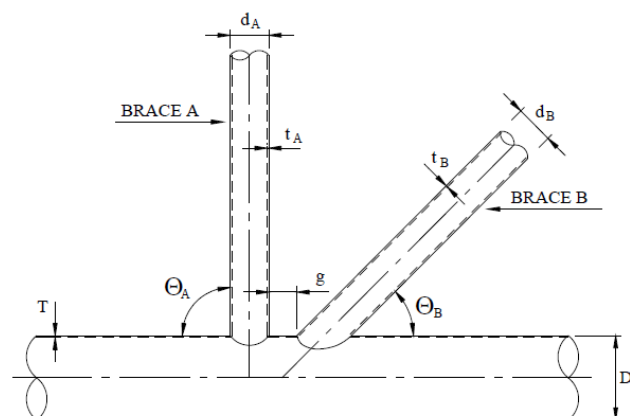


Figure 4-4: Axial loads at the critical hotspot (weld of brace m6qb to leg at level 1) at a) 13m/s mean wind speed and b) 7m/s mean wind speed showing there is no specific excitation at low frequencies dependent on the mean wind speed as is the case when 3P excitations are present.

#### 4.3.4 Stress Concentration Factors

The stress concentration factors have been calculated according to DNV RP C203 /11/. For a given joint, the calculation starts with its normalization. The joint's parameters are given by Figure 4-5.



$$\beta_A = \frac{d_A}{D} \quad \beta_B = \frac{d_B}{D}$$

$$\tau_A = \frac{t_A}{T} \quad \tau_B = \frac{t_B}{T}$$

$$\gamma = \frac{D}{2T} \quad \zeta = \frac{g}{D}$$

Figure 4-5: K-Joint parametrization (from DNV RP C203)

The characteristic stresses around the welds along with the stress concentration factors for the geometry in Figure 4-5 are given by the relations from DNV RP C203. From the hotspot's characteristic stresses,  $\sigma_i$ , the design stresses are obtained by:

$$\sigma_{di} = \gamma_f \cdot \gamma_m \cdot \gamma_n \cdot \gamma_x \sigma_{ni}$$

where the safety factors are taken from IEC 61400-1 ed.4 background document:

- $\gamma_f = 1.20$  is the partial safety factor associated to fatigue stress range counting;
- $\gamma_m = 1.25$  is the partial safety factor associated to the material properties;
- $\gamma_n = 1.10$  is the partial safety factor associated to the component's consequence of failure.
- $\gamma_x = 1.50$  is an additional partial safety factor due to increased uncertainty in stress concentration resulting from weld distortion or corrosion etc.

#### 4.3.5 SN-Curves

The stress ranges are obtained from the rainflow counting method applied on the design stress time series. The number of cycles,  $N$ , corresponding to full damage induced by a given stress range,  $\Delta\sigma$ , is obtained by the design S-N curve, i.e. the T-curve in sea water with cathodic protection as per DNV RP C203, which is described as:

$$\log N = \log \bar{a} - m \log \left( \Delta\sigma \left( \frac{t}{t_{ref}} \right)^k \right)$$

where

- $m$  and  $\log \bar{a}$  = are respectively the negative inverse slope of the S-N curve and the intercept of  $\log N$  axis. For S-N curves in seawater with cathodic protection, ( $m = 3$ ,  $\log \bar{a} = 11.764$ ) for  $N < 10^6$ , and ( $m = 5$ ,  $\log \bar{a} = 15.606$ ) for  $N > 10^6$ ;
- $t$  = is the thickness through which the crack will most likely grow;  $t = t_{ref}$  if  $t < t_{ref}$ ;
- $t_{ref}$  = is the reference thickness equal to 32 mm;
- $k$  = is the thickness exponent on fatigue strength.  $k = 0.25$  for  $SCF < 10.0$  and  $k = 0.30$  for  $SCF > 10.0$ .

#### 4.3.6 Damage Accumulation

Palmgren Miner's rule is applied to accumulate the induced damage. During one year, the accumulated damage is expressed as:

$$D_1 = \gamma_{FF} \sum_i \frac{n_i t_i}{N_i}$$

Where

- $\gamma_{FF}$  is the fatigue reserve factor = 3.0.
- $N_i$  is the number of cycles that can cause full damage under the stress range  $\Delta\sigma_i$ ;
- $n_i$  is the number of cycles corresponding to the stress range  $\Delta\sigma_i$ ; over 1 year
- $t_i$  is the Weibull time duration of occurrence of the stress range  $\Delta\sigma_i$ .

The damage accumulated during the lifetime of the structure, i.e. 25 yrs, is  $D_{25} = 25 D_1$ .

### 4.3.7 Fatigue Lifetime

Based on the one year accumulated fatigue damage, the fatigue lifetime in years is obtained by  $L = D_1^{-1}$ . Applied on the jackets in hand, it has been obtained a minimum fatigue lifetime of 12 years for the 3-legged jacket. This insufficient fatigue lifetime is due to the fact that the optimization settings were chosen to the lower bounds: the brace dimensions were constrained to be small in size. However for the 4 legged-jacket, the life at the hot spot was predicted to be 197 years, exclusive to the additional partial safety factor  $\gamma_x$ . However to compensate for the lack of stress concentration from corrosion or extra loading from marine growth, an additional partial safety factor  $\gamma_x$  was considered. Figure 4.6 shows the reduction in lifetime with increase in the added load factor  $\gamma_x$ . A  $\gamma_x = 1.5$  is a reasonable assumption as further increase in  $\gamma_x$  causes a much lower reduction in lifetime as compared to the change from 1 to 1.5.

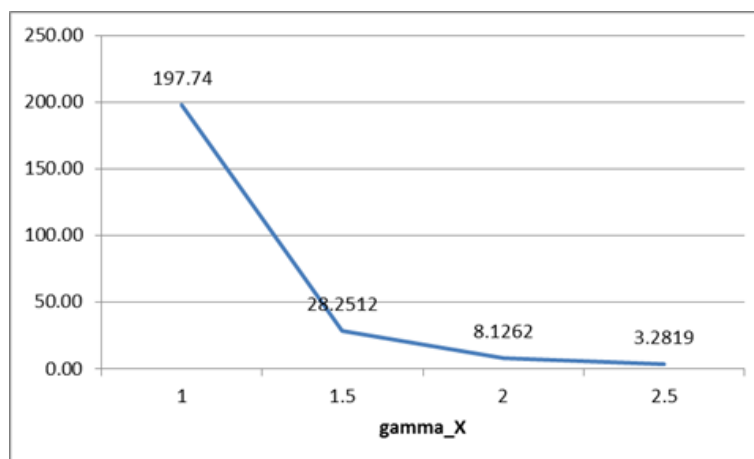


Figure 4-6: Reduction in lifetime of the hotspot with increase in added load partial safety factor

## 4.4 Monopile Design at 50 m Water Depth

### 4.4.1 Met-Ocean Conditions and Hydro-Servo-Aero-Elastic Load Simulation

In addition to the innovative jackets, a monopile substructure is proposed as a comparative concept to the developed jackets. The met-ocean conditions and the hydro-servo-aero-elastic simulation settings are the same with those of the jackets, except for some details on load cases. Indeed, three design load cases (DLC) are considered as defined by IEC 61400-3: DLC 1.2 for fatigue limit state, DLC 1.3 and DLC 6.2a for ultimate limit state. For DLC 1.2, the 11 wind speed bins are associated to six wind turbulence seeds each, and have been misaligned to the Pierson-Moskowitz type waves by  $0^\circ$  or  $\pm 10^\circ$ . This set of conditions provides  $11 \times 6 \times 3 \times 3 = 594$  scenarios.

DLC 1.3 is the ultimate loading resulting from extreme turbulence conditions with normal sea states. Six wind seeds for each of 11 wind speed bins are simulated, none with yaw error. The waves of JONSWAP type are aligned along the wind direction. The JONSWAP spectrum type has

been used for ultimate loading to capture the extreme load thanks to its peak. That provides  $11 \times 6 = 66$  scenarios. Table 4-6 presents the extreme turbulence intensity used for DLC 1.3; the expected wave states at each wind bin are read from Table 4-5. DLC 6.2a is the ultimate loading resulting from the turbulent extreme wind model with extreme sea states, coupled with loss of electrical power. A wind speed of 42.73 m/s is applied along 24 directions: from  $0^\circ$  to  $345^\circ$  with  $15^\circ$  bin size. A JONSWAP wave ( $H_s = 9.4$  m and  $T_p = 13.7$  s) is directed along the wind direction with  $\pm 30^\circ$  yaw error. With no active controller, the structure is loaded with an extreme current (1.2 m/s) of parabolic type at  $0^\circ$ . The blades are pitched to an angle of  $90^\circ$  with no dynamic induction. This leads to a total of  $24 \times 3 = 72$  scenarios.

**Table 4-6: Met-ocean conditions**

Wind speed [m/s]	5	7	9	11	13	15	17	19	21	23	25	42.73
Extreme TI [%]	43.85	33.30	27.43	23.70	21.12	19.23	17.78	16.63	15.71	14.94	14.30	11.00

#### 4.4.2 Predesign: Resonance Avoidance

Njomo et al. (2015), ref. /14/, have proposed a monopile design for the 10 MW reference turbine at 50 m water depth. The proposed monopile substructure had an outer diameter of 9500 mm, a wall thickness of 110 mm, and an embedded depth of 30 m. However, ref. /14/ has shown that the pile's penetration length was not sufficient to ensure that the soil remains elastic during the turbine lifetime. Therefore, the design has been modified herein while keeping the same natural frequency range. The new design possesses an outer diameter of 9500 mm, a wall thickness varying between 100 mm and 150 mm (see Appendix F – Geometry of the Monopile), and an embedded depth of 50 m.

The first natural frequencies of the new support structure are summarized in Table 4-7. The frequencies avoid the rotor harmonics, which range between [0.10 Hz 0.16 Hz] and between [0.30 Hz 0.48 Hz], and the wave frequencies, which are up to 0.225 Hz.

**Table 4-7: Natural frequencies of the monopile (D = 9.5m, t variable, penetration length = 50m)**

Mode	Frequency [Hz]
1 <sup>st</sup> bending mode Fore-Aft	0.2465
1 <sup>st</sup> bending mode Side-Side	0.2500
1 <sup>st</sup> Blade Asym. Flapwise Yaw	0.5561
1 <sup>st</sup> Blade Asym. Flapwise tilt	0.5827
1 <sup>st</sup> Blade Collective Flap	0.6262

#### 4.4.3 Load Assessment, Ultimate Limit State and Stability Limit State

Fully coupled hydro-servo-aero-elastic simulations have been carried out using HAWC2 for the three DLCs 1.2, 1.3, and 6.2a. Internal loads have been retrieved at different points along the monopile axis to evaluate the induced fatigue damage (DLC 1.2) and to compute the stresses (DLCs 1.3 and 6.2a) for ultimate and stability checks.

The internal loads generated for the ultimate design load cases have been used to check the monopile stresses at ultimate limit state and (local and global) buckling limit state. DLC 6.2a has been found to be more severe than DLC 1.3. The utilization ratios at ULS and local BLS for DLC 6.2a are presented in Figure 4-6. At critical locations, they are respectively 0.68 and 0.36.

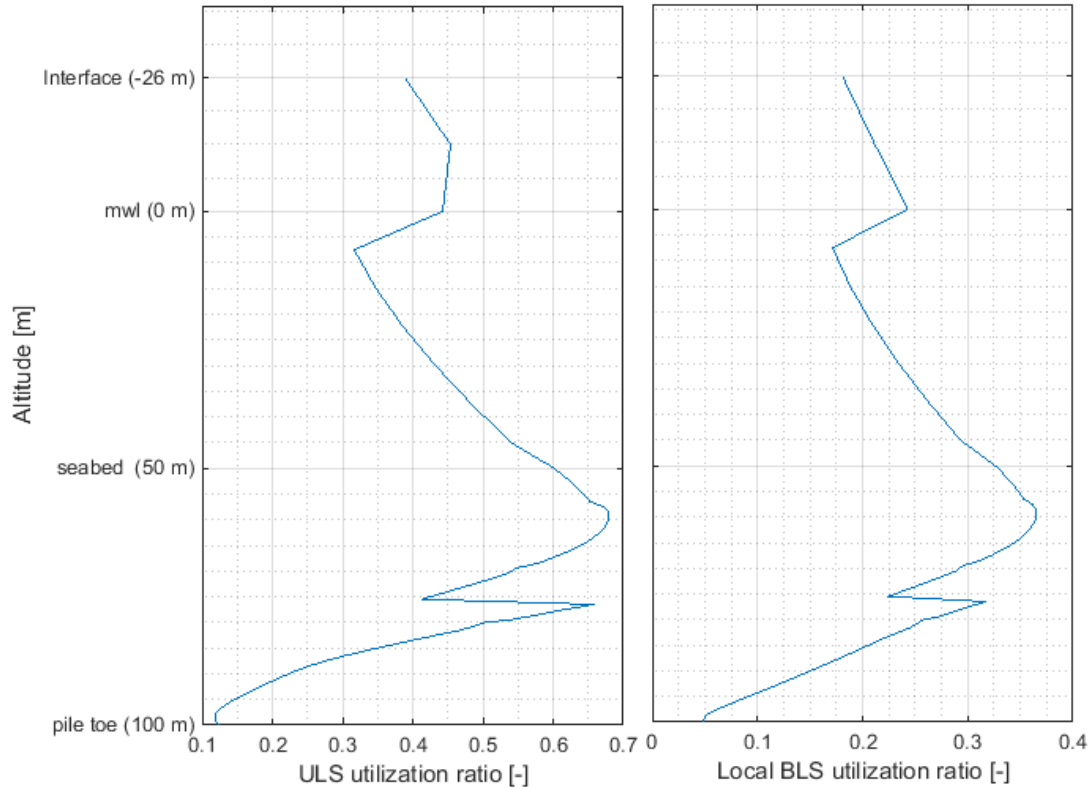


Figure 4-6: Utilization ratios along the monopile axis – (a) ultimate limit state; (b) local buckling limit state.

#### 4.4.4 Fatigue Limit State

A process similar to that of jacket fatigue evaluation has been applied for the monopile, considering merely the butt welds of the primary steel. The difference between the two processes lays on the estimation of the stress concentration factors. For monopile's butt weld connection of same nominal diameter and thickness, stress concentration factors are given by:

$$SCF = 1 + \frac{3\delta_m}{t} e^{-\sqrt{t/D}}$$

where  $D$  and  $t$  are respectively the outer diameter and the wall thickness,  $\delta_m$  is the resultant imperfection measure, whose components may be due to out of roundness or centre eccentricity. Herein, the imperfection measure has been taken as the maximum tolerance has recommended by DNV OS C401. At thickness changes from larger thickness  $T_2$  to smaller thickness  $T_1$ , stress concentration factors are calculated from:

$$SCF = 1 + \frac{6e}{T_1} \left( \frac{1}{1 + \left(\frac{T_2}{T_1}\right)^{1.5}} \right)$$

For conical transition from outer diameter  $D_L$  to  $D_s$  and wall thickness of the cone  $t_c$ , stress concentration factors are estimated by:

$$SCF = 1 + \frac{0.6t\sqrt{D_j(t+t_c)}}{t^2} \tan\alpha \quad \text{for the tubular side}$$

$$SCF = 1 + \frac{0.6t\sqrt{D_j(t+t_c)}}{t_c^2} \tan\alpha \quad \text{for the cone side}$$

With these stress concentration factors plugged into the above process, the fatigue lifetime at the critical location of the monopile has been estimated at 26 years. Figure 4-7 depicts the fatigue lifetime distribution along the monopile axis.

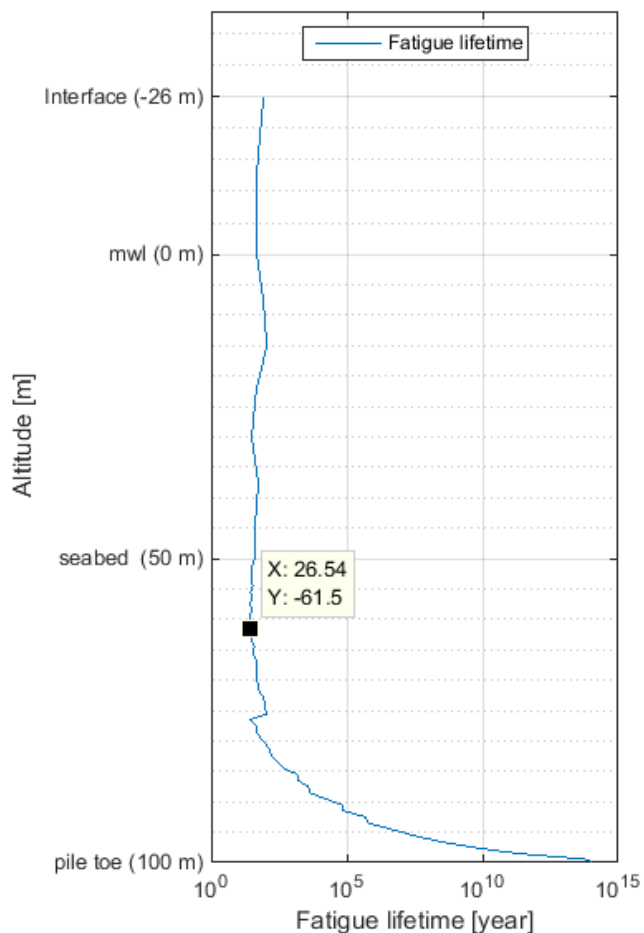


Figure 4-7: Fatigue lifetime distribution along the monopile axis.

#### 4.5 Summary of the three Developed Concepts

Table 4-8 summarizes the main properties of the three developed concepts and recalls those of the reference jacket. For the 4-legged jacket, the pile foundations are assumed to be the same as for the reference jacket. In estimating the cost of the structures, the unit costs are taken according to ref. /10/, i.e. 5000 €/t for the transition piece steel, 4800 €/t for the jacket steel, and 1200 €/t for the pile steel or 2000 €/t for the monopile steel.

Table 4-8: Summary of the four support structures

Criteria		Reference jacket	4-legged jacket	3-legged jacket	Monopile
Frequency [Hz]	Mode 1	0.2867	0.2267	0.2476	0.2465
Mass [t]	Transition piece	330	171	405	603
	Substructure	1210	654	820	1729
	Foundation	500	500	375	1472
	Total	2040	1325	1600	3804
Cost [million €]		8.06	4.59	6.41	7.61
Min. fatigue lifetime [years]		4	28	12	26

This study leads to the following inferences:

- The 4-legged jacket and the monopile satisfactorily demonstrate a fatigue lifetime not less than the intended lifetime. Jackets and monopile substructures can be good candidates for multi-megawatt wind turbines at 50+ m water depth.
- The modularized jackets have been successfully designed such that their first natural frequencies lay within the soft-stiff range. This proves that the optimization process is an effective tool for natural frequency placement.
- With overall natural frequency as objective function criterion, the system can lead to satisfactory design as in the 4-legged case. However, it may be important to set appropriate constraints in terms of member dimensions otherwise local failures may occur. In 4-legged jacket, the steel material is almost evenly distributed to both braces and legs to obtain medium size members: the legs are of about OD/WT = 700 mm / 50 mm, and the braces of about 540 mm / 20 mm. On contrary, for the 3-legged jacket, the steel material is mostly set for the legs: legs are of 1600 mm / 100 mm, and the braces are of 360 mm / 30 mm.
- Despite its high need in steel material, monopiles can be a desirable solution as its low manufacture cost helps to reduce the overall capital expenses. If applied on, an optimization process can lead to more competitive design.

## 5 CONCLUSIONS

The deliverables show the performance results of the innovative 10MW wind turbine model including the load mitigation from damping devices (tower mass dampers and a diagonal viscous damper). Subsequently, several design results of optimized support structures are given, which consists of an industry-oriented jacket design and designs using optimization procedures.

In Chapter 2 it is demonstrated that the addressed turbine size in combination with jacket substructures can lead to critical resonance issues, which need special attention during design iterations between WTG manufacturer and foundation designer. It should be the first choice to avoid resonance critical design. In most cases the upper natural frequency limit, resulting from the lowest blade passing frequency (3p), is critical. The 10MW INN WIND.EU reference wind turbine has the allowable frequency range between 0.16Hz-0.3Hz (without safety margin) for the first natural frequency. Critical operational ranges of the wind turbine can be avoided using a rotor speed exclusion zone, which is successfully implemented in the innovative 10MW wind turbine model. However, this option solely affects a small area of the rotor speed range and does not mitigate the loading at other operational states.

A general improvement of the loads is archived by introducing damping devices in the tower top. The damping mechanism responds to the horizontal deflection of the RNA and therefore the damping effect correlates with the strength of the deflections. In the present study it is shown that both longitudinal and lateral bending loads in the support structure are mitigated. However, the effect is stronger for sidewise motions. In fore-aft motion (along with the wind direction) the aerodynamic induced damping is strong and thus the tower top damping systems contributes less during normal operation. The result assessment is based on the change of damage equivalent loads at tower bottom, which are characteristic loads to compare the results of various (fatigue) load cases. A normal operation load case (oriented on DLC1.2) with single direction is considered. The sidewise bending moments are reduced up to approximately 29% and 59% for the TMD and viscous damper, respectively. However, it should be noted that in general all load components (i.e.  $F_x$ ,  $F_y$ ,  $F_z$ ,  $M_x$ ,  $M_y$ ,  $M_z$ ) are considered for the substructure design and thus the overall load reduction will be smaller in practice, but will have a positive effect on the design.

The reference jacket is optimized using different innovations from INN WIND.EU and the results are given in Chapter 3. Load mitigation due to increased damping, transition piece (TP) design optimization to improve the load transition into the jacket and general layout optimization of the jacket substructure are integrated. The design is carried out following the same guidelines, assumptions and same software as used in the reference jacket design (D4.31, ref. /1/). The improved jacket design is also driven by the tubular joint fatigue, which further affects the geometry of the free connecting members. Consequently ULS criteria (utilization < 1.0) are uncritical and in case can be easily secured. Fatigue life improvement across the jacket is achieved and the critical hot-spots fulfil the design lifetime of 81y (including design fatigue factor of three). Post-weld treatment is required to improve the fatigue life of critical K-Joints. The total primary steel mass of the jacket is decreased by approximately 9%.

Largest improvements are achieved using the innovative TP design, which also reduces the mass and further has strong reduced welding volume. Finally this leads to a cost saving of the entire substructure (i.e. TP, jacket and piles) of approximately 12.2% when applying the mass proportional cost model from Work Package 1. Alternatively the fabrication cost model (confidential) from Ramboll is applied, which addresses raw material, welding, assembly and preoperational work. Here the total cost reduction of approximately 17% is obtained, whereas the TP contributes the most.

The final improved jacket design is also available as a superelement for application in further wind turbine load calculations. Within the INN WIND.EU project one integrated load iteration is performed between the 10MW wind turbine and foundation. Compared to industry application this is not sufficient and further design optimization can be expected, when additional load iterations with control optimization are elaborated. The changes in the improved jacket are significant compared to the reference design. The first natural frequency is lower and thus 3p excitation is assumed to be mitigated and lower weight jacket structures can be expected. It is strongly recommended to aim for stronger interactions between the involved designers, i.e. wind turbine and foundation.

Chapter 4 presents modularized jacket designs using an optimization methodology. The optimization is decoupled from the design load calculation, which means that during the iteration loop the boundary conditions are constant. A realistic estimate of the ultimate loads and fatigue damage on the jacket are used as a constraint during the optimization process. A fully coupled aeroelastic simulation is used on the final jacket design upon convergence of the optimization routine. The considered jacket model uses clamped supports instead of non-linear pile-soil curves. The objective function is to minimize the first natural frequency. Upper and lower boundary conditions prescribe the design space for the leg and brace members.

The optimization is used to propose two different design concepts. The first is a jacket with four legs and four levels of X-braces. The second is a three legged jacket with four levels of X-braces. The natural frequencies of the two designs are strongly reduced eliminating 3P excitation and in general very light weight structures are achieved. The life of the optimal jacket structures is computed considering a large variation or uncertainty in the load level at the welded joints. The four legged optimal structure was found to have an expected fatigue life greater than 25 years. The optimal designs neglect the loading from secondary structures, as well as marine growth and do not consider manufacturing constraints, all of which may need to be accounted for before application to a real wind farm project.

The mass proportional cost model [€/ton] for the jacket, TP and piles is used. The four leg jacket results in a cost reduction of approximately 43%, the three leg jacket results in approximately 20.5% lower costs compared to the reference jacket /1/.

In addition to the two jackets, a monopile substructure is proposed as a comparative concept. The total primary steel mass of the monopile is 86% higher than the reference jacket and almost 190% higher than the promoted optimized 4-leg jacket. For the cost assessment a price of 2000 € per ton monopile steel is assumed, which considers the higher costs for a TP and internal platforms. The total costs of the monopile are approximately 5% lower compared to the reference jacket. The obtained results from the optimization methodology have to be validated against current design practise.

## 6 REFERENCES

- /1/ INNWIND.EU: Design Report – Reference Jacket, Deliverable D4.31, 2015
- /2/ IEC 61400-3, Wind turbines Part 3: Design requirements for offshore wind turbines, 2009
- /3/ DNV-OS-J101, Design of Offshore Wind Turbine Structures, 2014
- /4/ DNVGL-RP-0005, Recommended Practise for Fatigue Design of offshore steel structures, 2014
- /5/ NORSOK N-004: Design of Steel Structures. NORSOK Standard N-004, Rev. 2, October 2004.
- /6/ Craig R.R, Bampton, M.C.C. Coupling of Substructures for Dynamic Analysis, AIAA Journal 6(7): pages 1313-1319, 1968
- /7/ Innovations on component level (final report), Deliverable D4.13, INNWIND.EU project, 2015
- /8/ Validation of innovations by tests on component level, Deliverable D4.14, INNWIND.EU project, 2015
- /9/ Efthymiou, M.: Development of SCF formulae and generalized influence functions for use in fatigue analysis. Recent Developments in Tubular Joint Technology, OTJ'88, October 1988, London.
- /10/ INNWIND.EU: PI-based Assessment of Innovative Concepts (Methodological Issues), Deliverable D1.23, 2014
- /11/ DNV-RP-C203, Fatigue Design of Offshore Steel Structures, 2011
- /12/ INNWIND.EU: Innovative Concepts for Bottom-Mounted Structures, Deliverable D4.32, 2014
- /13/ Larsen, T.J., Hansen A.M.: How 2 HAWC2, the user's manual. DTU Risoe, 2014
- /14/ Njomo Wandji W, Natarajan A, Dimitrov N, Buhl T. Design of monopiles for multi-megawatt wind turbines at 50 m water depth. EWEA Paris 2015
- /15/ INNWIND.EU Deliverable D1.3.5- "System design assessment for innovative support structures", innwind.eu, accessed 2016-04-10
- /16/ Kuhnle, Bernd, and Kühn, Martin, Unfavourable trends of rotor speed and systems dynamics for very large offshore wind turbines – Analysis of the 10MW INNWIND.EU reference turbine, EWEA offshore 2015 conference, Copenhagen 2015.
- /17/ Lackner, Matthew A., and Mario A. Rotea. "Passive structural control of offshore wind turbines." Wind energy 14.3 (2011): 373-388.
- /18/ Carcangiu, C. E., Pineda, I., Fischer, T., Kuhnle, B., Scheu, M., & Martin, M. Wind Turbine Structural Damping Control for Tower Load Reduction. In Civil Engineering Topics, Volume 4 (pp. 141-153). Springer New York, 2011
- /19/ Karimi, Hamid Reza, Mauricio Zapateiro, and Ningsu Luo. "Semiactive vibration control of offshore wind turbine towers with tuned liquid column dampers using H8 output feedback control." Control applications (CCA), 2010 IEEE international conference on. IEEE, 2010.
- /20/ Caterino, Nicola. "Semi-active control of a wind turbine via magnetorheological dampers." Journal of Sound and Vibration 345 (2015): 1-17.
- /21/ Bossanyi E. GH Bladed user manual. GL-Garrad Hassan. Bristol, England; 2010.
- /22/ Hwang, Jenn-Shin, Yin-Nan Huang, and Ya-Hui Hung. "Analytical and experimental study of toggle-brace-damper systems." Journal of structural engineering 131.7 (2005): 1035-1043.

## APPENDIX A – JACKET SUPERELEMENT

In this appendix the Craig-Bampton superelement of the improved jacket from Chapter 3 is given. It contains 36 DOF in total (6 boundary DOFs and 30 internal DOFs). An Excel file with the data is located on the INNWIND.EU internal website.

The coordinate system of the model is as follows:

- x-axis points North,
- y-axis points west,
- z-axis points upwards.

The damping matrix is based on Rayleigh damping with the following parameters:

- alpha (mass proportional term) = 1.90813E-02
- beta (stiffness proportional term) = 1.50211E-03

### Mass matrix:

Mass matrix	Col 1	Col 2	Col 3	Col 4	Col 5	Col 6	Col 7	Col 8	Col 9	Col 10	Col 11	Col 12
Row 1	8.22E+05	-1.76E+01	-5.16E+02	-1.77E+03	-6.29E+06	-2.28E+04	2.82E+01	7.25E+02	-1.69E+01	5.17E+00	1.91E+00	1.23E+00
Row 2	-1.76E+01	8.22E+05	-5.25E+02	6.27E+06	3.03E+03	3.86E+04	-7.25E+02	2.79E+01	-1.54E+01	-4.81E+00	-1.99E+00	7.93E-01
Row 3	-5.16E+02	-5.25E+02	3.35E+05	-1.66E+02	-3.87E+03	9.59E+03	1.35E-01	1.29E-01	-1.55E-02	1.08E+00	-8.90E-03	-2.57E-03
Row 4	-1.77E+03	6.27E+06	-1.66E+02	5.21E+07	3.99E+04	3.06E+05	-6.32E+03	2.32E+02	-1.34E+02	-4.26E+01	-1.89E+01	5.37E+00
Row 5	-6.29E+06	3.03E+03	-3.87E+03	3.99E+04	5.23E+07	1.73E+05	-2.40E+02	-6.33E+03	1.48E+02	-4.67E+01	-1.61E+01	-8.44E+00
Row 6	-2.28E+04	3.86E+04	9.59E+03	3.06E+05	1.73E+05	8.76E+07	-1.08E+02	-9.11E+01	4.98E+00	8.83E+03	8.03E+00	-4.79E-01
Row 7	2.82E+01	-7.25E+02	1.35E-01	-6.32E+03	-2.40E+02	-1.08E+02	1.00E+00	1.38E-16	1.39E-16	-6.06E-16	2.40E-16	-5.44E-16
Row 8	7.25E+02	2.79E+01	1.29E-01	2.32E+02	-6.33E+03	-9.11E+01	1.38E-16	1.00E+00	4.56E-17	-2.11E-17	-3.60E-17	1.01E-16
Row 9	-1.69E+01	-1.54E+01	-1.55E-02	-1.34E+02	1.48E+02	4.98E+00	1.39E-16	4.56E-17	1.00E+00	-7.68E-16	4.03E-16	2.58E-16
Row 10	5.17E+00	-4.81E+00	1.08E+00	-4.26E+01	-4.67E+01	8.83E+03	-6.06E-16	-2.11E-17	-7.68E-16	1.00E+00	-4.03E-16	2.26E-16
Row 11	1.91E+00	-1.99E+00	-8.90E-03	-1.89E+01	-1.61E+01	8.03E+00	2.40E-16	-3.60E-17	4.03E-16	-4.03E-16	1.00E+00	-2.24E-17
Row 12	1.23E+00	7.93E-01	-2.57E-03	5.37E+00	-8.44E+00	-4.79E-01	-5.44E-16	1.01E-16	2.58E-16	2.26E-16	-2.24E-17	1.00E+00
Row 13	9.42E+00	-3.04E+02	6.00E-02	-2.43E+03	-1.54E+02	1.09E+01	-4.03E-17	-1.85E-16	7.74E-17	-7.63E-17	-3.54E-17	-4.81E-17
Row 14	-3.04E+02	-9.39E+00	-1.08E-01	-1.52E+02	2.44E+03	-9.41E+00	-2.69E-16	-7.60E-16	2.39E-16	-2.57E-16	6.90E-17	-7.09E-16
Row 15	1.16E+02	4.38E+01	-4.86E-01	3.23E+02	-1.23E+03	9.13E+00	3.39E-17	9.93E-17	-1.59E-16	1.78E-16	1.13E-16	1.49E-16
Row 16	-4.38E+01	1.16E+02	-6.51E-01	1.23E+03	3.25E+02	-8.68E+00	-8.44E-17	1.96E-16	-2.10E-16	1.97E-16	-4.49E-17	-3.29E-17
Row 17	1.08E+00	2.57E+00	3.93E+01	2.47E+01	-1.31E+01	-4.36E+01	7.00E-17	6.71E-17	-1.54E-16	5.23E-17	-1.75E-17	8.71E-17
Row 18	-1.78E-01	-1.87E-01	4.00E+01	-1.46E+00	1.04E+00	2.22E+01	4.17E-17	6.56E-17	-9.31E-17	-9.68E-17	-1.94E-16	-7.68E-18
Row 19	2.00E-01	2.48E-01	1.53E-03	7.96E-01	-2.56E-01	5.00E-01	1.16E-16	-1.96E-17	5.25E-17	-6.02E-17	-4.12E-17	1.03E-16
Row 20	-8.23E+01	8.39E+00	5.76E-02	4.58E+01	3.77E+02	5.41E+00	4.23E-17	9.32E-17	-5.21E-17	2.07E-17	-7.20E-17	-9.64E-17
Row 21	8.37E+00	8.24E+01	-7.94E-02	3.77E+02	-4.55E+01	4.09E+00	-5.22E-17	1.62E-17	-3.72E-17	8.93E-17	1.94E-17	1.58E-17
Row 22	-4.68E-02	-4.43E-02	1.73E+00	-1.90E-01	3.92E-02	-1.75E+01	7.76E-17	2.58E-17	-2.06E-17	2.38E-17	-2.36E-18	-7.59E-18
Row 23	6.18E+00	6.24E+00	-3.16E+02	1.72E+01	-1.62E+01	3.08E+01	-1.20E-17	3.12E-17	-9.74E-18	-1.65E-17	2.30E-17	7.40E-17
Row 24	-8.59E+00	-1.24E+02	-1.81E+01	-3.96E+02	3.45E+01	-1.09E+01	1.36E-16	-6.66E-17	-9.17E-17	1.21E-17	-1.28E-16	3.53E-17
Row 25	-1.24E+02	9.34E+00	-1.57E+01	3.67E+01	3.95E+02	1.41E+01	1.07E-16	-1.39E-16	-9.69E-17	-4.20E-17	-1.67E-16	-1.82E-17
Row 26	7.67E+00	6.97E+00	1.10E+00	2.09E+01	-2.48E+01	-2.29E+00	-5.81E-17	8.90E-18	6.50E-17	-1.08E-16	1.40E-16	-7.43E-18
Row 27	6.65E+00	-5.05E+00	-4.01E-01	-2.54E+01	-3.61E+01	-1.42E+00	1.64E-16	3.86E-17	2.75E-16	-4.70E-17	-7.57E-17	-3.88E-18
Row 28	4.54E+00	-8.55E+00	-1.54E+00	-4.81E+01	-2.65E+01	-1.97E+03	-8.97E-17	5.69E-19	-7.03E-17	5.37E-17	2.17E-17	-3.91E-17
Row 29	-8.81E+00	8.66E+00	6.72E+00	4.70E+01	4.81E+01	3.33E+02	5.61E-17	1.49E-17	1.10E-16	-6.79E-17	-2.37E-17	1.13E-16
Row 30	-2.44E+02	-7.95E+01	1.50E+00	-4.32E+02	1.30E+03	-2.71E+01	-9.91E-17	-1.30E-17	-9.89E-17	1.77E-17	3.17E-17	-9.09E-18
Row 31	7.92E+01	-2.44E+02	1.33E+00	-1.30E+03	-4.31E+02	7.56E+01	-4.71E-17	4.77E-18	3.28E-17	-4.10E-17	-1.26E-17	-3.57E-17
Row 32	-2.85E+00	9.74E+00	-8.60E-01	5.21E+01	1.98E+01	-1.64E+00	2.33E-17	1.03E-16	-1.64E-17	1.79E-16	1.05E-16	-2.35E-18
Row 33	9.59E+00	2.75E+00	-1.87E-01	1.95E+01	-5.15E+01	1.32E+01	-5.36E-17	-1.96E-17	4.90E-17	-1.69E-16	3.36E-18	-1.06E-17
Row 34	2.77E-01	-1.18E+00	-1.76E+02	-1.09E+01	5.02E+00	-1.18E+01	2.76E-18	-3.64E-18	-7.32E-17	8.48E-17	2.04E-16	-1.51E-17
Row 35	-1.35E+01	3.66E+00	1.57E+01	2.40E+01	7.63E+01	5.61E+00	-9.38E-18	5.12E-17	3.75E-18	-4.10E-17	-4.90E-17	2.77E-17
Row 36	-4.43E+00	-1.37E+01	5.26E+01	-7.70E+01	2.50E+01	-2.89E+00	-2.66E-17	7.16E-17	8.52E-18	-6.14E-17	-7.31E-17	1.08E-16

Col 13	Col 14	Col 15	Col 16	Col 17	Col 18	Col 19	Col 20	Col 21	Col 22	Col 23	Col 24
9.42E+00	-3.04E+02	1.16E+02	-4.38E+01	1.08E+00	-1.78E-01	2.00E-01	-8.23E+01	8.37E+00	-4.68E-02	6.18E+00	-8.59E+00
-3.04E+02	-9.39E+00	4.38E+01	1.16E+02	2.57E+00	-1.87E-01	2.48E-01	8.39E+00	8.24E+01	-4.43E-02	6.24E+00	-1.24E+02
6.00E-02	-1.08E-01	-4.86E-01	-6.51E-01	3.93E+01	4.00E+01	1.53E-03	5.76E-02	-7.94E-02	1.73E+00	-3.16E+02	-1.81E+01
-2.43E+03	-1.52E+02	3.23E+02	1.23E+03	2.47E+01	-1.46E+00	7.96E-01	4.58E+01	3.77E+02	-1.90E-01	1.72E+01	-3.96E+02
-1.54E+02	2.44E+03	-1.23E+03	3.25E+02	-1.31E+01	1.04E+00	-2.56E-01	3.77E+02	-4.55E+01	3.92E-02	-1.62E+01	3.45E+01
1.09E+01	-9.41E+00	9.13E+00	-8.68E+00	-4.36E+01	2.22E+01	5.00E-01	5.41E+00	4.09E+00	-1.75E+01	3.08E+01	-1.09E+01
-4.03E-17	-2.69E-16	3.39E-17	-8.44E-17	7.00E-17	4.17E-17	1.16E-16	4.23E-17	-5.22E-17	7.76E-17	-1.20E-17	1.36E-16
-1.85E-16	-7.60E-16	9.93E-17	1.96E-16	6.71E-17	6.56E-17	-1.96E-17	9.32E-17	1.62E-17	2.58E-17	3.12E-17	-6.66E-17
7.74E-17	2.39E-16	-1.59E-16	-2.10E-16	-1.54E-16	-9.31E-17	5.25E-17	-5.21E-17	-3.72E-17	-2.06E-17	-9.74E-18	-9.17E-17
-7.63E-17	-2.57E-16	1.78E-16	1.97E-16	5.23E-17	-9.68E-17	-6.02E-17	2.07E-17	8.93E-17	2.38E-17	-1.65E-17	1.21E-17
-3.54E-17	6.90E-17	1.13E-16	-4.49E-17	-1.75E-17	-1.94E-16	-4.12E-17	-7.20E-17	1.94E-17	-2.36E-18	2.30E-17	-1.28E-16
-4.81E-17	-7.09E-16	1.49E-16	-3.29E-17	8.71E-17	-7.68E-18	1.03E-16	-9.64E-17	1.58E-17	-7.59E-18	7.40E-17	3.53E-17
1.00E+00	-1.44E-16	1.10E-16	1.87E-16	-3.63E-17	4.03E-16	2.94E-16	6.03E-17	8.07E-17	-2.45E-16	-1.40E-18	-2.84E-16
-1.44E-16	1.00E+00	2.89E-16	2.17E-16	-5.69E-17	-1.72E-16	-1.61E-16	1.18E-16	-2.87E-17	-4.46E-17	-6.14E-17	1.36E-16
1.10E-16	2.89E-16	1.00E+00	1.01E-15	1.24E-16	-3.29E-16	-1.70E-16	1.21E-16	-1.59E-16	-1.69E-16	-5.03E-17	1.10E-16
1.87E-16	2.17E-16	1.01E-15	1.00E+00	-1.30E-17	-1.38E-16	-3.12E-16	2.57E-16	-5.46E-17	8.04E-17	2.05E-16	-3.82E-17
-3.63E-17	-5.69E-17	1.24E-16	-1.30E-17	1.00E+00	1.38E-16	8.11E-16	4.19E-17	-2.80E-17	3.52E-16	3.56E-17	-1.93E-17
4.03E-16	-1.72E-16	-3.29E-16	-1.38E-16	1.38E-16	1.00E+00	-7.21E-17	-8.23E-16	3.48E-16	1.88E-16	1.70E-16	-2.15E-17
2.94E-16	-1.61E-16	-1.70E-16	-3.12E-16	8.11E-16	-7.21E-17	1.00E+00	-6.17E-17	-8.27E-17	-4.48E-16	8.07E-17	-1.47E-16
6.03E-17	1.18E-16	1.21E-16	2.57E-16	4.19E-17	-8.23E-16	-6.17E-17	1.00E+00	1.14E-15	-2.13E-16	-2.30E-17	-3.70E-17
8.07E-17	-2.87E-17	-1.59E-16	-5.46E-17	-2.80E-17	3.48E-16	-8.27E-17	1.14E-15	1.00E+00	-4.37E-16	-1.94E-17	-1.31E-16
-2.45E-16	-4.46E-17	-1.69E-16	8.04E-17	3.52E-16	1.88E-16	-4.48E-16	-2.13E-16	-4.37E-16	1.00E+00	9.96E-17	-1.08E-16
-1.40E-18	-6.14E-17	-5.03E-17	2.05E-16	3.56E-17	1.70E-16	8.07E-17	-2.30E-17	-1.94E-17	9.96E-17	1.00E+00	-5.03E-16
-2.84E-16	1.36E-16	1.10E-16	-3.82E-17	-1.93E-17	-2.15E-17	-1.47E-16	-3.70E-17	-1.31E-16	-1.08E-16	-5.03E-16	1.00E+00
-3.40E-16	2.63E-16	1.10E-16	1.92E-16	2.12E-16	-1.01E-16	-1.84E-16	-9.22E-18	-1.92E-16	-2.23E-17	-4.79E-16	1.05E-16
-4.24E-16	-1.72E-16	-5.65E-17	-9.97E-18	-1.22E-16	5.88E-17	-4.62E-17	-2.10E-16	-2.04E-16	9.28E-17	-8.89E-16	-3.53E-16
-1.07E-16	-2.71E-16	1.45E-16	2.43E-17	8.86E-17	1.68E-16	1.14E-16	2.03E-16	2.80E-16	1.53E-16	2.30E-16	6.59E-17
-2.50E-17	-1.50E-17	-7.68E-17	6.96E-17	-3.28E-16	-9.02E-17	-1.16E-16	9.89E-18	1.85E-17	-8.11E-17	1.49E-16	4.24E-16
5.69E-17	8.95E-17	-4.72E-18	-9.80E-17	1.94E-16	-6.70E-18	1.97E-16	2.40E-17	-1.50E-16	1.27E-16	-4.20E-16	2.08E-17
7.77E-18	1.54E-16	3.10E-17	3.17E-17	-7.33E-17	3.16E-17	-1.71E-17	-2.97E-17	8.78E-17	-9.97E-17	2.91E-16	3.37E-16
-4.23E-18	-1.12E-16	4.47E-17	-7.26E-18	1.21E-17	-2.48E-17	5.87E-17	1.86E-17	-9.54E-17	3.80E-17	-2.14E-16	-1.33E-16
-9.16E-18	-8.32E-17	8.18E-17	5.34E-18	2.12E-17	8.13E-17	-1.56E-17	-4.69E-17	-1.02E-17	-1.81E-17	1.11E-16	3.37E-16
-1.51E-16	9.58E-17	1.45E-17	2.09E-17	-4.04E-17	4.52E-17	1.59E-17	3.99E-17	-2.30E-17	9.33E-18	1.07E-17	-1.77E-16
-5.99E-17	-5.25E-17	3.97E-18	6.24E-17	3.97E-17	7.11E-18	-7.47E-17	-1.38E-17	-4.57E-18	-9.28E-17	-3.08E-17	-1.33E-16
5.72E-17	-1.16E-16	-4.63E-17	-7.68E-17	-1.18E-17	-7.56E-17	4.88E-17	3.57E-17	-3.83E-17	4.41E-17	-2.23E-17	1.58E-16
2.66E-17	4.78E-17	1.27E-17	6.40E-18	-2.46E-18	-9.67E-17	-9.43E-17	2.82E-17	-2.21E-17	-2.71E-17	2.38E-17	4.14E-17

Col 25	Col 26	Col 27	Col 28	Col 29	Col 30	Col 31	Col 32	Col 33	Col 34	Col 35	Col 36
-1.24E+02	7.67E+00	6.65E+00	4.54E+00	-8.81E+00	-2.44E+02	7.92E+01	-2.85E+00	9.59E+00	2.77E-01	-1.35E+01	-4.43E+00
9.34E+00	6.97E+00	-5.05E+00	-8.55E+00	8.66E+00	-7.95E+01	-2.44E+02	9.74E+00	2.75E+00	-1.18E+00	3.66E+00	-1.37E+01
-1.57E+01	1.10E+00	-4.01E-01	-1.54E+00	6.72E+00	1.50E+00	1.33E+00	-8.60E-01	-1.87E-01	-1.76E+02	1.57E+01	5.26E+01
3.67E+01	2.09E+01	-2.54E+01	-4.81E+01	4.70E+01	-4.32E+02	-1.30E+03	5.21E+01	1.95E+01	-1.09E+01	2.40E+01	-7.70E+01
3.95E+02	-2.48E+01	-3.61E+01	-2.65E+01	4.81E+01	1.30E+03	-4.31E+02	1.98E+01	-5.15E+01	5.02E+00	7.63E+01	2.50E+01
1.41E+01	-2.29E+00	-1.42E+00	-1.97E+03	3.33E+02	-2.71E+01	7.56E+01	-1.64E+00	1.32E+01	-1.18E+01	5.61E+00	-2.89E+00
1.07E-16	-5.81E-17	1.64E-16	-8.97E-17	5.61E-17	-9.91E-17	-4.71E-17	2.33E-17	-5.36E-17	2.76E-18	-9.38E-18	-2.66E-17
-1.39E-16	8.90E-18	3.86E-17	5.69E-19	1.49E-17	-1.30E-17	4.77E-18	1.03E-16	-1.96E-17	-3.64E-18	5.12E-17	7.16E-17
-9.69E-17	6.50E-17	2.75E-16	-7.03E-17	1.10E-16	-9.89E-17	3.28E-17	-1.64E-17	4.90E-17	-7.32E-17	3.75E-18	8.52E-18
-4.20E-17	-1.08E-16	-4.70E-17	5.37E-17	-6.79E-17	1.77E-17	-4.10E-17	1.79E-16	-1.69E-16	8.48E-17	-4.10E-17	-6.14E-17
-1.67E-16	1.40E-16	-7.57E-17	2.17E-17	-2.37E-17	3.17E-17	-1.26E-17	1.05E-16	3.36E-18	2.04E-16	-4.90E-17	-7.31E-17
-1.82E-17	-7.43E-18	-3.88E-18	-3.91E-17	1.13E-16	-9.09E-18	-3.57E-17	-2.35E-18	-1.06E-17	-1.51E-17	2.77E-17	1.08E-16
-3.40E-16	-4.24E-16	-1.07E-16	-2.50E-17	5.69E-17	7.77E-18	-4.23E-18	-9.16E-18	-1.51E-16	-5.99E-17	5.72E-17	2.66E-17
2.63E-16	-1.72E-16	-2.71E-16	-1.50E-17	8.95E-17	1.54E-16	-1.12E-16	-8.32E-17	9.58E-17	-5.25E-17	-1.16E-16	4.78E-17
1.10E-16	-5.65E-17	1.45E-16	-7.68E-17	-4.72E-18	3.10E-17	4.47E-17	8.18E-17	1.45E-17	3.97E-18	-4.63E-17	1.27E-17
1.92E-16	-9.97E-18	2.43E-17	6.96E-17	-9.80E-17	3.17E-17	-7.26E-18	5.34E-18	2.09E-17	6.24E-17	-7.68E-17	6.40E-18
2.12E-16	-1.22E-16	8.86E-17	-3.28E-16	1.94E-16	-7.33E-17	1.21E-17	2.12E-17	-4.04E-17	3.97E-17	-1.18E-17	-2.46E-18
-1.01E-16	5.88E-17	1.68E-16	-9.02E-17	-6.70E-18	3.16E-17	-2.48E-17	8.13E-17	4.52E-17	7.11E-18	-7.56E-17	-9.67E-17
-1.84E-16	-4.62E-17	1.14E-16	-1.16E-16	1.97E-16	-1.71E-17	5.87E-17	-1.56E-17	1.59E-17	-7.47E-17	4.88E-17	-9.43E-17
-9.22E-18	-2.10E-16	2.03E-16	9.89E-18	2.40E-17	-2.97E-17	1.86E-17	-4.69E-17	3.99E-17	-1.38E-17	3.57E-17	2.82E-17
-1.92E-16	-2.04E-16	2.80E-16	1.85E-17	-1.50E-16	8.78E-17	-9.54E-17	-1.02E-17	-2.30E-17	-4.57E-18	-3.83E-17	-2.21E-17
-2.23E-17	9.28E-17	1.53E-16	-8.11E-17	1.27E-16	-9.97E-17	3.80E-17	-1.81E-17	9.33E-18	-9.28E-17	4.41E-17	-2.71E-17
-4.79E-16	-8.89E-16	2.30E-16	1.49E-16	-4.20E-16	2.91E-16	-2.14E-16	1.11E-16	1.07E-17	-3.08E-17	-2.23E-17	2.38E-17
1.05E-16	-3.53E-16	6.59E-17	4.24E-16	2.08E-17	3.37E-16	-1.33E-16	3.37E-16	-1.77E-16	-1.33E-16	1.58E-16	4.14E-17
1.00E+00	-8.02E-16	-2.35E-16	8.46E-17	-6.80E-16	1.11E-16	-4.17E-17	-7.46E-17	-5.55E-17	2.10E-16	-7.20E-17	-1.36E-17
-8.02E-16	1.00E+00	5.52E-16	1.18E-16	-1.63E-16	1.97E-17	-7.96E-17	-2.47E-17	-1.08E-19	-3.55E-17	-9.29E-17	-5.20E-17
-2.35E-16	5.52E-16	1.00E+00	4.36E-17	-3.71E-16	2.17E-16	9.15E-17	3.46E-17	-7.57E-17	9.47E-17	5.38E-17	3.74E-17
8.46E-17	1.18E-16	4.36E-17	1.00E+00	-8.22E-16	3.18E-16	-1.31E-16	2.43E-17	1.58E-16	-2.94E-16	8.84E-17	6.32E-17
-6.80E-16	-1.63E-16	-3.71E-16	-8.22E-16	1.00E+00	-7.77E-17	-3.18E-17	-3.10E-16	1.52E-16	-1.54E-16	1.39E-17	7.68E-17
1.11E-16	1.97E-17	2.17E-16	3.18E-16	-7.77E-17	1.00E+00	-5.23E-16	7.30E-18	-2.07E-16	-2.45E-16	-8.64E-17	-1.44E-16
-4.17E-17	-7.96E-17	9.15E-17	-1.31E-16	-3.18E-17	-5.23E-16	1.00E+00	-3.45E-17	8.43E-17	6.34E-17	-6.97E-17	-2.34E-17
-7.46E-17	-2.47E-17	3.46E-17	2.43E-17	-3.10E-16	7.30E-18	-3.45E-17	1.00E+00	9.96E-16	1.77E-16	3.75E-18	-2.02E-16
-5.55E-17	-1.08E-19	-7.57E-17	1.58E-16	1.52E-16	-2.07E-16	8.43E-17	9.96E-16	1.00E+00	3.51E-16	-1.15E-16	-7.23E-17
2.10E-16	-3.55E-17	9.47E-17	-2.94E-16	-1.54E-16	-2.45E-16	6.34E-17	1.77E-16	3.51E-16	1.00E+00	4.89E-16	5.43E-16
-7.20E-17	-9.29E-17	5.38E-17	8.84E-17	1.39E-17	-8.64E-17	-6.97E-17	3.75E-18	-1.15E-16	4.89E-16	1.00E+00	-1.37E-16
-1.36E-17	-5.20E-17	3.74E-17	6.32E-17	7.68E-17	-1.44E-16	-2.34E-17	-2.02E-16	-7.23E-17	5.43E-16	-1.37E-16	1.00E+00

## Damping matrix

Damping matrix	Col 1	Col 2	Col 3	Col 4	Col 5	Col 6	Col 7	Col 8	Col 9	Col 10	Col 11	Col 12
Row 1	1.55E+05	-2.92E+00	2.22E+01	6.88E+02	-1.46E+06	-4.42E+02	5.38E-01	1.38E+01	-3.22E-01	9.87E-02	3.65E-02	2.36E-02
Row 2	-2.92E+00	1.55E+05	-2.55E+01	1.45E+06	1.85E+03	9.69E+02	-1.38E+01	5.32E-01	-2.93E-01	-9.18E-02	-3.79E-02	1.51E-02
Row 3	2.22E+01	-2.55E+01	1.74E+06	-1.74E+03	-3.21E+03	-5.07E+03	2.58E-03	2.46E-03	-2.95E-04	2.07E-02	-1.68E-04	-4.92E-05
Row 4	6.88E+02	1.45E+06	-1.74E+03	1.18E+08	6.43E+04	1.25E+04	-1.21E+02	4.42E+00	-2.56E+00	-8.12E-01	-3.61E-01	1.02E-01
Row 5	-1.46E+06	1.85E+03	-3.21E+03	6.43E+04	1.19E+08	-5.98E+03	-4.58E+00	-1.21E+02	2.83E+00	-8.92E-01	-3.08E-01	-1.61E-01
Row 6	-4.42E+02	9.69E+02	-5.07E+03	1.25E+04	-5.98E+03	5.02E+07	-2.06E+00	-1.74E+00	9.50E-02	1.68E+02	1.53E-01	-9.15E-03
Row 7	5.38E-01	-1.38E+01	2.58E-03	-1.21E+02	-4.58E+00	-2.06E+00	2.33E-01	4.82E-10	1.72E-10	-5.22E-09	8.63E-09	1.68E-10
Row 8	1.38E+01	5.32E-01	2.46E-03	4.42E+00	-1.21E+02	-1.74E+00	4.82E-10	2.33E-01	-5.44E-10	-5.76E-09	-2.22E-09	-1.75E-10
Row 9	-3.22E-01	-2.93E-01	-2.95E-04	-2.56E+00	2.83E+00	9.50E-02	1.72E-10	-5.44E-10	2.40E-01	-8.76E-10	3.76E-10	7.82E-11
Row 10	9.87E-02	-9.18E-02	2.07E-02	-8.12E-01	-8.92E-01	1.68E+02	-5.22E-09	-5.76E-09	-8.76E-10	2.99E-01	2.92E-10	-1.92E-10
Row 11	3.65E-02	-3.79E-02	-1.68E-04	-3.61E-01	-3.08E-01	1.53E-01	8.63E-09	-2.22E-09	3.76E-10	1.92E-10	3.24E-01	-3.64E-11
Row 12	2.36E-02	1.51E-02	-4.92E-05	1.02E-01	-1.61E-01	-9.15E-03	1.68E-10	-1.75E-10	7.82E-11	-1.92E-10	-3.64E-11	4.71E-01
Row 13	1.80E-01	-5.80E+00	1.14E-03	-4.64E+01	-2.94E+00	2.08E-01	2.09E-09	-1.61E-10	1.11E-10	-4.35E-09	6.51E-09	2.63E-10
Row 14	-5.81E+00	-1.79E-01	-2.06E-03	-2.90E+00	4.65E+01	-1.80E-01	4.30E-10	-5.31E-09	3.27E-10	3.62E-09	2.61E-09	4.99E-10
Row 15	2.22E+00	8.35E-01	-9.27E-03	6.16E+00	-2.34E+01	1.74E-01	-4.10E-10	4.62E-09	-2.70E-10	-7.01E-09	-2.54E-10	-4.78E-10
Row 16	-8.36E-01	2.22E+00	-1.24E-02	2.34E+01	6.19E+00	-1.66E-01	-2.02E-09	-1.13E-10	-2.30E-10	2.75E-09	-1.79E-09	1.06E-10
Row 17	2.05E-02	4.90E-02	7.50E-01	4.71E-01	-2.49E-01	-8.32E-01	1.17E-10	-3.75E-10	-2.60E-10	3.12E-10	-9.18E-10	-8.51E-11
Row 18	-3.39E-03	-3.56E-03	7.64E-01	-2.79E-02	1.99E-02	4.24E-01	-7.28E-10	1.37E-10	-1.19E-11	-9.50E-11	5.71E-10	3.01E-11
Row 19	3.82E-03	4.72E-03	2.93E-05	1.52E-02	-4.90E-03	9.54E-03	-6.35E-10	1.33E-09	1.68E-11	5.14E-11	-7.24E-11	-5.43E-11
Row 20	-1.57E+00	1.60E-01	1.10E-03	8.73E-01	7.19E+00	1.03E-01	2.33E-10	6.43E-10	-2.72E-10	-3.62E-09	-2.22E-10	-2.64E-10
Row 21	1.60E-01	1.57E+00	-1.52E-03	7.19E+00	-8.69E-01	7.81E-02	-5.97E-11	2.72E-11	1.90E-10	-1.75E-09	9.03E-10	1.37E-10
Row 22	-8.93E-04	-8.45E-04	3.30E-02	-3.61E-03	7.51E-04	-3.34E-01	-4.88E-10	-2.94E-10	-4.11E-11	-4.74E-11	-6.28E-10	-3.02E-11
Row 23	1.18E-01	1.19E-01	-6.03E+00	3.28E-01	-3.09E-01	5.88E-01	1.05E-08	1.68E-09	7.37E-10	-6.37E-10	7.55E-09	-2.14E-10
Row 24	-1.64E-01	-2.36E+00	-3.46E-01	-7.55E+00	6.58E-01	-2.07E-01	-4.28E-09	5.19E-11	-4.96E-10	4.89E-09	8.55E-09	-5.78E-10
Row 25	-2.36E+00	1.78E-01	-3.00E-01	7.01E-01	7.54E+00	2.70E-01	6.08E-10	2.35E-09	-7.64E-11	-7.47E-09	2.68E-09	-6.89E-10
Row 26	1.46E-01	1.33E-01	2.09E-02	3.99E-01	-4.73E-01	-4.37E-02	-4.07E-09	7.40E-09	-1.76E-09	1.02E-08	-6.62E-10	-1.06E-09
Row 27	1.27E-01	-9.63E-02	-7.66E-03	-4.84E-01	-6.89E-01	-2.70E-02	3.22E-09	-1.12E-09	-8.23E-10	-5.31E-10	4.50E-09	6.86E-10
Row 28	8.67E-02	-1.63E-01	-2.94E-02	-9.18E-01	-5.06E-01	-3.76E+01	-1.23E-09	-2.74E-09	-3.79E-10	1.87E-09	-1.89E-10	6.83E-10
Row 29	-1.68E-01	1.65E-01	1.28E-01	8.97E-01	9.17E-01	6.35E+00	4.74E-09	2.28E-09	-5.07E-10	-4.85E-09	6.51E-10	1.21E-09
Row 30	-4.66E+00	-1.52E+00	2.85E-02	-8.23E+00	2.48E+01	-5.17E-01	4.95E-11	3.44E-09	-5.40E-10	-2.49E-09	-3.44E-09	-8.50E-11
Row 31	1.51E+00	-4.65E+00	2.53E-02	-2.48E+01	-8.22E+00	1.44E+00	-1.67E-09	-2.09E-09	2.63E-11	1.42E-10	-5.13E-09	1.53E-10
Row 32	-5.44E-02	1.86E-01	-1.64E-02	9.94E-01	3.77E-01	-3.13E-02	-5.37E-10	-1.38E-10	1.08E-09	7.29E-10	9.80E-10	5.48E-10
Row 33	1.83E-01	5.24E-02	-3.58E-03	3.72E-01	-9.82E-01	2.52E-01	5.38E-10	-7.88E-11	-5.01E-10	-1.65E-09	-8.05E-10	-7.13E-10
Row 34	5.28E-03	-2.25E-02	-3.35E+00	-2.08E-01	9.58E-02	-2.26E-01	-2.07E-10	-5.36E-10	1.52E-10	-8.03E-10	6.50E-11	-2.66E-10
Row 35	-2.58E-01	6.98E-02	2.99E-01	4.58E-01	1.46E+00	1.07E-01	2.34E-10	-7.43E-11	-2.81E-10	-5.28E-09	6.36E-10	-2.91E-10
Row 36	-8.45E-02	-2.62E-01	1.00E+00	-1.47E+00	4.78E-01	-5.51E-02	4.06E-10	-1.70E-09	-5.44E-10	-6.75E-10	9.60E-10	-1.16E-09

Col 13	Col 14	Col 15	Col 16	Col 17	Col 18	Col 19	Col 20	Col 21	Col 22	Col 23	Col 24
1.80E-01	-5.81E+00	2.22E+00	-8.36E-01	2.05E-02	-3.39E-03	3.82E-03	-1.57E+00	1.60E-01	-8.93E-04	1.18E-01	-1.64E-01
-5.80E+00	-1.79E-01	8.35E-01	2.22E+00	4.90E-02	-3.56E-03	4.72E-03	1.60E-01	1.57E+00	-8.45E-04	1.19E-01	-2.36E+00
1.14E-03	-2.06E-03	-9.27E-03	-1.24E-02	7.50E-01	7.64E-01	2.93E-05	1.10E-03	-1.52E-03	3.30E-02	-6.03E+00	-3.46E-01
-4.64E+01	-2.90E+00	6.16E+00	2.34E+01	4.71E-01	-2.79E-02	1.52E-02	8.73E-01	7.19E+00	-3.61E-03	3.28E-01	-7.55E+00
-2.94E+00	4.65E+01	-2.34E+01	6.19E+00	-2.49E-01	1.99E-02	-4.90E-03	7.19E+00	-8.69E-01	7.51E-04	-3.09E-01	6.58E-01
2.08E-01	-1.80E-01	1.74E-01	-1.66E-01	-8.32E-01	4.24E-01	9.54E-03	1.03E-01	7.81E-02	-3.34E-01	5.88E-01	-2.07E-01
2.09E-09	4.30E-10	-4.10E-10	-2.02E-09	1.17E-10	-7.28E-10	-6.35E-10	2.33E-10	-5.97E-11	-4.88E-10	1.05E-08	-4.28E-09
-1.61E-10	-5.31E-09	4.62E-09	-1.13E-10	-3.75E-10	1.37E-10	1.33E-09	6.43E-10	2.72E-11	-2.94E-10	1.68E-09	5.19E-11
1.11E-10	3.27E-10	-2.70E-10	-2.30E-10	-2.60E-10	-1.19E-11	1.68E-11	-2.72E-10	1.90E-10	-4.11E-11	7.37E-10	-4.96E-10
-4.35E-09	3.62E-09	-7.01E-09	2.75E-09	3.12E-10	-9.50E-11	5.14E-11	-3.62E-09	-1.75E-09	-4.74E-11	-6.37E-10	4.89E-09
6.51E-09	2.61E-09	-2.54E-10	-1.79E-09	-9.18E-10	5.71E-10	-7.24E-11	-2.22E-10	9.03E-10	-6.28E-10	7.55E-09	8.55E-09
2.63E-10	4.99E-10	-4.78E-10	1.06E-10	-8.51E-11	3.01E-11	-5.43E-11	-2.64E-10	1.37E-10	-3.02E-11	-2.14E-10	-5.78E-10
5.09E-01	-2.52E-10	7.66E-10	-1.52E-09	1.44E-10	-3.36E-10	-3.56E-10	1.24E-10	1.98E-10	-2.71E-10	6.40E-09	-3.42E-09
-2.52E-10	5.09E-01	-3.05E-09	-2.53E-10	1.07E-09	-3.69E-10	-1.09E-09	-3.54E-10	-4.04E-11	8.02E-11	-7.57E-10	-6.14E-10
7.66E-10	-3.05E-09	5.45E-01	2.45E-10	-1.23E-09	3.14E-10	1.01E-09	3.99E-10	1.40E-11	-1.53E-10	1.40E-09	1.82E-10
-1.52E-09	-2.53E-10	2.45E-10	5.45E-01	-3.55E-10	4.68E-10	4.51E-10	-1.53E-10	7.66E-11	2.31E-10	-7.25E-09	3.40E-09
1.44E-10	1.07E-09	-1.23E-09	-3.55E-10	5.48E-01	1.94E-10	1.55E-10	-8.47E-10	4.05E-10	-1.62E-10	-1.09E-09	-1.15E-09
-3.36E-10	-3.69E-10	3.14E-10	4.68E-10	1.94E-10	6.09E-01	-6.50E-11	1.62E-10	-2.34E-10	8.34E-11	-1.58E-09	-9.35E-10
-3.56E-10	-1.09E-09	1.01E-09	4.51E-10	1.55E-10	-6.50E-11	7.07E-01	3.29E-10	-1.75E-10	-2.93E-11	-2.50E-10	6.14E-10
1.24E-10	-3.54E-10	3.99E-10	-1.53E-10	-8.47E-10	1.62E-10	3.29E-10	7.77E-01	-1.56E-10	2.45E-11	8.98E-10	3.72E-10
1.98E-10	-4.04E-11	1.40E-11	7.66E-11	4.05E-10	-2.34E-10	-1.75E-10	-1.56E-10	7.77E-01	-1.37E-10	2.29E-09	-1.84E-09
-2.71E-10	8.02E-11	-1.53E-10	2.31E-10	-1.62E-10	8.34E-11	-2.93E-11	2.45E-11	-1.37E-10	8.92E-01	-1.24E-09	-8.04E-10
6.40E-09	-7.57E-10	1.04E-09	-7.25E-09	-1.09E-09	-1.58E-09	-2.50E-10	8.98E-10	2.29E-09	-1.24E-09	1.61E+00	1.27E-08
-3.42E-09	-6.14E-10	1.82E-10	3.40E-09	-1.15E-09	-9.35E-10	6.14E-10	3.72E-10	-1.84E-09	-8.04E-10	1.27E-08	1.67E+00
5.48E-10	-2.06E-09	2.77E-09	-4.99E-10	-8.16E-12	4.88E-10	8.02E-10	1.70E-09	-6.74E-12	4.92E-10	-5.52E-09	1.53E-09
-2.45E-09	-6.15E-09	6.08E-09	2.62E-09	5.43E-10	-9.80E-11	2.93E-09	2.68E-09	-1.78E-09	3.76E-11	-2.83E-09	1.22E-08
3.29E-09	7.00E-10	-9.02E-10	-2.58E-09	4.52E-10	2.94E-10	-3.78E-10	3.25E-10	7.17E-10	3.37E-10	-4.88E-09	6.27E-09
-2.27E-09	1.98E-09	-2.38E-09	1.68E-09	2.77E-11	-2.06E-10	3.40E-10	-1.54E-09	2.49E-11	-3.04E-10	2.87E-10	3.24E-09
4.12E-09	-5.93E-10	8.04E-10	-3.98E-09	-3.83E-10	-5.89E-11	-4.54E-10	1.29E-10	1.98E-09	-1.70E-10	1.11E-09	-8.66E-09
6.56E-10	-2.35E-09	1.62E-09	-2.14E-10	4.24E-10	3.05E-10	4.45E-10	5.95E-10	-7.77E-11	2.61E-10	-4.12E-09	1.28E-09
-1.57E-09	8.54E-10	-1.22E-09	1.18E-09	5.00E-10	9.33E-10	-2.88E-11	-5.61E-10	-3.85E-10	6.54E-10	-1.13E-08	3.61E-09
8.72E-11	-1.10E-09	9.40E-10	-7.92E-11	9.18E-11	8.95E-11	5.32E-10	-1.41E-09	9.26E-10	-5.61E-10	3.06E-09	-5.07E-10
5.88E-10	1.06E-09	-8.28E-10	-1.34E-09	-2.36E-10	6.37E-11	-2.55E-10	4.13E-10	-2.84E-10	1.19E-10	-8.86E-11	-2.30E-09
-5.98E-10	4.29E-10	-1.23E-09	-2.32E-10	3.77E-10	7.99E-11	8.30E-11	-6.46E-10	2.12E-10	1.42E-11	-1.24E-09	8.29E-10
5.62E-10	-9.18E-11	3.19E-10	-2.55E-10	-2.62E-11	1.21E-10	2.28E-10	4.65E-10	1.97E-10	1.85E-10	-2.19E-09	-1.13E-09
3.22E-11	1.19E-09	-8.60E-10	-3.05E-10	-4.31E-10	-4.86E-10	-1.62E-10	1.03E-09	-9.62E-10	7.68E-11	3.44E-09	5.04E-09

Col 25	Col 26	Col 27	Col 28	Col 29	Col 30	Col 31	Col 32	Col 33	Col 34	Col 35	Col 36
-2.36E+00	1.46E-01	1.27E-01	8.67E-02	-1.68E-01	-4.66E+00	1.51E+00	-5.44E-02	1.83E-01	5.28E-03	-2.58E-01	-8.45E-02
1.78E-01	1.33E-01	-9.63E-02	-1.63E-01	1.65E-01	-1.52E+00	-4.65E+00	1.86E-01	5.24E-02	-2.25E-02	6.98E-02	-2.62E-01
-3.00E-01	2.09E-02	-7.66E-03	-2.94E-02	1.28E-01	2.85E-02	2.53E-02	-1.64E-02	-3.58E-03	-3.35E+00	2.99E-01	1.00E+00
7.01E-01	3.99E-01	-4.84E-01	-9.18E-01	8.97E-01	-8.23E+00	-2.48E+01	9.94E-01	3.72E-01	-2.08E-01	4.58E-01	-1.47E+00
7.54E+00	-4.73E-01	-6.89E-01	-5.06E-01	9.17E-01	2.48E+00	-8.22E+00	3.77E-01	-9.82E-01	9.58E-02	1.46E+00	4.78E-01
2.70E-01	-4.37E-02	-2.70E-02	-3.76E+01	6.35E+00	-5.17E-01	1.44E+00	-3.13E-02	2.52E-01	-2.26E-01	1.07E-01	-5.51E-02
6.08E-10	-4.07E-09	3.22E-09	-1.23E-09	4.74E-09	4.95E-11	-1.67E-09	-5.37E-10	5.38E-10	-2.07E-10	2.34E-10	4.06E-10
2.35E-09	7.40E-09	-1.12E-09	-2.74E-09	2.28E-09	3.44E-09	-2.09E-09	-1.38E-10	-7.88E-11	-5.36E-10	-7.43E-11	-1.70E-09
-7.64E-11	-1.76E-09	-8.23E-10	-3.79E-10	-5.07E-10	-5.40E-10	2.63E-11	1.08E-09	-5.01E-10	1.52E-10	-2.81E-10	-5.44E-10
-7.47E-09	1.02E-08	-5.31E-10	1.87E-09	-4.85E-09	-2.49E-09	1.42E-10	7.29E-10	-1.65E-09	-8.03E-10	-5.28E-09	-6.75E-10
2.68E-09	-6.62E-10	4.50E-09	-1.89E-10	6.51E-10	-3.44E-09	-5.13E-09	9.80E-10	-8.05E-10	6.50E-11	6.36E-10	9.60E-10
-6.89E-10	-1.06E-09	6.86E-10	6.83E-10	1.21E-09	-8.50E-11	1.53E-10	5.48E-10	-7.13E-10	-2.66E-10	-2.91E-10	-1.16E-09
5.48E-10	-2.45E-09	3.29E-09	-2.27E-09	4.12E-09	6.56E-10	-1.57E-09	8.72E-11	5.88E-10	-5.98E-10	5.62E-10	3.22E-11
-2.06E-09	-6.15E-09	7.00E-10	1.98E-09	-5.93E-10	-2.35E-09	8.54E-10	-1.10E-09	1.06E-09	4.29E-10	-9.18E-11	1.19E-09
2.77E-09	6.08E-09	-9.02E-10	-2.38E-09	8.04E-10	1.62E-09	-1.22E-09	9.40E-10	-8.28E-10	-1.23E-09	3.19E-10	-8.60E-10
-4.99E-10	2.62E-09	-2.58E-09	1.68E-09	-3.98E-09	-2.14E-10	1.18E-09	-7.92E-11	-1.34E-09	-2.32E-10	-2.55E-10	-3.05E-10
-8.16E-12	5.43E-10	4.52E-10	2.77E-11	-3.83E-10	4.24E-10	5.00E-10	9.18E-11	-2.36E-10	3.77E-10	-2.62E-11	-4.31E-10
4.88E-10	-9.80E-11	2.94E-10	-2.06E-10	-5.89E-11	3.05E-10	9.33E-10	8.95E-11	6.37E-11	7.99E-11	1.21E-10	-4.86E-10
8.02E-10	2.93E-09	-3.78E-10	3.40E-10	-4.54E-10	4.45E-10	-2.88E-11	5.32E-10	-2.55E-10	8.30E-11	2.28E-10	-1.62E-10
1.70E-09	2.68E-09	3.25E-10	-1.54E-09	1.29E-10	5.95E-10	-5.61E-10	-1.41E-09	4.13E-10	-6.46E-10	4.65E-10	1.03E-09
-6.74E-12	-1.78E-09	7.17E-10	2.49E-11	1.98E-09	-7.77E-11	-3.85E-10	9.26E-10	-2.84E-10	2.12E-10	1.97E-10	-9.62E-10
4.92E-10	3.76E-11	3.37E-10	-3.04E-10	-1.70E-10	2.61E-10	6.54E-10	-5.61E-10	1.19E-10	1.42E-11	1.85E-10	7.68E-11
-5.52E-09	-2.83E-09	-4.88E-09	2.87E-10	1.11E-09	-4.12E-09	-1.13E-08	3.06E-09	-8.86E-11	-1.24E-09	-2.19E-09	3.44E-09
1.53E-09	1.22E-08	6.27E-09	3.24E-09	-8.66E-09	1.28E-09	3.61E-09	-5.07E-10	-2.30E-09	8.29E-10	-1.13E-09	5.04E-09
1.67E+00	1.53E-08	9.46E-10	-3.64E-09	7.00E-09	-5.66E-09	1.73E-09	-1.28E-09	-2.58E-11	-7.20E-10	6.81E-09	1.13E-09
1.53E-08	1.74E+00	-2.74E-09	2.78E-09	-6.10E-09	3.96E-09	-1.23E-09	2.40E-09	1.43E-09	-5.08E-10	2.62E-09	4.35E-09
9.46E-10	-2.74E-09	2.03E+00	-7.51E-10	-1.30E-09	-2.43E-09	-3.41E-09	3.81E-10	2.64E-09	1.21E-10	3.46E-11	3.11E-09
-3.64E-09	2.78E-09	-7.51E-10	2.20E+00	-8.73E-10	-1.48E-09	7.73E-10	9.46E-10	-1.70E-10	3.44E-10	-2.05E-09	-6.50E-10
7.00E-09	-6.10E-09	-1.30E-09	-8.73E-10	2.32E+00	1.54E-10	3.09E-10	-7.61E-10	1.61E-09	1.23E-09	1.80E-09	1.48E-09
-5.66E-09	3.96E-09	-2.43E-09	-1.48E-09	1.54E-10	2.43E+00	-1.75E-09	-3.26E-11	1.41E-09	-4.96E-10	-1.48E-09	-1.35E-09
1.73E-09	-1.23E-09	-3.41E-09	7.73E-10	3.09E-10	-1.75E-09	2.43E+00	1.38E-11	-4.45E-10	3.15E-10	9.58E-10	-7.44E-10
-1.28E-09	2.40E-09	3.81E-10	9.46E-10	-7.61E-10	-3.26E-11	1.38E-11	2.56E+00	1.27E-09	1.71E-09	-1.13E-10	1.15E-09
-2.58E-11	1.43E-09	2.64E-09	-1.70E-10	1.61E-09	1.41E-09	-4.45E-10	1.27E-09	2.56E+00	9.72E-11	9.02E-10	-1.34E-09
-7.20E-10	-5.08E-10	1.21E-10	3.44E-10	1.23E-09	-4.96E-10	3.15E-10	1.71E-09	9.72E-11	3.06E+00	4.42E-10	-9.99E-11
6.81E-09	2.62E-09	3.46E-11	-2.05E-09	1.80E-09	-1.48E-09	9.58E-10	-1.13E-10	9.02E-10	4.42E-10	3.09E+00	-3.61E-10
1.13E-09	4.35E-09	3.11E-09	-6.50E-10	1.48E-09	-1.35E-09	-7.44E-10	1.15E-09	-1.34E-09	-9.99E-11	-3.61E-10	3.09E+00

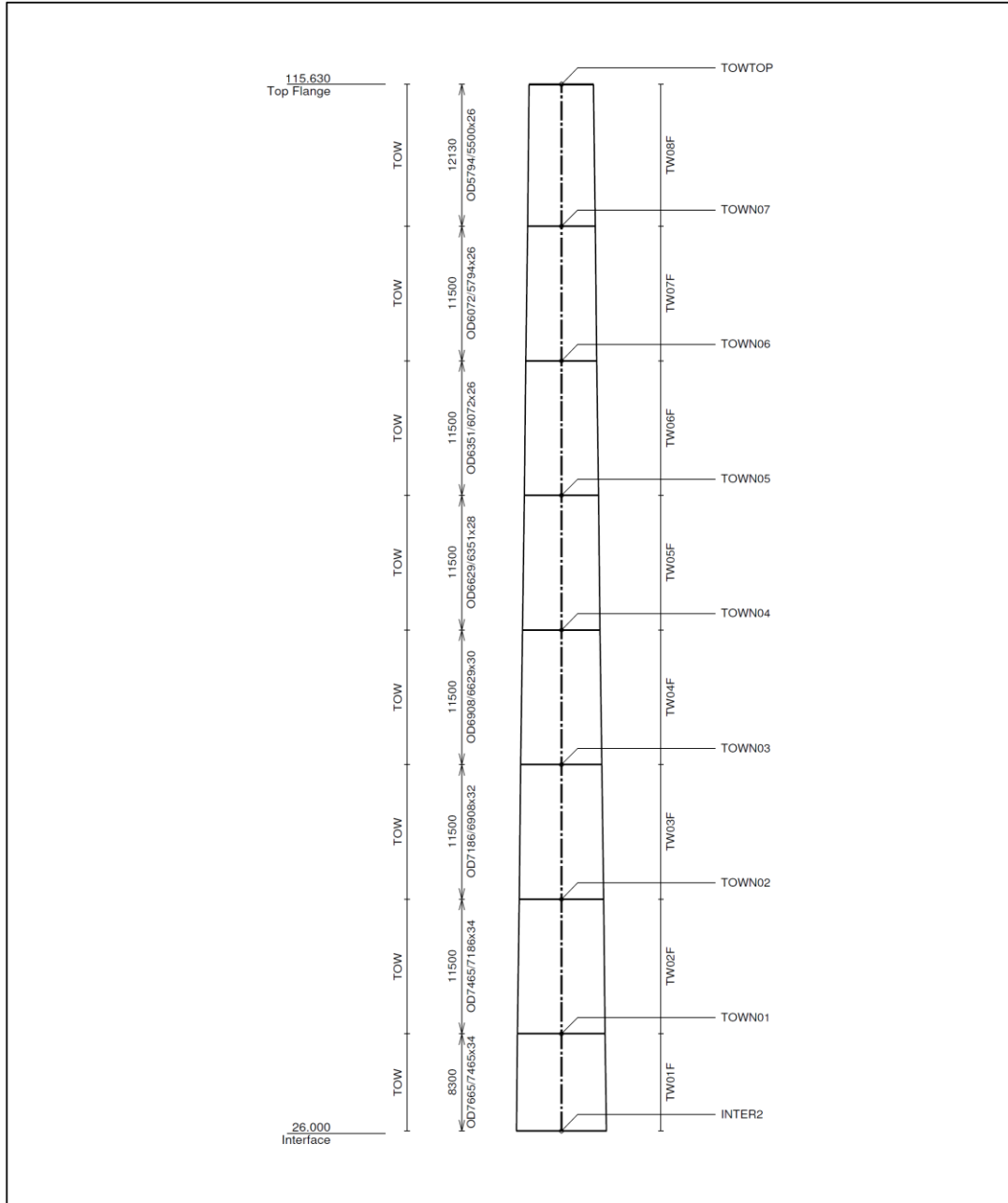
## Stiffness matrix

Stiffness matrix	Col 1	Col 2	Col 3	Col 4	Col 5	Col 6	Col 7	Col 8	Col 9	Col 10	Col 11	Col 12
Row 1	9.27E+07	-1.72E+03	2.13E+04	4.81E+05	-8.89E+08	-4.34E+03	1.81E-04	1.30E-03	-2.35E-04	-2.44E-03	-8.02E-04	-1.06E-04
Row 2	-1.72E+03	9.27E+07	-1.03E+04	8.88E+08	1.19E+06	1.55E+05	-9.40E-04	-1.66E-04	-1.09E-04	1.99E-03	-5.48E-03	-2.95E-06
Row 3	2.13E+04	-1.03E+04	1.15E+09	-1.15E+06	-2.09E+06	-3.50E+06	-1.69E-03	-2.24E-05	6.64E-05	-3.39E-05	1.08E-03	-7.55E-05
Row 4	4.81E+05	8.88E+08	-1.15E+06	7.82E+10	4.23E+07	4.43E+06	-8.56E-03	-2.10E-03	-1.50E-03	2.35E-02	-4.58E-02	3.54E-04
Row 5	-8.89E+08	1.19E+06	-2.09E+06	4.23E+07	7.83E+10	-6.18E+06	-2.23E-03	-1.19E-02	3.07E-03	2.85E-02	7.27E-03	3.45E-04
Row 6	-4.34E+03	1.55E+05	-3.50E+06	4.43E+06	-6.18E+06	3.23E+10	-3.16E-02	-3.36E-02	-6.28E-04	3.25E-02	1.56E-03	-1.96E-03
Row 7	1.81E-04	-9.40E-04	-1.69E-03	-8.56E-03	-2.23E-03	-3.16E-02	1.42E+02	3.21E-07	1.15E-07	-3.47E-06	5.74E-06	1.12E-07
Row 8	1.30E-03	-1.66E-04	-2.24E-05	-2.10E-03	-1.19E-02	-3.36E-02	3.21E-07	1.42E+02	-3.62E-07	-3.83E-06	-1.48E-06	-1.17E-07
Row 9	-2.35E-04	-1.09E-04	6.64E-05	-1.50E-03	3.07E-03	-6.28E-04	1.15E-07	-3.62E-07	1.47E+02	-5.83E-07	2.50E-07	5.21E-08
Row 10	-2.44E-03	1.99E-03	-3.39E-05	2.35E-02	2.85E-02	3.25E-02	-3.47E-06	-3.83E-06	-5.83E-07	1.87E+02	1.95E-07	-1.28E-07
Row 11	-8.02E-04	-5.48E-03	1.08E-03	-4.58E-02	7.27E-03	1.56E-03	5.74E-06	-1.48E-06	2.50E-07	1.95E-07	2.03E+02	-2.42E-08
Row 12	-1.06E-04	-2.95E-06	-7.55E-05	3.54E-04	3.45E-04	-1.96E-03	1.12E-07	-1.17E-07	5.21E-08	-1.28E-07	-2.42E-08	3.01E+02
Row 13	5.43E-05	-5.12E-04	-1.39E-03	-1.04E-02	8.68E-04	-2.16E-02	1.39E-06	-1.07E-07	7.36E-08	-2.89E-06	4.33E-06	1.75E-07
Row 14	-2.81E-03	-1.34E-04	4.52E-04	-3.17E-03	2.67E-02	2.02E-02	2.86E-07	-3.54E-06	2.18E-07	2.41E-06	1.74E-06	3.32E-07
Row 15	2.21E-03	1.72E-04	-5.57E-05	1.73E-03	-2.31E-02	-3.64E-02	-2.73E-07	3.08E-06	-1.80E-07	-4.67E-06	-1.69E-07	-3.18E-07
Row 16	-5.01E-05	7.74E-04	5.39E-04	9.06E-03	4.88E-04	1.42E-02	-1.34E-06	-7.54E-08	-1.53E-07	1.83E-06	-1.19E-06	7.07E-08
Row 17	-2.83E-04	-3.37E-04	1.16E-07	-3.11E-03	2.79E-03	-5.53E-04	7.78E-08	-2.50E-07	-1.73E-07	2.08E-07	-6.11E-07	-5.67E-08
Row 18	7.68E-05	4.47E-04	1.47E-04	3.88E-03	-7.76E-04	-1.20E-05	-4.84E-07	9.11E-08	-7.92E-09	-6.32E-08	3.80E-07	2.00E-08
Row 19	5.46E-04	2.88E-04	-1.30E-05	3.23E-03	-6.33E-03	1.51E-04	-4.23E-07	8.83E-07	1.12E-08	3.42E-08	-4.82E-08	-3.61E-08
Row 20	3.63E-04	-9.78E-05	-6.93E-05	-8.32E-04	-3.10E-03	-1.83E-02	1.55E-07	4.28E-07	-1.81E-07	-2.41E-06	-1.48E-07	-1.76E-07
Row 21	5.06E-06	1.68E-05	-2.58E-04	1.81E-04	-1.10E-05	-8.83E-03	-3.97E-08	1.81E-08	1.27E-07	-1.16E-06	6.01E-07	9.10E-08
Row 22	-1.85E-04	2.55E-04	1.36E-04	2.05E-03	1.47E-03	-1.13E-04	-3.25E-07	-1.96E-07	-2.74E-08	-3.16E-08	-4.18E-07	-2.01E-08
Row 23	1.29E-03	-6.05E-03	-3.04E-03	-5.11E-02	-1.08E-02	-4.39E-03	6.96E-06	1.12E-06	4.91E-07	-4.24E-07	5.03E-06	-1.43E-07
Row 24	-9.51E-05	1.31E-03	-2.23E-03	2.15E-02	1.33E-04	2.57E-02	-2.85E-06	3.46E-08	-3.30E-07	3.26E-06	5.69E-06	-3.85E-07
Row 25	1.33E-04	-2.06E-04	7.12E-04	-1.27E-03	-1.18E-02	-3.83E-02	4.05E-07	1.56E-06	-5.08E-08	-4.97E-06	1.78E-06	-4.59E-07
Row 26	3.13E-03	1.81E-03	2.43E-04	2.07E-02	-3.68E-02	5.07E-02	-2.71E-06	4.93E-06	-1.17E-06	6.76E-06	-4.41E-07	-7.08E-07
Row 27	-5.02E-04	-2.40E-03	1.03E-03	-1.90E-02	4.41E-03	-1.27E-03	2.15E-06	-7.44E-07	-5.48E-07	-3.54E-07	3.00E-06	4.57E-07
Row 28	-1.26E-03	3.38E-04	8.10E-05	8.13E-03	1.28E-02	9.06E-03	-8.17E-07	-1.83E-06	-2.52E-07	1.24E-06	-1.26E-07	4.55E-07
Row 29	1.04E-03	-2.39E-03	-6.77E-05	-2.44E-02	-1.28E-02	-2.54E-02	3.15E-06	1.51E-06	-3.38E-07	-3.23E-06	4.34E-07	8.04E-07
Row 30	2.26E-03	-1.49E-04	7.28E-04	-4.20E-05	-1.73E-02	-1.34E-02	3.30E-08	2.29E-06	-3.59E-07	-1.66E-06	-2.29E-06	-5.66E-08
Row 31	-1.31E-03	7.48E-04	1.95E-03	7.61E-03	1.06E-02	9.33E-04	-1.11E-06	-1.39E-06	1.75E-08	9.45E-08	-3.41E-06	1.02E-07
Row 32	1.10E-04	5.01E-04	-2.26E-04	-1.97E-03	2.17E-03	8.92E-04	-3.58E-07	-9.18E-08	7.20E-07	4.85E-07	6.52E-07	3.65E-07
Row 33	-4.44E-05	-3.74E-04	-8.06E-05	-3.03E-03	5.86E-04	-8.02E-03	3.58E-07	-5.25E-08	-3.33E-07	-1.10E-06	-5.36E-07	-4.75E-07
Row 34	-1.43E-04	-1.11E-04	4.75E-04	2.15E-04	2.28E-03	-5.55E-03	-1.38E-07	-3.57E-07	1.01E-07	-5.35E-07	4.32E-08	-1.77E-07
Row 35	-4.87E-04	-2.97E-05	2.45E-04	7.14E-04	2.97E-04	-2.41E-02	1.56E-07	-4.95E-08	-1.87E-07	-3.52E-06	4.24E-07	-1.94E-07
Row 36	-8.60E-04	-4.46E-04	-8.71E-04	9.96E-05	7.11E-03	-3.90E-03	2.70E-07	-1.13E-06	-3.62E-07	-4.49E-07	6.39E-07	-7.74E-07

Col 13	Col 14	Col 15	Col 16	Col 17	Col 18	Col 19	Col 20	Col 21	Col 22	Col 23	Col 24
5.43E-05	-2.81E-03	2.21E-03	-5.01E-05	-2.83E-04	7.68E-05	5.46E-04	3.63E-04	5.06E-06	-1.85E-04	1.29E-03	-9.51E-05
-5.12E-04	-1.34E-04	1.72E-04	7.74E-04	-3.37E-04	4.47E-04	2.88E-04	-9.78E-05	1.68E-05	2.55E-04	-6.05E-03	1.31E-03
-1.39E-03	4.52E-04	-5.57E-05	5.39E-04	1.16E-07	1.47E-04	-1.30E-05	-6.93E-05	-2.58E-04	1.36E-04	-3.04E-03	-2.23E-03
-1.04E-02	-3.17E-03	1.73E-03	9.06E-03	-3.11E-03	3.88E-03	3.23E-03	-8.32E-04	1.81E-04	2.05E-03	-5.11E-02	2.15E-02
8.68E-04	2.67E-02	-2.31E-02	4.88E-04	2.79E-03	-7.76E-04	-6.33E-03	-3.10E-03	-1.10E-05	1.47E-03	-1.08E-02	1.33E-04
-2.16E-02	2.02E-02	-3.64E-02	1.42E-02	-5.53E-04	-1.20E-05	1.51E-04	-1.83E-02	-8.83E-03	-1.13E-04	-4.39E-03	2.57E-02
1.39E-06	2.86E-07	-2.73E-07	-1.34E-06	7.78E-08	-4.84E-07	-4.23E-07	1.55E-07	-3.97E-08	-3.25E-07	6.96E-06	-2.85E-06
-1.07E-07	-3.54E-06	3.08E-06	-7.54E-08	-2.50E-07	9.11E-08	8.83E-07	4.28E-07	1.81E-08	-1.96E-07	1.12E-06	3.46E-08
7.36E-08	2.18E-07	-1.80E-07	-1.53E-07	-1.73E-07	-7.92E-09	1.12E-08	-1.81E-07	1.27E-07	-2.74E-08	4.91E-07	-3.30E-07
-2.89E-06	2.41E-06	-4.67E-06	1.83E-06	2.08E-07	-6.32E-08	3.42E-08	-2.41E-06	-1.16E-06	-3.16E-08	-4.24E-07	3.26E-06
4.33E-06	1.74E-06	-1.69E-07	-1.19E-06	-6.11E-07	3.80E-07	-4.82E-08	-1.48E-07	6.01E-07	-4.18E-07	5.03E-06	5.69E-06
1.75E-07	3.32E-07	-3.18E-07	7.07E-08	-5.67E-08	2.00E-08	-3.61E-08	-1.76E-07	9.10E-08	-2.01E-08	-1.43E-07	-3.85E-07
3.26E+02	-1.68E-07	5.10E-07	-1.01E-06	9.59E-08	-2.24E-07	-2.37E-07	8.28E-08	1.32E-07	-1.81E-07	4.26E-06	-2.28E-06
-1.68E-07	3.26E+02	-2.03E-06	-1.68E-07	7.15E-07	-2.46E-07	-7.26E-07	-2.36E-07	-2.69E-08	5.34E-08	-5.04E-07	-4.08E-07
5.10E-07	-2.03E-06	3.50E+02	1.63E-07	-8.17E-07	2.09E-07	6.73E-07	2.66E-07	9.32E-09	-1.02E-07	6.90E-07	1.21E-07
-1.01E-06	-1.68E-07	1.63E-07	3.50E+02	-2.37E-07	3.12E-07	3.00E-07	-1.02E-07	5.10E-08	1.54E-07	-4.83E-06	2.26E-06
9.59E-08	7.15E-07	-8.17E-07	-2.37E-07	3.52E+02	1.29E-07	1.03E-07	-5.64E-07	2.69E-07	-1.08E-07	-7.29E-07	-7.66E-07
-2.24E-07	-2.46E-07	2.09E-07	3.12E-07	1.29E-07	3.93E+02	-4.33E-08	1.08E-07	-1.56E-07	5.55E-08	-1.05E-06	-6.23E-07
-2.37E-07	-7.26E-07	6.73E-07	3.00E-07	1.03E-07	-4.33E-08	4.58E+02	2.19E-07	-1.17E-07	-1.95E-08	-1.67E-07	4.09E-07
8.28E-08	-2.36E-07	2.66E-07	-1.02E-07	-5.64E-07	1.08E-07	2.19E-07	5.05E+02	-1.04E-07	1.63E-08	5.98E-07	2.48E-07
1.32E-07	-2.69E-08	9.32E-09	5.10E-08	2.69E-07	-1.56E-07	-1.17E-07	-1.04E-07	5.05E+02	-9.13E-08	1.52E-06	-1.22E-06
-1.81E-07	5.34E-08	-1.02E-07	1.54E-07	-1.08E-07	5.55E-08	-1.95E-08	1.63E-08	-9.13E-08	5.81E+02	-8.24E-07	-5.35E-07
4.26E-06	-5.04E-07	6.90E-07	-4.83E-06	-7.29E-07	-1.05E-06	-1.67E-07	5.98E-07	1.52E-06	-8.24E-07	1.06E+03	8.44E-06
-2.28E-06	-4.08E-07	1.21E-07	2.26E-06	-7.66E-07	-6.23E-07	4.09E-07	2.48E-07	-1.22E-06	-5.35E-07	8.44E-06	1.10E+03
3.65E-07	-1.37E-06	1.84E-06	-3.32E-07	-5.43E-09	3.25E-07	5.34E-07	1.13E-06	-4.49E-09	3.28E-07	-3.68E-06	1.02E-06
-1.63E-06	-4.09E-06	4.05E-06	1.75E-06	3.62E-07	-6.52E-08	1.95E-06	1.78E-06	-1.19E-06	2.50E-08	-1.89E-06	8.14E-06
2.19E-06	4.66E-07	-6.01E-07	-1.72E-06	3.01E-07	1.96E-07	-2.52E-07	2.16E-07	4.77E-07	2.24E-07	-3.25E-06	4.17E-06
-1.51E-06	1.32E-06	-1.58E-06	1.12E-06	1.84E-08	-1.37E-07	2.27E-07	-1.03E-06	1.65E-08	-2.02E-07	1.91E-07	2.16E-06
2.74E-06	-3.95E-07	5.35E-07	-2.65E-06	-2.55E-07	-3.92E-08	-3.02E-07	8.59E-08	1.32E-06	-1.13E-07	7.41E-07	-5.77E-06
4.37E-07	-1.56E-06	1.08E-06	-1.43E-07	2.82E-07	2.03E-07	2.96E-07	3.96E-07	-5.17E-08	1.74E-07	-2.74E-06	8.54E-07
-1.05E-06	5.68E-07	-8.13E-07	7.86E-07	3.33E-07	6.21E-07	-1.92E-08	-3.73E-07	-2.56E-07	4.35E-07	-7.50E-06	2.40E-06
5.81E-08	-7.31E-07	6.26E-07	-5.27E-08	6.11E-08	5.96E-08	3.54E-07	-9.37E-07	6.16E-07	-3.74E-07	2.04E-06	-3.37E-07
3.91E-07	7.09E-07	-5.51E-07	-8.94E-07	-1.57E-07	4.24E-08	-1.70E-07	2.75E-07	-1.89E-07	7.90E-08	-5.90E-08	-1.53E-06
-3.98E-07	2.86E-07	-8.18E-07	-1.55E-07	2.51E-07	5.32E-08	5.52E-08	-4.30E-07	1.41E-07	9.42E-09	-8.27E-07	5.52E-07
3.74E-07	-6.11E-08	2.12E-07	-1.70E-07	-1.74E-08	8.02E-08	1.52E-07	3.10E-07	1.31E-07	1.23E-07	-1.46E-06	-7.49E-07
2.14E-08	7.93E-07	-5.73E-07	-2.03E-07	-2.87E-07	-3.23E-07	-1.08E-07	6.83E-07	-6.41E-07	5.12E-08	2.29E-06	3.36E-06

Col 25	Col 26	Col 27	Col 28	Col 29	Col 30	Col 31	Col 32	Col 33	Col 34	Col 35	Col 36
1.33E-04	3.13E-03	-5.02E-04	-1.26E-03	1.04E-03	2.26E-03	-1.31E-03	1.10E-04	-4.44E-05	-1.43E-04	-4.87E-04	-8.60E-04
-2.06E-04	1.81E-03	-2.40E-03	3.38E-04	-2.39E-03	-1.49E-04	7.48E-04	5.01E-04	-3.74E-04	-1.11E-04	-2.97E-05	-4.46E-04
7.12E-04	2.43E-04	1.03E-03	8.10E-05	-6.77E-05	7.28E-04	1.95E-03	-2.26E-04	-8.06E-05	4.75E-04	2.45E-04	-8.71E-04
-1.27E-03	2.07E-02	-1.90E-02	8.13E-03	-2.44E-02	-4.20E-05	7.61E-03	-1.97E-03	-3.03E-03	2.15E-04	7.14E-04	9.96E-05
-1.18E-02	-3.68E-02	4.41E-03	1.28E-02	-1.28E-02	-1.73E-02	1.06E-02	2.17E-03	5.86E-04	2.28E-03	2.97E-04	7.11E-03
-3.83E-02	5.07E-02	-1.27E-03	9.06E-03	-2.54E-02	-1.34E-02	9.33E-04	8.92E-04	-8.02E-03	-5.55E-03	-2.41E-02	-3.90E-03
4.05E-07	-2.71E-06	2.15E-06	-8.17E-07	3.15E-06	3.30E-08	-1.11E-06	-3.58E-07	3.58E-07	-1.38E-07	1.56E-07	2.70E-07
1.56E-06	4.93E-06	-7.44E-07	-1.83E-06	1.51E-06	2.29E-06	-1.39E-06	-9.18E-08	-5.25E-08	-3.57E-07	-4.95E-08	-1.13E-06
-5.08E-08	-1.17E-06	-5.48E-07	-2.52E-07	-3.38E-07	-3.59E-07	1.75E-08	7.20E-07	-3.33E-07	1.01E-07	-1.87E-07	-3.62E-07
-4.97E-06	6.76E-06	-3.54E-07	1.24E-06	-3.23E-06	-1.66E-06	9.45E-08	4.85E-07	-1.10E-06	-5.35E-07	-3.52E-06	-4.49E-07
1.78E-06	-4.41E-07	3.00E-06	-1.26E-07	4.34E-07	-2.29E-06	-3.41E-06	6.52E-07	-5.36E-07	4.32E-08	4.24E-07	6.39E-07
-4.59E-07	-7.08E-07	4.57E-07	4.55E-07	8.04E-07	-5.66E-08	1.02E-07	3.65E-07	-4.75E-07	-1.77E-07	-1.94E-07	-7.74E-07
3.65E-07	-1.63E-06	2.19E-06	-1.51E-06	2.74E-06	4.37E-07	-1.05E-06	5.81E-08	3.91E-07	-3.98E-07	3.74E-07	2.14E-08
-1.37E-06	-4.09E-06	4.66E-07	1.32E-06	-3.95E-07	-1.56E-06	5.68E-07	-7.31E-07	7.09E-07	2.86E-07	-6.11E-08	7.93E-07
1.84E-06	4.05E-06	-6.01E-07	-1.58E-06	5.35E-07	1.08E-06	-8.13E-07	6.26E-07	-5.51E-07	-8.18E-07	2.12E-07	-5.73E-07
-3.32E-07	1.75E-06	-1.72E-06	1.12E-06	-2.65E-06	-1.43E-07	7.86E-07	-5.27E-08	-8.94E-07	-1.55E-07	-1.70E-07	-2.03E-07
-5.43E-09	3.62E-07	3.01E-07	1.84E-08	-2.55E-07	2.82E-07	3.33E-07	6.11E-08	-1.57E-07	2.51E-07	-1.74E-08	-2.87E-07
3.25E-07	-6.52E-08	1.96E-07	-1.37E-07	-3.92E-08	2.03E-07	6.21E-07	5.96E-08	4.24E-08	5.32E-08	8.02E-08	-3.23E-07
5.34E-07	1.95E-06	-2.52E-07	2.27E-07	-3.02E-07	2.96E-07	-1.92E-08	3.54E-07	-1.70E-07	5.52E-08	1.52E-07	-1.08E-07
1.13E-06	1.78E-06	2.16E-07	-1.03E-06	8.59E-08	3.96E-07	-3.73E-07	-9.37E-07	2.75E-07	-4.30E-07	3.10E-07	6.83E-07
-4.49E-09	-1.19E-06	4.77E-07	1.65E-08	1.32E-06	-5.17E-08	-2.56E-07	6.16E-07	-1.89E-07	1.41E-07	1.31E-07	-6.41E-07
3.28E-07	2.50E-08	2.24E-07	-2.02E-07	-1.13E-07	1.74E-07	4.35E-07	-3.74E-07	7.90E-08	9.42E-09	1.23E-07	5.12E-08
-3.68E-06	-1.89E-06	-3.25E-06	1.91E-07	7.41E-07	-2.74E-06	-7.50E-06	2.04E-06	-5.90E-08	-8.27E-07	-1.46E-06	2.29E-06
1.02E-06	8.14E-06	4.17E-06	2.16E-06	-5.77E-06	8.54E-07	2.40E-06	-3.37E-07	-1.53E-06	5.52E-07	-7.49E-07	3.36E-06
1.10E+03	1.02E-05	6.30E-07	-2.43E-06	4.66E-06	-3.77E-06	1.15E-06	-8.51E-07	-1.72E-08	-4.79E-07	4.54E-06	7.51E-07
1.02E-05	1.15E+03	-1.82E-06	1.85E-06	-4.06E-06	2.64E-06	-8.20E-07	1.60E-06	9.54E-07	-3.38E-07	1.75E-06	2.90E-06
6.30E-07	-1.82E-06	1.34E+03	-5.00E-07	-8.65E-07	-1.62E-06	-2.27E-06	2.54E-07	1.76E-06	8.08E-08	2.30E-08	2.07E-06
-2.43E-06	1.85E-06	-5.00E-07	1.45E+03	-5.81E-07	-9.88E-07	5.14E-07	6.30E-07	-1.13E-07	2.29E-07	-1.37E-06	-4.33E-07
4.66E-06	-4.06E-06	-8.65E-07	-5.81E-07	1.54E+03	1.02E-07	2.05E-07	-5.06E-07	1.07E-06	8.19E-07	1.20E-06	9.85E-07
-3.77E-06	2.64E-06	-1.62E-06	-9.88E-07	1.02E-07	1.60E+03	-1.17E-06	-2.17E-08	9.37E-07	-3.31E-07	-9.88E-07	-8.98E-07
1.15E-06	-8.20E-07	-2.27E-06	5.14E-07	2.05E-07	-1.17E-06	1.61E+03	9.16E-09	-2.96E-07	2.10E-07	6.38E-07	-4.95E-07
-8.51E-07	1.60E-06	2.54E-07	6.30E-07	-5.06E-07	-2.17E-08	9.16E-09	1.69E+03	8.43E-07	1.14E-06	-7.53E-08	7.62E-07
-1.72E-08	9.54E-07	1.76E-06	-1.13E-07	1.07E-06	9.37E-07	-2.96E-07	8.43E-07	1.69E+03	6.47E-08	6.00E-07	-8.92E-07
-4.79E-07	-3.38E-07	8.08E-08	2.29E-07	8.19E-07	-3.31E-07	2.10E-07	1.14E-06	6.47E-08	2.02E+03	2.94E-07	-6.65E-08
4.54E-06	1.75E-06	2.30E-08	-1.37E-06	1.20E-06	-9.88E-07	6.38E-07	-7.53E-08	6.00E-07	2.94E-07	2.04E+03	-2.40E-07
7.51E-07	2.90E-06	2.07E-06	-4.33E-07	9.85E-07	-8.98E-07	-4.95E-07	7.62E-07	-8.92E-07	-6.65E-08	-2.40E-07	2.04E+03

## APPENDIX B – TOWER MODEL



### NOTES

1. All dimensions in millimeters.
2. All levels in meters.
3. Nominal weight of steel on this drawing:  
TOW 427.95 tonnes
4. Steel density 7850kg/m<sup>3</sup>

Rev.	Date	Drw.	Chkd.	Appr.	Description
0	2016.05.xx	DAKA	xxxx	xxxx	FOR INFORMATION
Client <b>INN WIND.EU</b>					
Planner <b>Ramboll Wind</b>					
Title <b>INN WIND 10MW Design</b>					
Title <b>TOWER - COMPUTER MODEL</b>					
Scale	Size	Drawing No.			Rev.
1:467	A4	For information			0

## APPENDIX C – SOIL PROFILE

DESIGN PARAMETERS FOR SOIL IN01 WITH PILE A0P0P											
depth (m)	Soil type	$\gamma'$ (kN/m <sup>3</sup> )	$I_p$ (%)	$q_u$ (MPa)	$\phi$ (deg)	$c_u$ (kPa)	E (MPa)	$\epsilon_{50}$ (%)	$t_c$ (kPa)	$t_t$ (kPa)	q (MPa)
2.0	SAND	9.00			35.0		5.7		0.0	0.0	0.0
3.3	SAND	9.00			35.0		5.7		0.0	0.0	0.0
9.0	SAND	9.00			35.0		13.7		15.1	15.1	1.1
10.0	SAND	9.00			35.0		16.6		32.8	32.8	2.4
15.0	SAND	9.00			35.0		19.7		47.0	47.0	3.4
20.0	SAND	10.00			35.0		24.4		71.1	71.1	5.1
22.5	SAND	10.50			35.0		27.5		89.8	89.8	6.5
29.0	SAND	11.00			35.0		30.8		105.5	105.5	8.1
32.0	SAND	11.00			35.0		34.0		115.0	115.0	9.9
38.0	SAND	11.00			35.0		36.8		115.0	115.0	11.2
40.0	SAND	11.00			35.0		39.1		115.0	115.0	12.0
90.0	SAND	11.00			35.0		50.3		115.0	115.0	12.0

$\gamma'$  : Submerged unit weight  
 $I_p$  : Plasticity index  
 $q_u$  : Unconfined compression strength  
 $\phi$  : Characteristic angle of internal friction  
 $c_u$  : Characteristic undrained shear strength  
E : Modulus of elasticity  
 $\epsilon_{50}$  : Strain which occurs at one-half of the maximum stress in laboratory undrained compression test  
 $t_c$  : Unit skin friction, compression  
 $t_t$  : Unit skin friction, tension  
q : Unit tip resistance, compression

Design code: DNV-J101  
Partial coefficient on angle of internal friction: 1.00  
Partial coefficient on undrained shear strength: 1.00  
Partial coefficient on axial bearing capacity: 1.00

Scour: Local scour: 3.3 m  
Global scour: 0.0 m  
Scour angle: 18.0 deg

 Pile tip depth: 38.00 m  
Pile tip diameter: 2540.0 mm  
Pile tip thickness: 31.8 mm

## Ramboll Wind

Subject: InnWind Soil Profile

Prepared: TVB

Checked: BJOS

Approved: TIMF

Program: ROSA 5.00

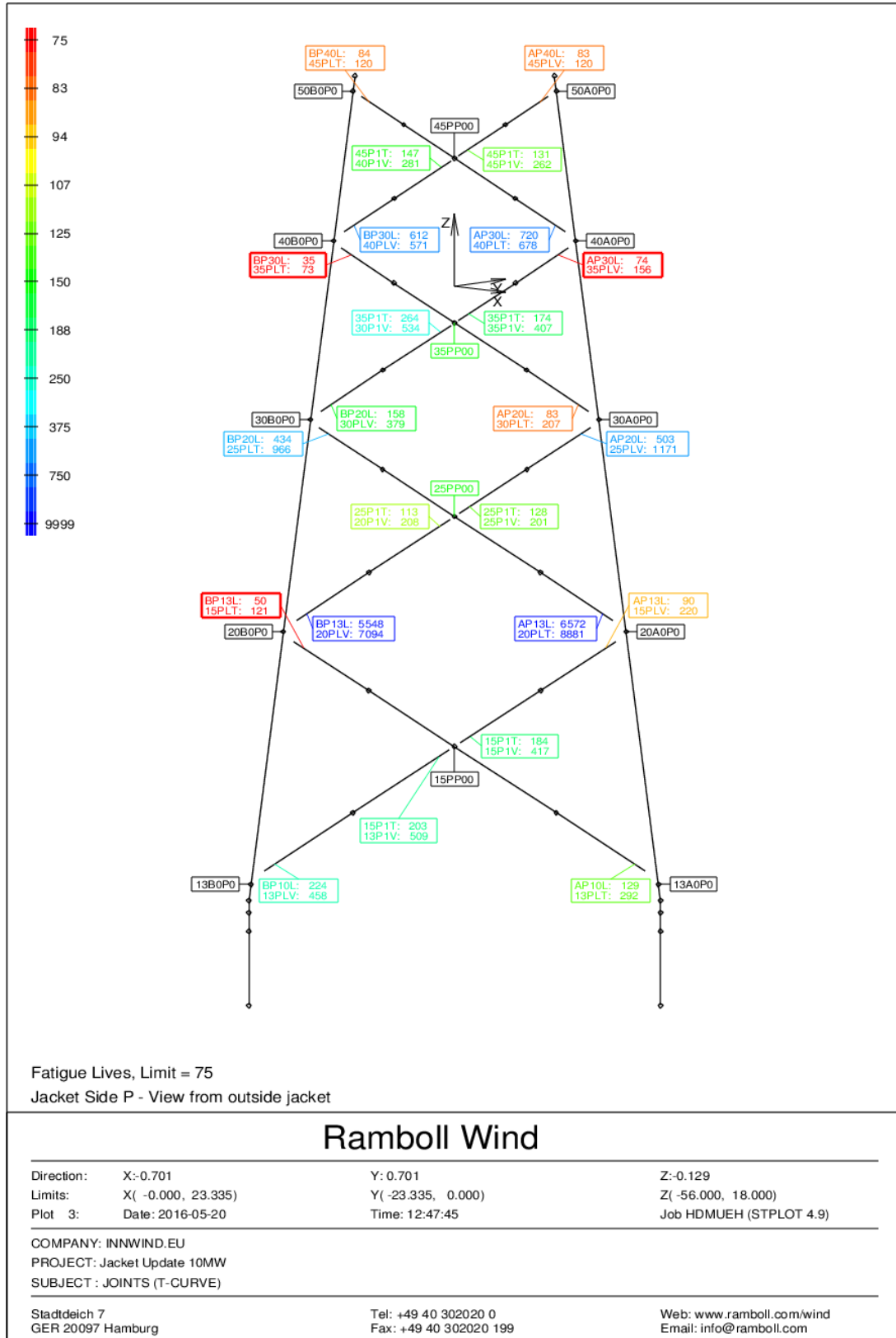
Rev. 0 Date: 2013-09-25

Staddeich 7  
GER 20097 Hamburg

Tel: +49 40 302020 0  
Fax: +49 40 302020 199

Web: [www.ramboll.com/wind](http://www.ramboll.com/wind)  
Email: [info@ramboll.com](mailto:info@ramboll.com)

## APPENDIX D – FATIGUE LIVES OF TUBULAR JOINTS

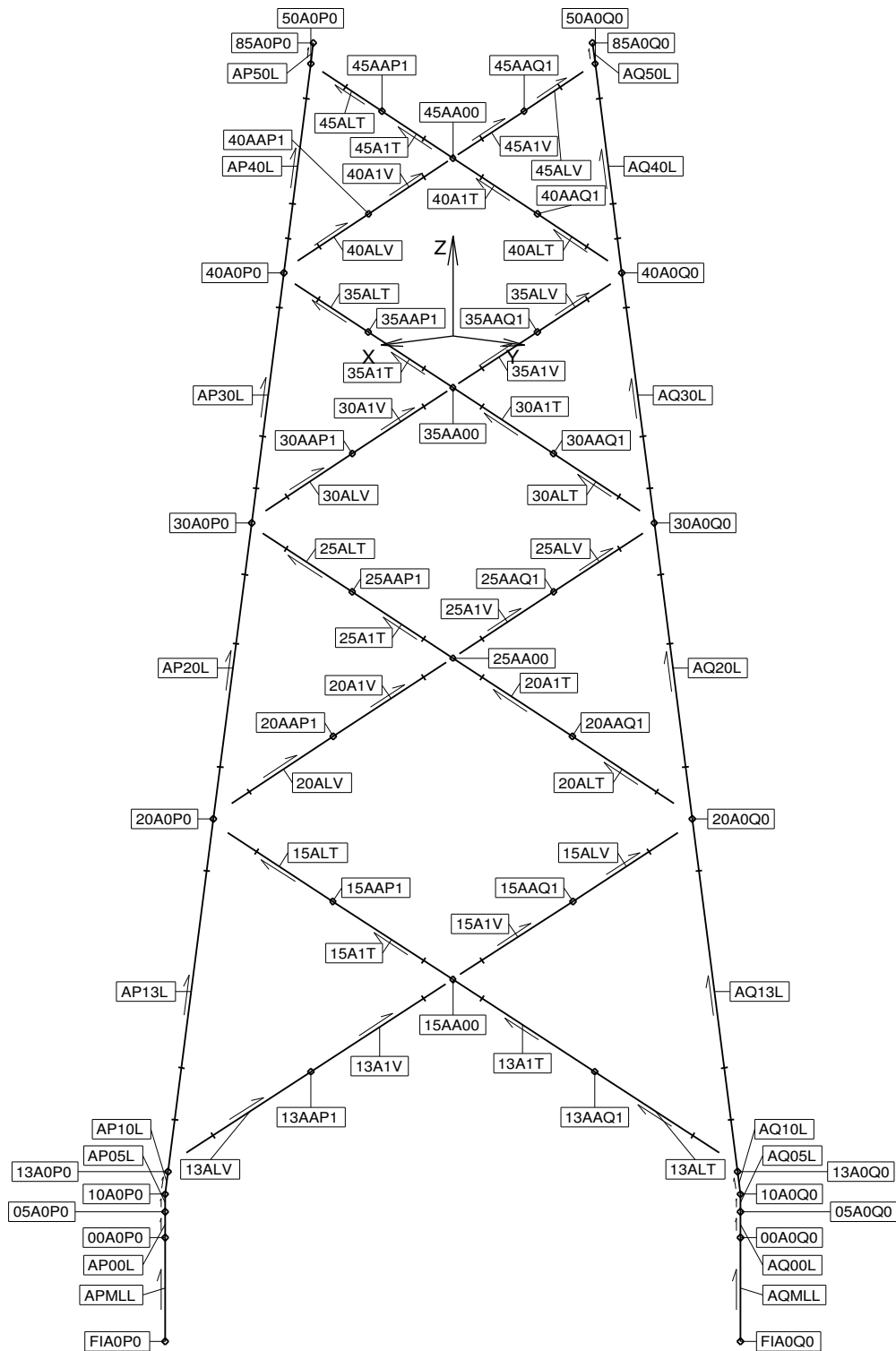


## APPENDIX E – GEOMETRY OF THE JACKET

This appendix contains:

- Node and element naming convention
- Node coordinates
- Overview of cross sections
- Length of jacket members
- Material assignment

of the improved steel jacket design presented in Chapter 3.



Node and Element Names  
Jacket Side A - View from outside jacket

# Ramboll Wind

Direction:	X:-0.701	Y:-0.701	Z:-0.129
Limits:	X( 0.000, 23.335)	Y( 0.000, 23.335)	Z( -56.000, 18.000)
Plot 1:	Date: 2016-05-20	Time: 09:54:54	Job HDJXFK (STPLOT 5.0)

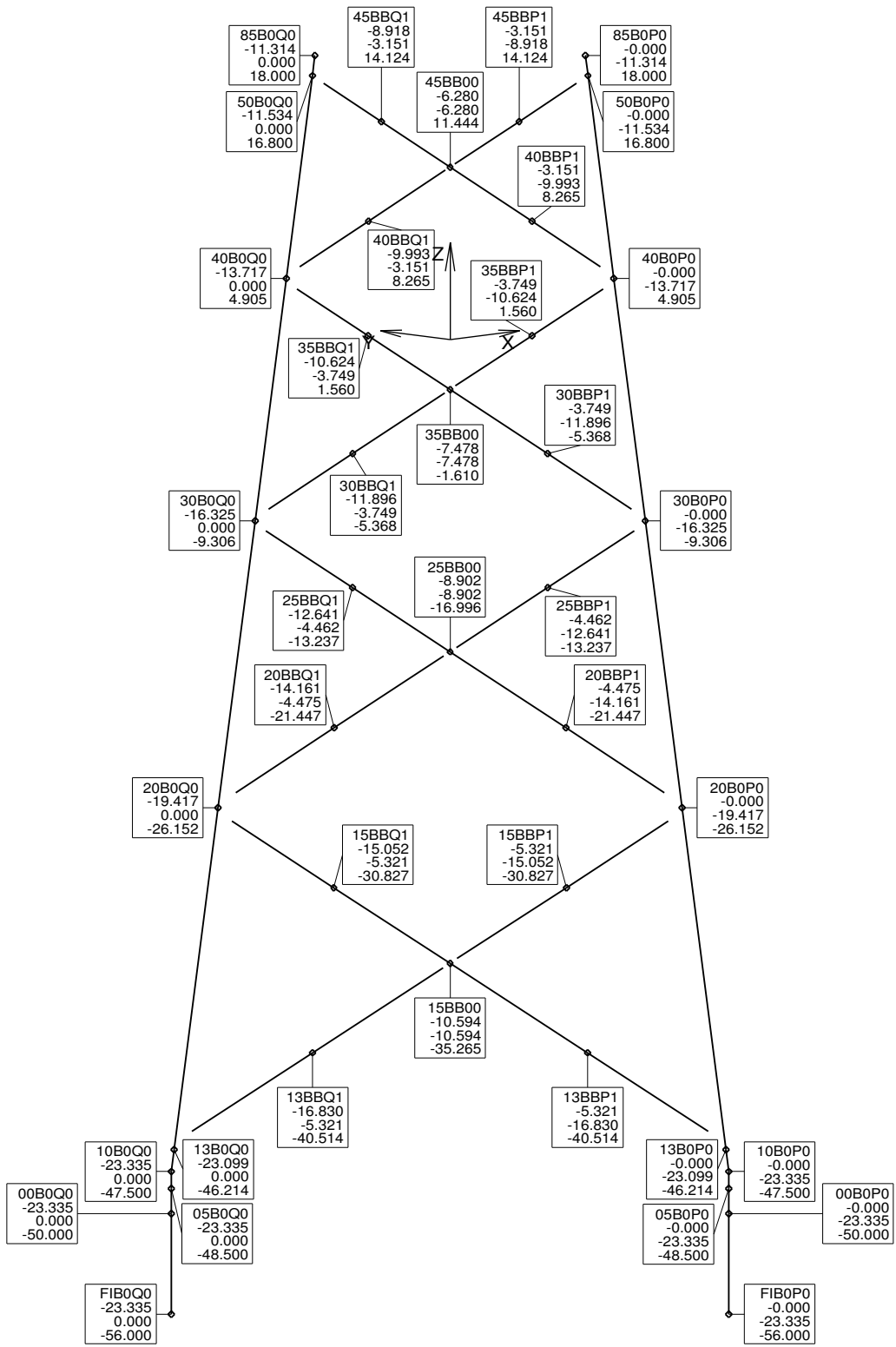
COMPANY: INNWIND.EU  
PROJECT: Jacket Update 10MW  
SUBJECT: 4-LEG, 4-STOREY, FATIGUE CONFIG

Stadtdeich 7  
GER 20097 Hamburg

Tel: +49 40 302020 0  
Fax: +49 40 302020 199

Web: [www.ramboll.com/wind](http://www.ramboll.com/wind)  
Email: [info@ramboll.com](mailto:info@ramboll.com)





Node coordinates (m)  
Jacket Side B - View from outside jacket

## Ramboll Wind

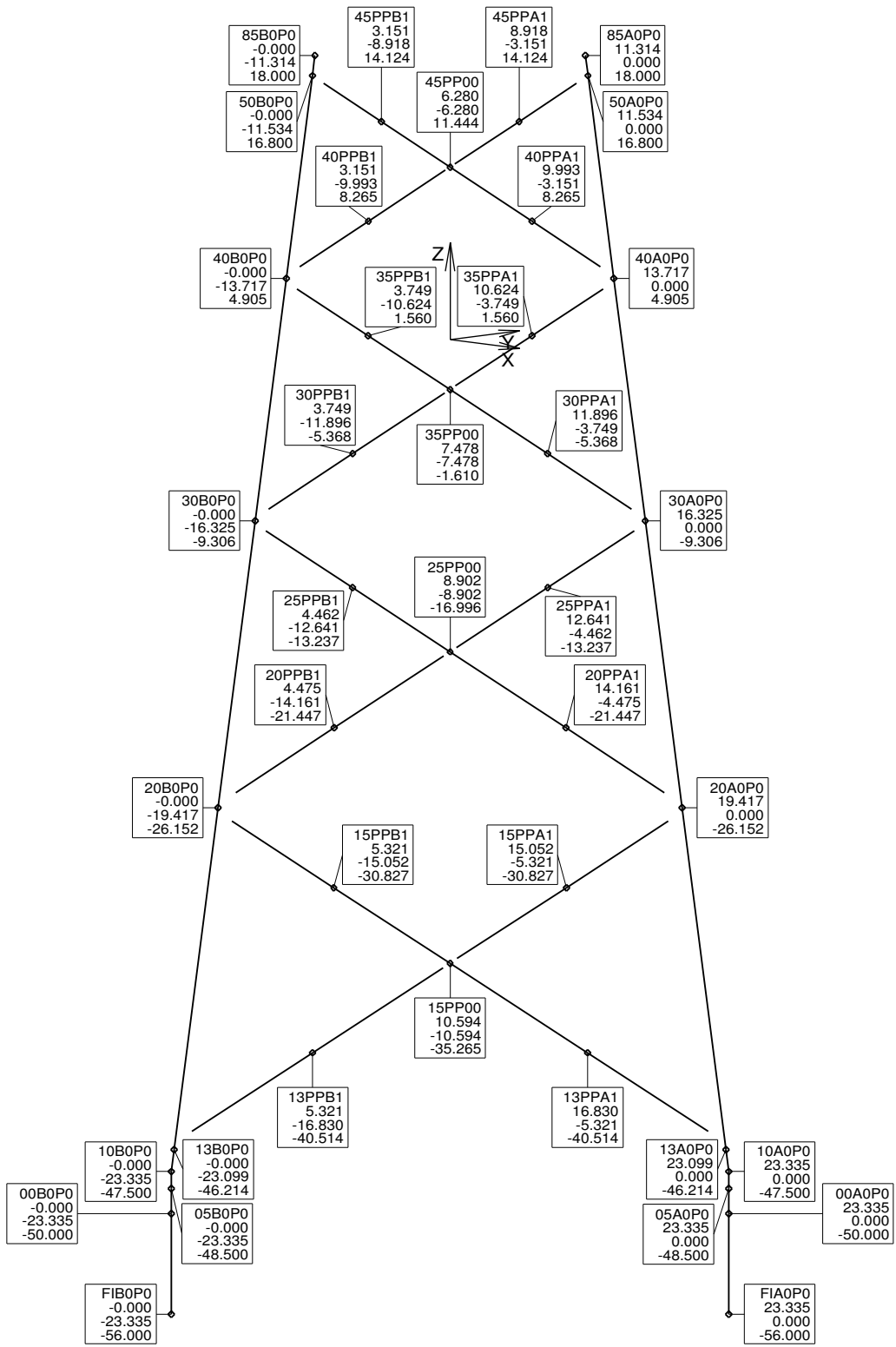
Direction:	X: 0.701	Y: 0.701	Z: -0.129
Limits:	X(-23.335, -0.000)	Y(-23.335, 0.000)	Z(-56.000, 18.000)
Plot 2:	Date: 2016-05-20	Time: 09:54:54	Job HDJXFK (STPLOT 5.0)

COMPANY: INNWIND.EU  
PROJECT: Jacket Update 10MW  
SUBJECT: 4-LEG, 4-STOERY, FATIGUE CONFIG

Stadtdeich 7  
GER 20097 Hamburg

Tel: +49 40 302020 0  
Fax: +49 40 302020 199

Web: www.ramboll.com/wind  
Email: info@ramboll.com



Node coordinates (m)  
 Jacket Side P - View from outside jacket

# Ramboll Wind

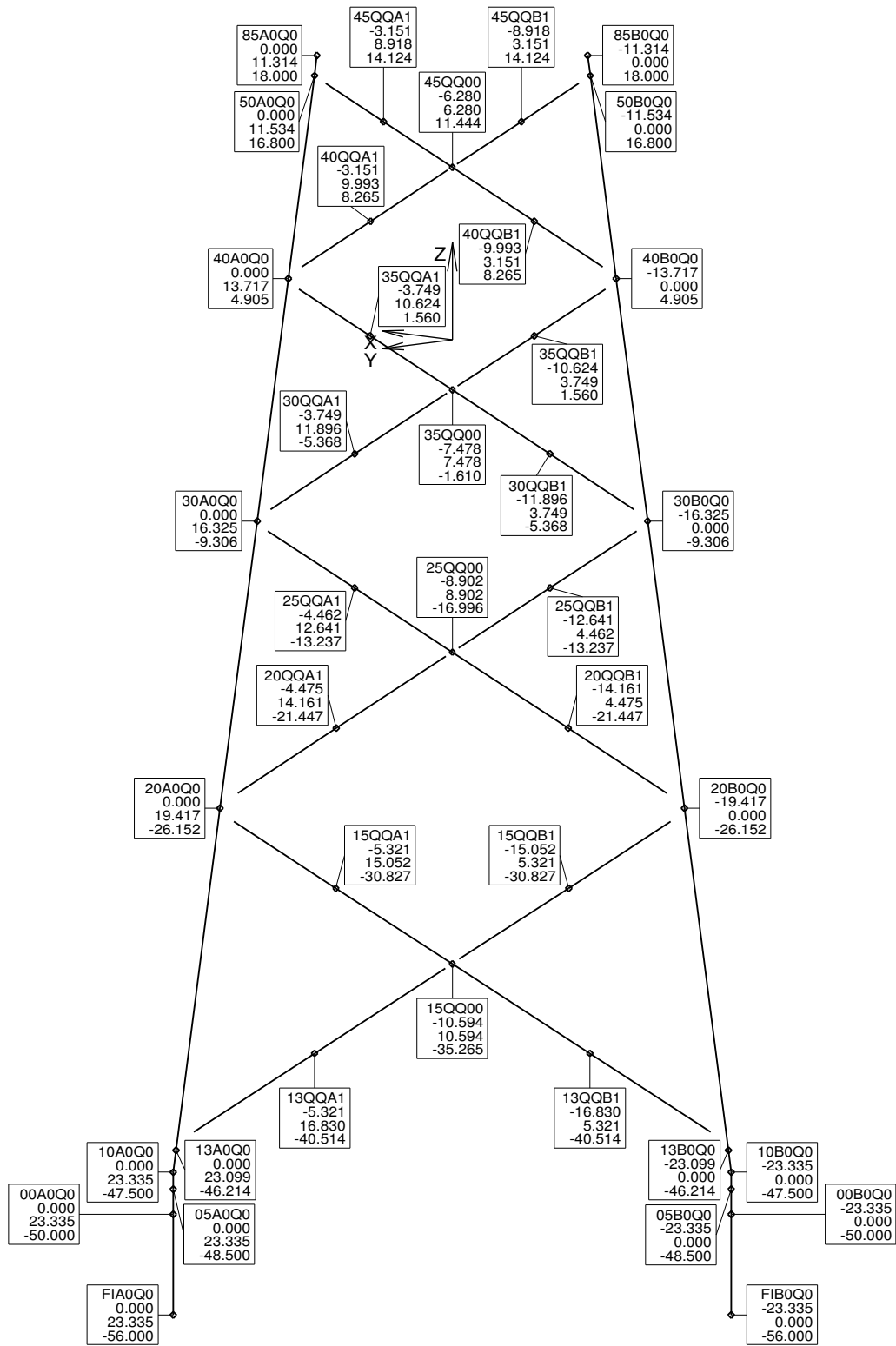
Direction:	X: -0.701	Y: 0.701	Z: -0.129
Limits:	X( -0.000, 23.335)	Y( -23.335, 0.000)	Z( -56.000, 18.000)
Plot 3:	Date: 2016-05-20	Time: 09:54:54	Job HDJXFK (STPLOT 5.0)

COMPANY: INNWIND.EU  
 PROJECT: Jacket Update 10MW  
 SUBJECT: 4-LEG, 4-STOERY, FATIGUE CONFIG

Stadtdeich 7  
 GER 20097 Hamburg

Tel: +49 40 302020 0  
 Fax: +49 40 302020 199

Web: www.ramboll.com/wind  
 Email: info@ramboll.com



Node coordinates (m)  
Jacket Side Q - View from outside jacket

## Ramboll Wind

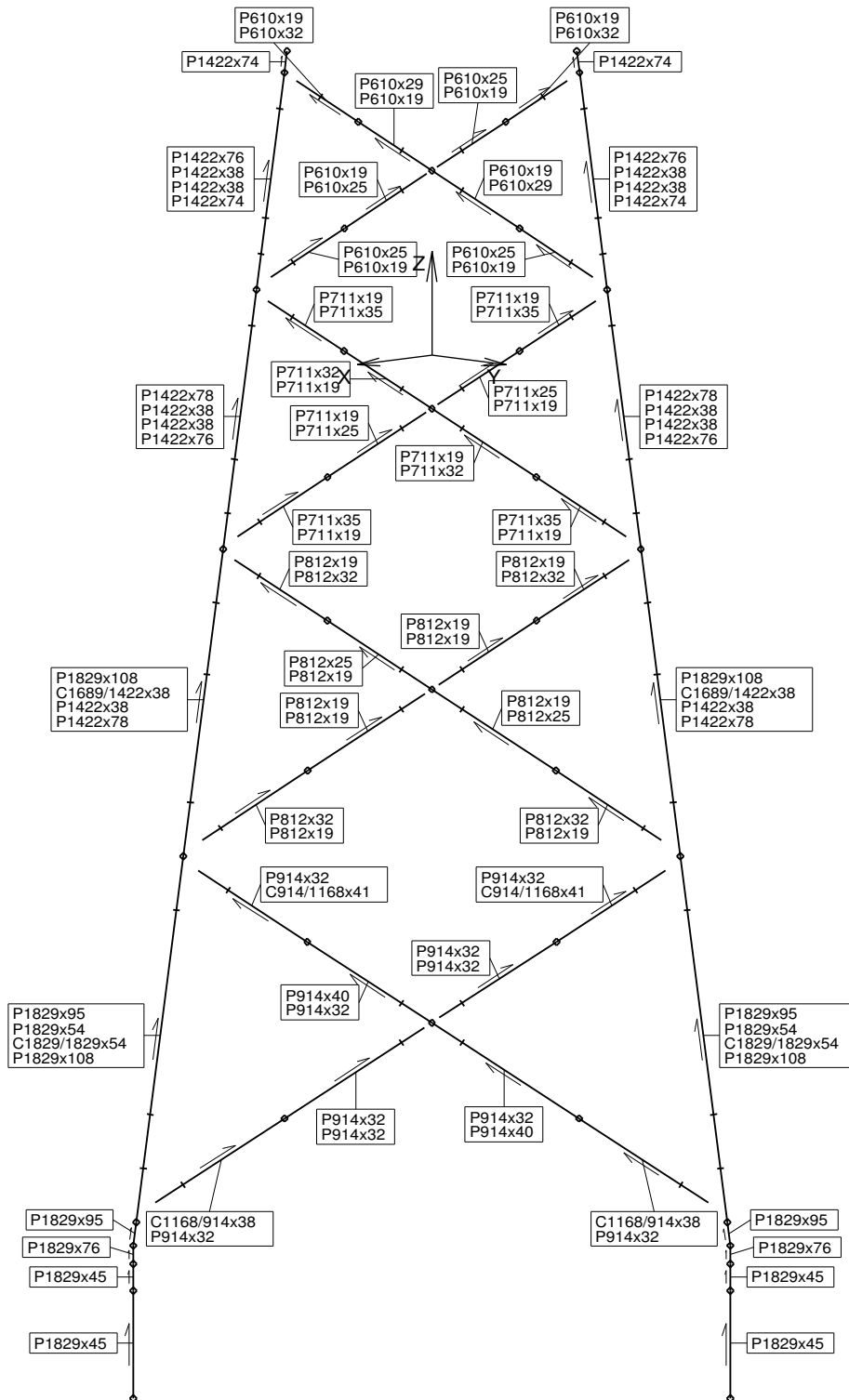
Direction:	X: 0.701	Y: -0.701	Z: -0.129
Limits:	X( -23.335, 0.000)	Y( 0.000, 23.335)	Z( -56.000, 18.000)
Plot 4:	Date: 2016-05-20	Time: 09:54:54	Job HDJXFK (STPLOT 5.0)

COMPANY: INNWIND.EU  
PROJECT: Jacket Update 10MW  
SUBJECT: 4-LEG, 4-STOERY, FATIGUE CONFIG

Stadtdeich 7  
GER 20097 Hamburg

Tel: +49 40 302020 0  
Fax: +49 40 302020 199

Web: [www.ramboll.com/wind](http://www.ramboll.com/wind)  
Email: [info@ramboll.com](mailto:info@ramboll.com)



Jacket Side A - View from outside jacket

## Ramboll Wind

Direction:	X: -0.701	Y: -0.701	Z: -0.129
Limits:	X( 0.000, 23.335)	Y( 0.000, 23.335)	Z( -56.000, 18.000)
Plot 1:	Date: 2016-05-20	Time: 09:54:54	Job HDJXFK (STPLOT 5.0)

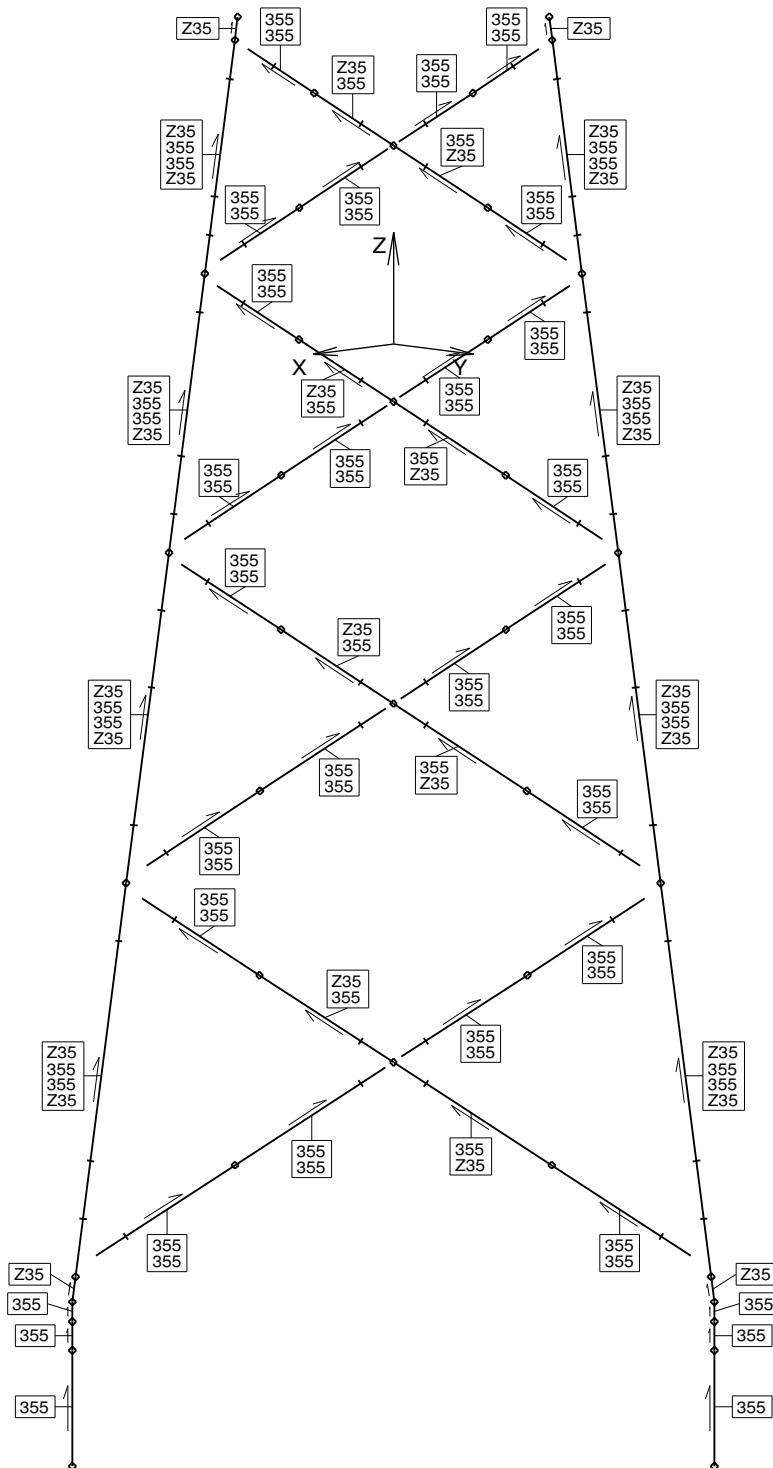
COMPANY: INNWIND.EU  
 PROJECT: Jacket Update 10MW  
 SUBJECT: 4-LEG, 4-STOREY, FATIGUE CONFIG

Stadtdeich 7  
 GER 20097 Hamburg

Tel: +49 40 302020 0  
 Fax: +49 40 302020 199

Web: [www.ramboll.com/wind](http://www.ramboll.com/wind)  
 Email: [info@ramboll.com](mailto:info@ramboll.com)





**Material Names**

Jacket Side A - View from outside jacket

# Ramboll Wind

Direction:	X:-0.701	Y:-0.701	Z:-0.129
Limits:	X( 0.000, 23.335)	Y( 0.000, 23.335)	Z( -56.000, 18.000)
Plot 1:	Date: 2016-05-20	Time: 09:54:55	Job HDJXFK (STPLOT 5.0)

COMPANY: INNWIND.EU  
 PROJECT: Jacket Update 10MW  
 SUBJECT: 4-LEG, 4-STOERY, FATIGUE CONFIG

Stadtdeich 7  
 GER 20097 Hamburg

Tel: +49 40 302020 0  
 Fax: +49 40 302020 199

Web: [www.ramboll.com/wind](http://www.ramboll.com/wind)  
 Email: [info@ramboll.com](mailto:info@ramboll.com)

## APPENDIX F – GEOMETRY OF THE MONOPILE

	Height or Depth [m]	Outer Diameter [mm]	Wall thickness [mm]
Interface	26.000	9500	100
Mean sea level	0.000	9500	100
	- 0.001	9500	150
mudline	-50.000	9500	150
	-76.500	9500	150
	-76.501	9500	102
Pile toe	-100.000	9500	102